Mechanophore Strategies for the Development of Polymers with Mechanically Gated Responsive Behavior

Thesis by

Ross William Barber

In Partial Fulfillment of the Requirements for the

Degree of

Doctor of Philosophy

2023

(Defended May 1, 2023)

© 2023

Ross William Barber

ORCID: 0000-0003-0434-847X

Acknowledgements

It is difficult to put into words the incredible appreciation I have for the people in my life who supported me during the years summarized in this document. Through no small effort have they continually inspired me to be the best scientist, coworker, friend, brother, and son that I could be. The people named below, and several others I have not the time to appropriately recognize, will always have a special place in my heart.

First I would like to thank my advisor Professor Maxwell Robb for welcoming me so wholeheartedly into his research group. His constant attention and tutelage have forged me into the scientist I am today, and I will always remember him by the wisdom he has imparted to me. I consider it a distinct privilege to have worked with him during the first years of his professorial career.

My thesis committee, led by Brian Stoltz and consisting of Theo Agapie, Hosea Nelson, and Bob Grubbs, has been invaluable for my professional and scientific development. I am lucky to have been mentored by such incredible scientists and supportive people. I would not be where I am today without them and will sorely miss their guidance and perspective as I continue my professional career.

I would next like to sincerely thank all current and former members of the Robb group: Molly McFadden, Quan Gan, Chelsea Edwards, Anna Overholts, Corey Husic, Brooke Versaw, May Zeng, Isabel Klein, Skylar Osler, Stella Luo, Yan Sun, Debbie Tseng, Jolly Patro, David Kovacs, Nicolas Choquette, Maria Azcona-Baez, Wendy Granados Razo, Liam Ordner, Sean Hu, and Peng Liu. There is no doubt that the positive impact left on me by every single one of these incredible scientists helped shape me into the researcher I am today, and for that I am truly grateful.

Confining a summary of the positive relationships I formed outside of the lab during my time at Caltech to a paragraph of acceptable length is one of the hardest things I have had to do during the course of assembling this document. I am incredibly lucky to have spent my time here with some of the brightest and most memorable people I will ever meet. As members of my cohort, in no particular order, Molly McFadden, Josh Zak, Sarah Bevilacqua, Matt O'Rourke, Alex Shimozono, Gracie Zhang, Ailiena Maggiolo, Juner Zhang, Alex Barth, James Lawniczak, Nick Hafeman, and Axl LeVan were invaluable companions from the very beginning. I leave Caltech wishing to remain close to each and every one of them. Game nights will not be the same without Bryce Hickam, Isabel Klein, Jonathan Michelsen, Anna Overholts, Kshitij Sadasivan, May Zeng, Molly McFadden, Skylar Osler, Stella Luo, or Yan Sun, even if Isabel never actually played. Neither will rock climbing without Skylar Osler, Anna Overholts, Kshitij Sadasivan, Stella Luo, or Bryce Hickam. Though their names have already been mentioned several times, special thanks go to Skylar Osler, Molly McFadden, Stella Luo, and Yan Sun for being great friends both on and off campus. Finally, shout out to all members of the Churchgoers softball team for drinking brews and hitting dingers!

At the risk of sounding like a broken record, I want to extend heartfelt recognition to Molly McFadden. Though she is an excellent coworker, I find truer value in her undying and unwavering friendship. None of what I accomplished during that time would be possible without her constant advice and positivity. The thought of leaving her and her fiancé William Hargis on the west coast feels like leaving parts of myself behind.

Finally, I want to thank my mom, Heather, dad, Chuck, and two brothers Colin and Kyle. I struggle to find the words to describe what you all mean to me. The difficult periods I

faced during grad school were eased by knowing you all love and support me. I consider the time I spend with you to be the best of my life.

Abstract

The development of mechanically sensitive molecules has recently enabled mechanical force to induce specific changes in polymeric materials. This document details efforts in the development of such mechanophores in which mechanical activation is used to gate the desired functional responses.

Chapter 1 is an introduction to polymer mechanochemistry and delineates the state of the field as it relates to color changing mechanophores used for damage detection. Special emphasis is placed on a system developed by our lab in which mechanical force gates the photoresponsive behavior of a diarylethene molecular switch.

Chapter 2 details the design of a new mechanically gated photoswitch whose synthesis and activity are improved from the previous iteration. The modular design enables a late-stage synthetic intermediate to be differentiated into a small library of masked photoswitches that produce unique colors following mechanical activation and ultraviolet irradiation. Notably, these mechanophores show activity in solution phase experiments as well as in bulk polymeric materials.

Published Content and Contributions

Barber, R.W.; McFadden, M.E.; Hu, X.; Robb, M.J. Mechanically Gated Photoswitching: Expanding the Scope of Polymer Mechanochromism. *Synlett* **2019**, *30*, 1725–1732. DOI: 10.1055/s-0037-1611858.

R.W.B. wrote the manuscript.

Barber, R.W.; Robb, M. J. A Modular Approach to Mechanically Gated Photoswitching with Color-Tunable Force Probes. *Chem. Sci.* **2021**, *12*, 11703-11709. DOI: 10.1039/D1SC02890A.

R.W.B. conceived of some ideas, performed all experimental work and wrote the manuscript.

Table of Contents

Chapter 1

Mechanically Gated Photoswitching: Expanding the Scope of Polymer Mechanochromism

Adapted with permission from Barber, R. W.; McFadden, M. E.; Hu, X.; and Robb, M. J.

Synlett **2019**, *30*, 1725–1732.

Copyright 2019 Georg Thieme Verlag KG

Abstract

Mechanophores are molecules that undergo productive, covalent chemical transformations in response to mechanical force. Over the last decade, a variety of mechanochromic mechanophores have been developed that enable the direct visualization of stress in polymers and polymeric materials through changes in color and chemiluminescence. The recent introduction of mechanochemically gated photoswitching extends the repertoire of polymer mechanochromism by decoupling the mechanical activation from the visible response, enabling the mechanical history of polymers to be recorded and read on-demand using light. Here, we discuss advances in mechanochromic mechanophores and present our design of a cyclopentadiene–maleimide Diels–Alder adduct that undergoes a force-induced retro-[4+2] cycloaddition reaction to reveal a latent diarylethene photoswitch. Following mechanical activation, UV light converts the colorless diarylethene molecule to the colored isomer via a 6π electrocyclic ring-closing reaction. Mechanically gated photoswitching expands on the fruitful developments in mechanochromic polymers and provides a promising platform for further innovation in materials applications including stress sensing, patterning, and information storage.

Introduction to Polymer Mechanochemistry

The burgeoning field of polymer mechanochemistry explores the use of mechanical force to promote specific, and sometimes unusual, chemical reactions.[1,2] Polymer chains transduce external forces to particular covalent bonds in mechanically sensitive molecules known as mechanophores, resulting in productive chemical transformations.[3] Since the seminal report on site-specific activation of azo-linked polymers by Moore and coworkers in 2005,[4] the field has evolved to identify an exponentially growing number of

mechanophores that display a wide variety of functionality. Force-driven reactivity includes activation of catalysts,[5] triggered depolymerization,[6] generation of reactive functional groups,[7–10] switching of electrical conductivity,[11] chemiluminescence,[12]and changes in color.[13–23] Mechanical force has also been shown to promote formally forbidden pericyclic reactions such as the disrotatory electrocyclic ring-opening reaction of cis-1,2-disubstituted benzocyclobutene[24,25] and the conrotatory ring-opening reactions of gem-dihalocyclopropanes.[26,27] Computational studies have established that the unique reactivity of mechanophores originates from a distortion of the potential energy surface under large forces, which fundamentally changes the reaction landscape and leads to different reaction pathways.[28–30]

Mechanochromic Reactions for Stress Sensing

Mechanophores that produce a visible change in color upon mechanical activation are particularly appealing targets for stress sensing. At the molecular scale, mechanical stress causes degradation typically characterized by homolytic bond scission along polymer backbones. As individual chains rupture, the mechanical integrity of a material diminishes and the likelihood of failure increases. Mechanochromic molecular force probes provide a convenient approach for visually detecting critical stress and/or strain in polymeric materials. Early reports of molecular strain sensors relied on changes in the fluorescent properties of dye aggregates in polymer blends;[31] however, the development of mechanophores has provided a platform for precisely tailoring the stress-responsive properties of materials within the framework of synthetic and physical organic chemistry.

The mechanically activated ring-opening reaction of spiropyran is one of the most ubiquitous transformations in the field of polymer mechanochemistry. Spiropyran is a well-

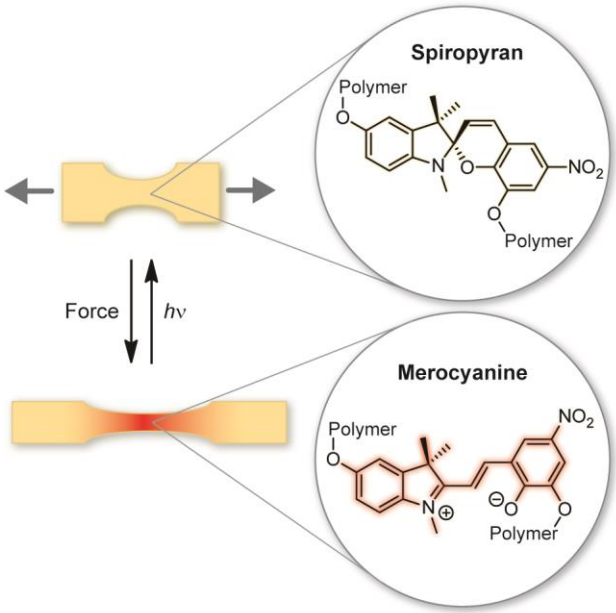

Figure 1.1. Mechanical activation of spiropyran in polymeric materials induces a 6π electrocyclic ring-opening reaction to generate the colored merocyanine species. Irradiation with visible light regenerates the ring-closed isomer.

known photochromic molecule that undergoes a 6π electrocyclic ring-opening reaction upon irradiation with UV light to generate a highly colored merocyanine dye. In 2007, Moore and coworkers discovered that this same electrocyclic ring-opening reaction is promoted by mechanical force applied across the spiro C–O bond.[13] The mechanochromic transformation of spiropyran was originally demonstrated in solution by sonicating poly(methyl acrylate) (PMA) polymers containing a single spiropyran mechanophore located near the center of the chains, where sonication-induced elongational forces are maximized. Later, in 2009, Sottos and coworkers demonstrated that the mechanochemical activation of spiropyran covalently incorporated into PMA and poly(methyl methacrylate) (PMMA) could be achieved in bulk polymeric materials (**Figure 1.1**).[14] An intense color change corresponding to generation of the ring-opened merocyanine dye was observed in

the materials under tensile loading, establishing a promising new strategy for stress sensing in polymers. Control experiments confirmed that the reactivity was mechanical in origin and the merocyanine dye was shown to convert back to the spiropyran form under visible light after stress relaxation.

In the decade following the discoveries of spiropyran mechanochromism in polymers, a number of additional mechanophores that display mechanochromic properties have been developed. In addition to ring-opening and pericyclic reactions, Otsuka and coworkers have pioneered another strategy to achieve mechanochromic materials that relies on homolytic dissociation of mechanophores into a pair of stable, colored free radicals under force. The mechanochromism of diarylbibenzofuranone (DABBF) was first demonstrated in polyurethane gels by freezing-induced mechanical activation (**Scheme 1.1**).[18] Formation of the blue-colored arylbenzofuranone radicals was confirmed using EPR spectroscopy. Low temperatures were required to suppress radical recombination. Subsequent research demonstrated that mechanochemical activation of DABBF could be

Scheme 1.1. Force-induced homolytic cleavage of dynamic-covalent mechanophores generates colored, stable radical fragments. The radical species thermally recombine to regenerate the mechanophores.

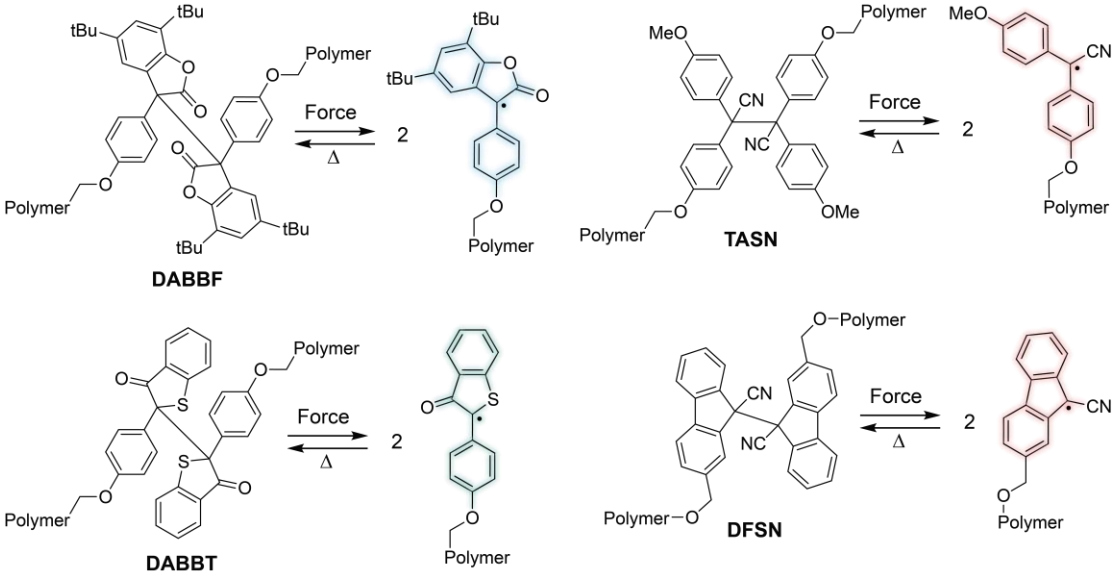

achieved in elastomeric linear polyurethanes under uniaxial tension for colorimetric stress sensing.[32] The same group has also identified tetraarylsuccinonitrile (TASN)[33] and diarylbibenzothiophenone (DABBT)[34] as mechanophores capable of producing pink and green colored radical fragments, respectively. The intrinsic thermal instability of these radical-type dynamic covalent molecules, however, limits their range of applications. To overcome this limitation, a thermally stable difluorenylsuccinonitrile (DFSN) mechanophore was recently introduced[35] that extends the utility of radical-type mechanochromic molecules and, importantly, enables their incorporation into well-defined materials prepared using controlled radical polymerization techniques.

An unprecedented mechanochromic transformation was introduced in 2017 by Xia, Burns, Martinez, and coworkers with the demonstration of polyladderene mechanochemistry.[11] Mechanochemical unzipping of polyladderene in solution using ultrasound was revealed to generate semiconducting polylacetylene (**Scheme 1.2**). The initially colorless insulating polymer developed a deep purple color characteristic of polyacetylene with highly extended conjugation. Interestingly, resonance Raman and infrared spectroscopy suggested that mechanochemical activation of polyladderene forms exclusively trans-polyacetylene, requiring that a cis-to-trans isomerization of the terminal olefins also occurs simultaneously during chain extension. Calculations of the force-

Scheme 1.2. Polyladderene unzips under ultrasound-induced elongational forces to generate conjugated polyacetylene.

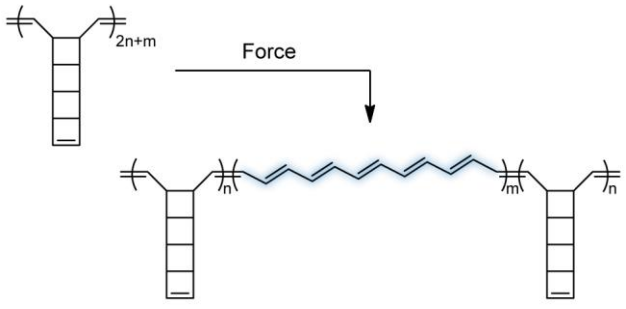

modified potential energy surface suggested that the mechanochemical reaction occurs via a multistep mechanism involving two diradical transition-state structures that becomes barrierless above 3.0 nN of force.

A seminal report by Sijbesma and coworkers in 2012 described the mechanochemically induced chemiluminescent reaction of a 1,2-dioxetane mechanophore (**Scheme 1.3**).[12] Dioxetane and its derivatives are known to emit light in response to chemical or thermal stimuli by a reaction that generates a short-lived electronically excited ketone, which relaxes to the ground state through a radiative process. Mechanochemical activation of a bis(adamantyl)-1,2-dioxetane mechanop hore covalently linked to PMA generated chemiluminescence upon ultrasonication. This effect was extended to the solid state by activating crosslinked PMA under tension and the color of emission was tuned via energy transfer to different fluorescent dye molecules incorporated into the polymeric material. While not technically a mechanochromic transformation, chemiluminescence provides an advantage in stress sensing applications due to the absence of background signal, enabling highly sensitive detection of polymer chain scission events with excellent temporal and spatial resolution.[36,37] Nevertheless, the transience of chemiluminescence

Scheme 1.3. Mechanical activation of polymers containing a bis(adamantyl)-1,2-dioxetane mechanophore generates light via chemiluminescence.

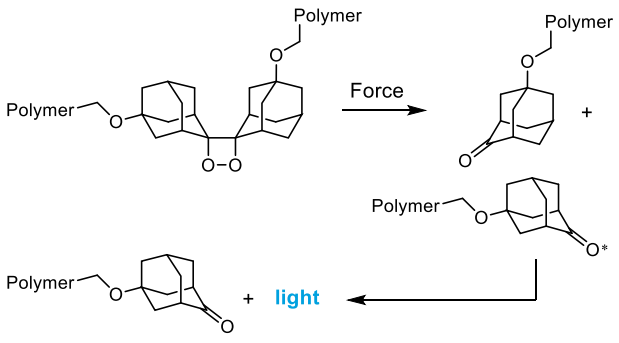

emission precludes any record of the stress history of materials. It is interesting to note that bis(adamantyl)-1,2-dioxetane remains the only reported chemiluminescent mechanophore.

Regiochemical Effects on Mechanophore Activation

Regiochemistry has been implicated as a critical structural parameter that influences mechanochemical reactivity. In 2016, Moore and coworkers demonstrated the regioisomer-specific mechanochromism of naphthopyran, which undergoes a 6π electrocyclic ring-opening reaction under force to generate a yellow merocyanine dye (**Figure 1.2a**).[20] Three naphthopyran regioisomers were prepared, each having a different polymer attachment point on the naphthalene ring. Remarkably, only the naphthopyran molecule substituted at the 5-position exhibited mechanochromic behavior in crosslinked polydimethylsiloxane (PDMS) elastomers under tension. This trend was also supported by density functional theory (DFT) calculations. The mechanochemical reactivity of naphthopyran substituted at the 5-position was attributed to more efficient chemomechanical coupling due to better alignment of the C–O pyran bond with the direction of external force applied along the reaction coordinate. The angle between the C–O pyran bond and the external force vector at maximum extension was calculated to be a relatively narrow 31°, while the same angle was significantly wider for the other two

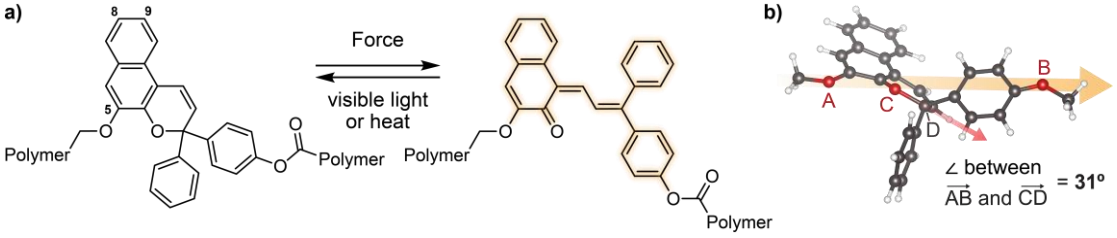

Figure 1.2. a) The naphthopyran regioisomer substituted at the 5-position undergoes a mechanically-facilitated 6π electrocyclic ring-opening reaction in polymeric materials to produce a colored merocyanine dye, while regioisomers with polymers attached at the 8- and 9- position are mechanochemically inert. b) Regioisomer-specific mechanochromism is attributed to better alignment of the force vector with the C–O pyran bond along the reaction coordinate. Adapted with permission.[20] Copyright 2016, American Chemical Society.

unreactive naphthopyran regioisomers (**Figure 1.2b**). It was proposed that mechanical activation of a specific covalent bond is achieved only when it is sufficiently aligned with the force vector, introducing a useful conceptual framework for the design of new mechanophores.

Another important class of mechanochemical transformations are retro-[4+2] cycloaddition reactions, which have been demonstrated for anthracene–maleimide,[38–40] anthracene–triazolinedione,[16] furan–acetylene,[41] and furan–maleimide[42–45] Diels–Alder adducts. The geometrical analysis used for naphthopyran was extended to furan–maleimide adducts in a key paper by Stevenson and De Bo in 2017, which further elucidated the effects of regiochemistry and stereochemistry on mechanochemical reactivity (**Figure 1.3**).[45] Four different isomers, constructed with an *endo* or *exo* configuration and *proximal* or *distal* pulling geometry, were incorporated into PMA polymer chains and their mechanochemical activity was investigated in solution using ultrasonication. In contrast to

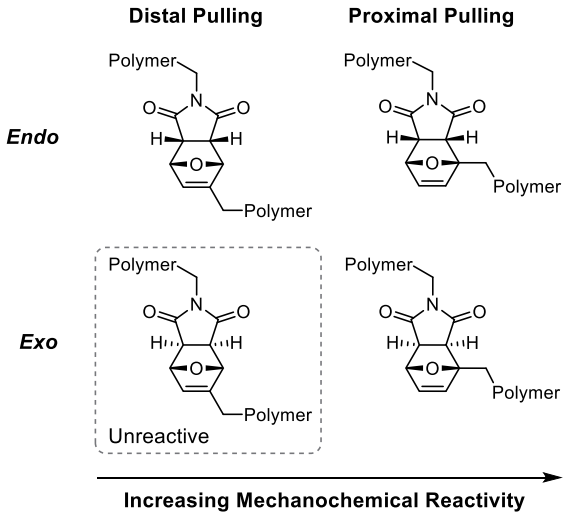

Figure 1.3. Furan–maleimide adducts with an *endo* or *exo* configuration and *distal* or *proximal* polymer attachment geometry display different rates of mechanochemical activation using ultrasound. In contrast to the thermal reactivity, the regiochemistry of polymer attachment critically influences mechanochemical activity. The *distal-exo* adduct is mechanochemically inert due to poor alignment of the scissile bonds with the direction of applied force.

thermal activation in which *endo* and *exo* stereochemistry primarily dictates the relative reactivity, the regiochemistry of polymer attachment to the furan–maleimide adducts was determined to be crucial to the mechanochemical activity. Adducts with *endo* and *exo* stereochemistry bearing a pulling position α (*proximal*) to the diene/maleimide junction reacted faster than the *distal-endo* adduct with one of the polymer chains attached at the β position. Interestingly, the *distal-exo* adduct was mechanochemically unreactive due to weak chemomechanical coupling, which arises from poor geometrical alignment between the scissile bonds and the external force vector.

Mechanochemically Gated Photoswitching

The mechanochromic mechanophores presented previously undergo force-induced covalent bond transformations that lead directly to a visible color change or chemiluminescence, which reports on critical stress and/or strain in materials and signals potential damage caused by polymer chain scission. Despite their utility, mechanochromic transformations are often transient, which limits some applications. For example, the ring-opening reactions of spiropyran and naphthopyran are reversible under visible light; radical-type mechanophores undergo radical recombination; and the oxidative instability of polyacetylene leads to degradation. The development of alternative strategies for visible stress sensing in which mechanical activation is decoupled from the visible response would allow the mechanical history of a material to be more permanently preserved for future detection.

Chemical reactivity can be gated in certain systems, wherein desired chemical changes occur only after specific regulating events. In 2016, Craig and Boulatov reported the mechanically gated reaction of a molecule containing two distinct mechanochemically active groups that underwent sequential activation in response to mechanical force.[46] In this example, activation of the second mechanophore unit was gated by the first. The gating concept is conventionally applied to photoswitching reactions, where light either triggers a chemical change to reveal a new structure with unique reactivity, or a chemical reaction generates a photochemically active motif. Otsuka and coworkers have elegantly expanded the former concept by establishing the photochemical modulation of thermally[47] and mechanochemically induced polymer chain scission.[48]

A notable early example of photogated reactivity was reported by Branda and coworkers in which the photoactivation of a diarylethene (DAE) molecular switch regulated a retro-Diels–Alder reaction for light-triggered small molecule release.[49] DAE photoswitches undergo 6π electrocyclic ring-closing reactions under UV irradiation to generate intensely colored conjugated species, while the colorless ring-opened form is regenerated using visible light. The authors leveraged the reorganization of π bonds that accompanies the electrocyclic ring-closing reaction of DAEs to photochemically lock a reversible dithienylfulvene–dicyanofumarate Diels–Alder adduct in a thermally stable state (**Scheme 1.4**). Upon irradiation of the ring-closed DAE photoswitch with visible light, the two exocyclic double bonds isomerized to regenerate the dithienylethene architecture, facilitating the retro-Diels–Alder reaction that proceeded at room temperature to release the dienophile.

Scheme 1.4. Isomerization of π bonds upon photoirradiation of a thermally locked, ring-closed DAE photoswitch with visible light enables a retro-[4+2] cycloaddition reaction to release the dicyanofumarate dienophile.

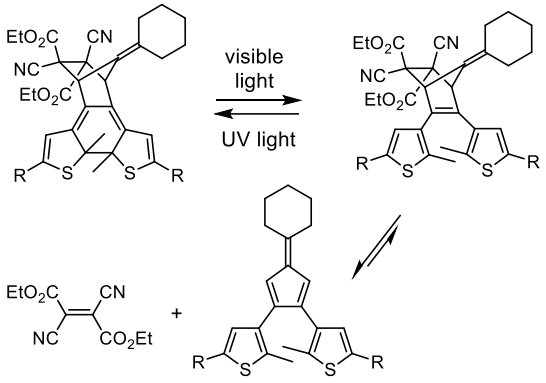

Inspired by Branda's work, we recently set out to design a system using the gating concept to mechan ically regulate the formation of a photochromic switch in polymers.[50] Materials with mechanochemically gated photoswitching capabilities are promising for applications in stress sensing, enabling the mechanical history of a material to be recorded and then read on-demand using light. In addition to stress sensing, we envisioned that the spatial control provided by mechanochemical activation would make this concept useful for lithographic and information storage applications, where patterns written by mechanical force could be visualized under UV light and subsequently erased with visible light.

Our strategy for achieving mechanochemically gated photoswitching is illustrated in **Scheme 1.5**. We designed a cyclopentadiene–maleimide Diels–Alder adduct (**1.1**) that was anticipated to generate the dithienylethene photoswitch **DAE$_{open}$** via a mechanochemical retro-[4+2] cycloaddition reaction. Following mechanical activation of **1.1**, **DAE$_{open}$** would reversibly photoisomerize between the colorless ring-opened and colored ring-closed states upon irradiation with UV and visible light. Importantly, the

Scheme 1.5. Mechanochemically gated photoswitching. Mechanical activation of a polymer chain-centered cyclopentadiene–maleimide mechanophore (**1.1**) generates a diarylethene photoswitch (**DAE$_{open}$**), which is converted to the colored ring-closed isomer (**DAE$_{closed}$**) under UV light. No photochromic transformation occurs in the absence of mechanical force. Adapted with permission.[50] Copyright 2018, American Chemical Society.

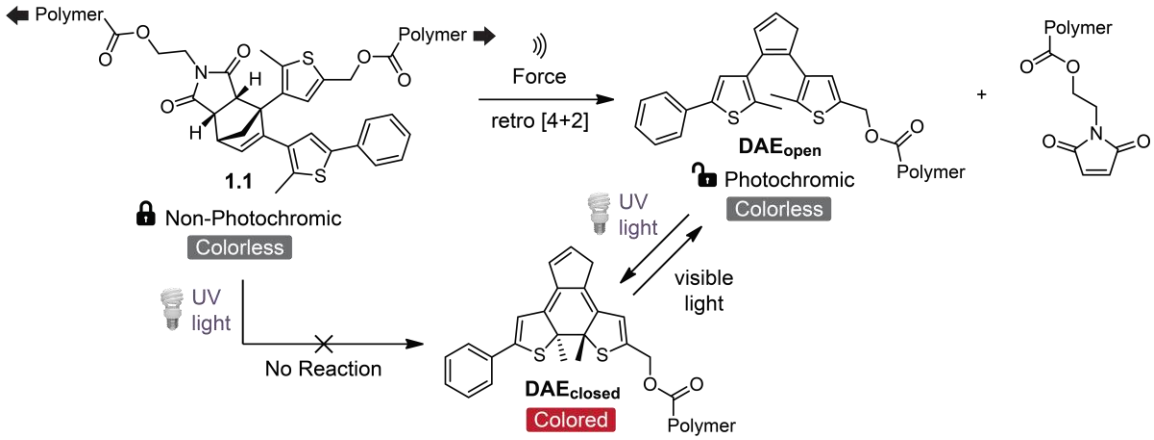

Diels–Alder adduct is photochemically inert because it does not possess the 6π electronic framework necessary for electrocyclization, so no photoswitching reaction should occur in the absence of mechanical force. Moreover, cyclopentadiene–maleimide adducts are known to possess high thermal stability,[51] suggesting that the transformation would be selective toward mechanical activation.

To initially test our hypothesis, we performed DFT calculations using the Constrained Geometries simulate External Force (CoGEF) method,[52,53] which qualitatively predicted the desired retro-[4+2] cycloaddition reaction upon molecular elongation. Encouraged by this result, we set out to synthesize a polymer containing the cyclopentadiene–maleimide Diels–Alder adduct in order to investigate its mechanochemical behavior experimentally (**Scheme 1.6**). Dithienylethene **1.2** was prepared via an acylation reaction between 2-chloro-5-methylthiophene and glutaryl dichloride, followed by a McMurry reaction to form the annulated product, and finally Suzuki-Miyaura coupling to install a single phenyl substituent.[54,55] The phenyl substituent

Scheme 1.6. Synthesis of poly(methyl acrylate) polymer **1.1** incorporating a chain-centered cyclopentadiene–maleimide mechanophore for mechanochemically gated photoswitching. Adapted with permission.[50] Copyright 2018, American Chemical Society.

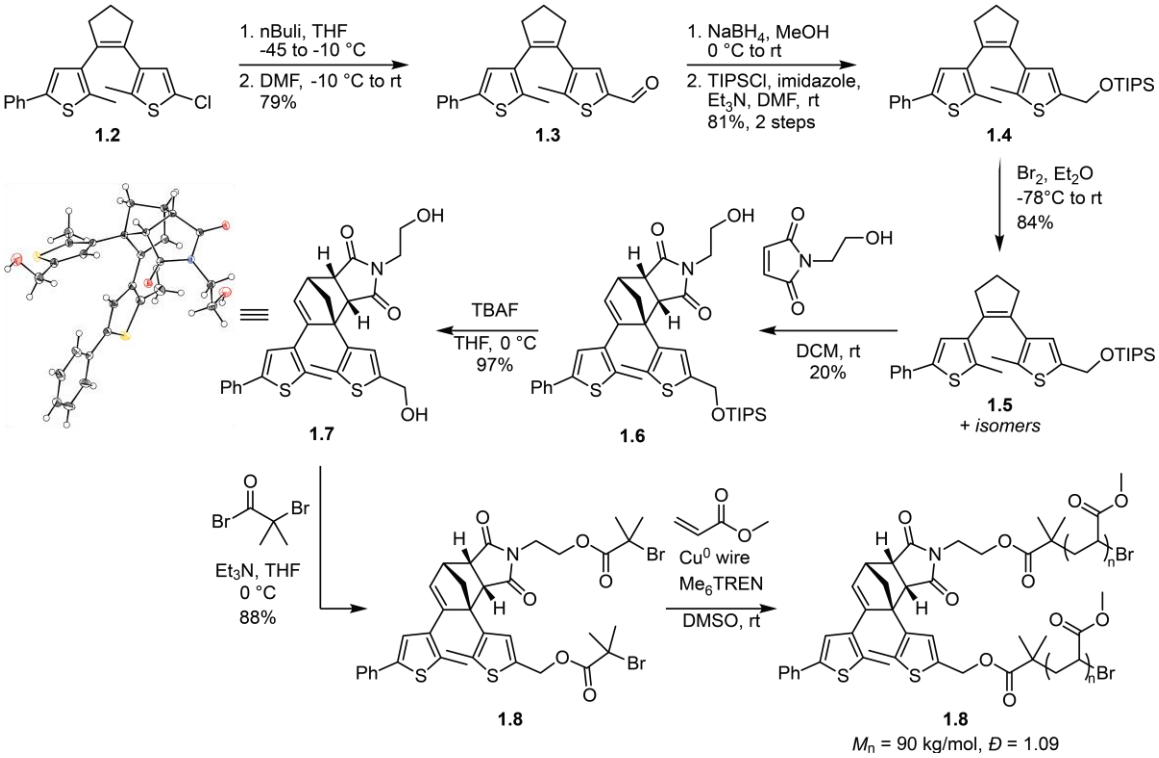

was included to extend the conjugation and shift the absorption of the ring-closed DAE compound to longer visible wavelengths. Formylation of the chloro-substituted DAE afforded aldehyde **1.3**, which was reduced to the alcohol and protected to generate **1.4**. Oxidation of the cyclopentene to a cyclopentadiene was facilitated by bromine, resulting in a mixture of three different cyclopentadiene tautomers. Reacting this mixture with N-(2-hydroxyethyl)maleimide afforded a mixture of Diels-Alder adducts which were separated chromatographically. Based on the analysis by De Bo on the regio- and stereochemical effects on the mechanochemical activity of furan–maleimide adducts,[45] we focused our investigation on the *endo* cyclopentadiene–maleimide adduct with a *proximal* pulling geometry. Removal of the TIPS protecting group with TBAF afforded dihydroxy compound **1.7**, which was unambiguously characterized by single crystal X-ray diffraction.

Finally, installation of α-bromoisobutryl esters provided **1.8**, which was used as a difunctional initiator for the controlled radical polymerization of methyl acrylate using the Cu/Me_6TREN catalyst system in DMSO to afford chain-centered PMA polymer **1.1** with a number average molecular weight of 90 kg/mol and a dispersity of 1.09.

Pulsed ultrasonication was used to evaluate the mechanochemical activity of polymer **1.1** incorporating the chain-centered cyclopentadiene–maleimide adduct. The molecular weight of the polymer steadily decreased with increasing sonication time, as characterized by gel permeation chromatography (GPC) with refractive index and multi-angle laser light scattering detectors. Attenuation of the original polymer peak and formation of a new peak at approximately one-half the original molecular weight was observed, which is characteristic of a process involving mid-chain scission. Remarkably, photoirradiation of the sonicated samples with UV light immediately prior to analysis by GPC revealed a new elution peak measured using a UV-vis absorption detector monitoring at 460–550 nm. The retention time of this new peak matched the low molecular weight fragment peak in the refractive index traces, indicating that a photochromic moiety covalently bound to the polymer was generated during ultrasonication.

UV-vis absorption spectroscopy was performed to further probe the photochemical changes that accompanied ultrasound-induced mechanical activation of polymer **1.1** (**Figure 1.4**). Over the course of 90 minutes of sonication, the solution remained colorless and displayed changes in absorption only at wavelengths below approximately 350 nm. Irradiation of the sonicated polymer solution with UV light (λ = 311 nm), however,

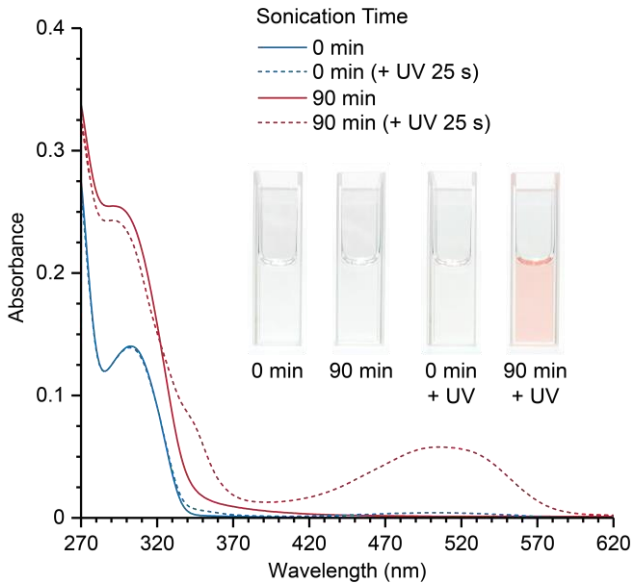

Figure 1.4. UV-vis absorption spectra of **1.1** before and after ultrasonication for 90 min and subsequent UV irradiation. Ultrasound-induced mechanical activation generates a diarylethene (DAE) photoswitch that photoisomerizes under UV light to form the colored ring-closed species. Both mechanical force and UV light are required to cause the color change. Reproduced with permission.[50] Copyright 2018, American Chemical Society.

revealed a new absorption peak centered at 505 nm that increased in optical density with longer ultrasonication times. These spectroscopic changes associated with mechanical activation of **1.1** were reflected in the color of the polymer solution, which changed from colorless to red upon UV irradiation. Importantly, no color change was observed under UV light without prior mechanical activation and the absorption spectra obtained after sonication and subsequent UV irradiation matched that of the isolated ring-closed DAE small molecule. In addition, the photoswitching behavior of polymer **1.1** after mechanical activation was reversible over several cycles of alternating UV and visible light irradiation. Control experiments performed on a polymer containing the cyclopentadiene–maleimide adduct at the chain end, which is not subjected to mechanical force during ultrasonication, did not result in the generation of a photochromic product, indicating that the reactivity observed for **1.1** was mechanochemical in nature.

Conclusions

Mechanochromic reactions are an important class of mechanochemical transformations that enable the direct visualization of stress in polymers. We recently introduced the concept of mechanochemically gated photoswitching, which expands the scope of mechanochromic reactions by decoupling the mechanical activation of a mechanophore from the visible response. We designed a cyclopentadiene–maleimide Diels–Alder adduct that produces a diarylethene (DAE) photoswitch via a retro-[4+2] cycloaddition reaction. Once generated mechanochemically, the photoswitch isomerizes under UV light to form an intensely colored species via a 6π electrocyclic ring-closing reaction that is reversible using visible light. Conceptually, this strategy provides a promising platform for recording the mechanical history of materials, which can be revealed on-demand using light. Ongoing research is exploring new chemistries and the translation of mechanically gated photoswitching from solution to solid state polymeric materials for a range of applications including patterning, information storage, and stress sensing.

References

(1) Beyer, M. K.; Clausen-Schaumann, H. Mechanochemistry: The Mechanical Activation of Covalent Bonds. *Chem. Rev.* **2005**, *105* (8), 2921–2948.

(2) Caruso, M. M.; Davis, D. A.; Shen, Q.; Odom, S. A.; Sottos, N. R.; White, S. R.; Moore, J. S. Mechanically-Induced Chemical Changes in Polymeric Materials. *Chem. Rev.* **2009**, *109* (11), 5755–5798.

(3) Li, J.; Nagamani, C.; Moore, J. S. Polymer Mechanochemistry: From Destructive to Productive. *Acc. Chem. Res.* **2015**, *48* (8), 2181–2190.

(4) Berkowski, K. L.; Potisek, S. L.; Hickenboth, C. R.; Moore, J. S. Ultrasound-Induced Site-Specific Cleavage of Azo-Functionalized Poly(Ethylene Glycol). *Macromolecules* **2005**, *38* (22), 8975–8978.

(5) Piermattei, A.; Karthikeyan, S.; Sijbesma, R. P. Activating Catalysts with Mechanical Force. *Nat. Chem.* **2009**, *1* (2), 133–137.

(6) Diesendruck, C. E.; Peterson, G. I.; Kulik, H. J.; Kaitz, J. A.; Mar, B. D.; May, P. A.; White, S. R.; Martínez, T. J.; Boydston, A. J.; Moore, J. S. Mechanically Triggered Heterolytic Unzipping of a Low-Ceiling-Temperature Polymer. *Nat. Chem.* **2014**, *6* (7), 623–628.

(7) Ramirez, A. L. B.; Kean, Z. S.; Orlicki, J. A.; Champhekar, M.; Elsakr, S. M.; Krause, W. E.; Craig, S. L. Mechanochemical Strengthening of a Synthetic Polymer in Response to Typically Destructive Shear Forces. *Nat. Chem.* **2013**, *5* (9), 757–761.

(8) Wang, J.; Piskun, I.; Craig, S. L. Mechanochemical Strengthening of a Multi-Mechanophore Benzocyclobutene Polymer. *ACS Macro Lett.* **2015**, *4* (8), 834–837.

(9) Robb, M. J.; Moore, J. S. A Retro-Staudinger Cycloaddition: Mechanochemical Cycloelimination of a β-Lactam Mechanophore. *J. Am. Chem. Soc.* **2015**, *137* (34), 10946–10949.

(10) Zhang, H.; Gao, F.; Cao, X.; Li, Y.; Xu, Y.; Weng, W.; Boulatov, R. Mechanochromism and Mechanical-Force-Triggered Cross-Linking from a Single Reactive Moiety Incorporated into Polymer Chains. *Angew. Chem. Int. Ed.* **2016**, *55* (9), 3040–3044.

(11) Chen, Z.; Mercer, J. A. M.; Zhu, X.; Romaniuk, J. A. H.; Pfattner, R.; Cegelski, L.; Martinez, T. J.; Burns, N. Z.; Xia, Y. Mechanochemical Unzipping of Insulating Polyladderene to Semiconducting Polyacetylene. *Science* **2017**, *357* (6350), 475–479.

(12) Chen, Y.; Spiering, A. J. H.; Karthikeyan, S.; Peters, G. W. M.; Meijer, E. W.; Sijbesma, R. P. Mechanically Induced Chemiluminescence from Polymers Incorporating a 1,2-Dioxetane Unit in the Main Chain. *Nat. Chem.* **2012**, *4* (7), 559–562.

(13) Potisek, S. L.; Davis, D. A.; Sottos, N. R.; White, S. R.; Moore, J. S. Mechanophore-Linked Addition Polymers. *J. Am. Chem. Soc.* **2007**, *129* (45), 13808–13809.

(14) Davis, D. A.; Hamilton, A.; Yang, J.; Cremar, L. D.; Van Gough, D.; Potisek, S. L.; Ong, M. T.; Braun, P. V.; Martínez, T. J.; White, S. R.; Moore, J. S.; Sottos, N. R. Force-Induced Activation of Covalent Bonds in Mechanoresponsive Polymeric Materials. *Nature* **2009**, *459* (7243), 68–72.

(15) Verstraeten, F.; Göstl, R.; Sijbesma, R. P. Stress-Induced Colouration and Crosslinking of Polymeric Materials by Mechanochemical Formation of Triphenylimidazolyl Radicals. *Chem. Commun.* **2016**, *52* (55), 8608–8611.

(16) Gossweiler, G. R.; Hewage, G. B.; Soriano, G.; Wang, Q.; Welshofer, G. W.; Zhao, X.; Craig, S. L. Mechanochemical Activation of Covalent Bonds in Polymers with Full and Repeatable Macroscopic Shape Recovery. *ACS Macro Lett.* **2014**, *3* (3), 216–219.

(17) Göstl, R.; Sijbesma, R. P. π-Extended Anthracenes as Sensitive Probes for Mechanical Stress. *Chem. Sci.* **2016**, *7* (1), 370–375.

(18) Imato, K.; Irie, A.; Kosuge, T.; Ohishi, T.; Nishihara, M.; Takahara, A.; Otsuka, H. Mechanophores with a Reversible Radical System and Freezing- Induced Mechanochemistry in Polymer Solutions and Gels*. *Angew. Chem. Int. Ed.* **2015**, 5.

(19) Wang, Z.; Ma, Z.; Wang, Y.; Xu, Z.; Luo, Y.; Wei, Y.; Jia, X. A Novel Mechanochromic and Photochromic Polymer Film: When Rhodamine Joins Polyurethane. *Adv. Mater.* **2015**, *27* (41), 6469–6474.

(20) Robb, M. J.; Kim, T. A.; Halmes, A. J.; White, S. R.; Sottos, N. R.; Moore, J. S. Regioisomer-Specific Mechanochromism of Naphthopyran in Polymeric Materials. *J. Am. Chem. Soc.* **2016**, *138* (38), 12328–12331.

(21) Li, Z.; Toivola, R.; Ding, F.; Yang, J.; Lai, P.-N.; Howie, T.; Georgeson, G.; Jang, S.-H.; Li, X.; Flinn, B. D.; Jen, A. K.-Y. Highly Sensitive Built-In Strain Sensors for Polymer Composites: Fluorescence Turn-On Response through Mechanochemical Activation. *Adv. Mater.* **2016**, *28* (31), 6592–6597.

(22) Wang, T.; Zhang, N.; Dai, J.; Li, Z.; Bai, W.; Bai, R. Novel Reversible Mechanochromic Elastomer with High Sensitivity: Bond Scission and Bending-Induced Multicolor Switching. *ACS Appl. Mater. Interfaces* **2017**, *9* (13), 11874–11881.

(23) Kosuge, T.; Zhu, X.; Lau, V. M.; Aoki, D.; Martinez, T. J.; Moore, J. S.; Otsuka, H. Multicolor Mechanochromism of a Polymer/Silica Composite with Dual Distinct Mechanophores. *J. Am. Chem. Soc.* **2019**, *141* (5), 1898–1902.

(24) Hickenboth, C. R.; Moore, J. S.; White, S. R.; Sottos, N. R.; Baudry, J.; Wilson, S. R. Biasing Reaction Pathways with Mechanical Force. *Nature* **2007**, *446* (7134), 423–427.

(25) Ribas-Arino, J.; Shiga, M.; Marx, D. Unravelling the Mechanism of Force-Induced Ring-Opening of Benzocyclobutenes. *Chem. - Eur. J.* **2009**, *15* (48), 13331–13335.

(26) Wang, J.; Kouznetsova, T. B.; Niu, Z.; Ong, M. T.; Klukovich, H. M.; Rheingold, A. L.; Martinez, T. J.; Craig, S. L. Inducing and Quantifying Forbidden Reactivity with Single-Molecule Polymer Mechanochemistry. *Nat. Chem.* **2015**, *7* (4), 323–327.

(27) Wollenhaupt, M.; Krupička, M.; Marx, D. Should the Woodward-Hoffmann Rules Be Applied to Mechanochemical Reactions? *ChemPhysChem* **2015**, *16* (8), 1593–1597.

(28) Ribas-Arino, J.; Shiga, M.; Marx, D. Understanding Covalent Mechanochemistry. *Angew. Chem. Int. Ed.* **2009**, *48* (23), 4190–4193.

(29) Stauch, T.; Dreuw, A. Quantum Chemical Strain Analysis For Mechanochemical Processes. *Acc. Chem. Res.* **2017**, *50* (4), 1041–1048.

(30) Roessler, A. G.; Zimmerman, P. M. Examining the Ways To Bend and Break Reaction Pathways Using Mechanochemistry. *J. Phys. Chem. C* **2018**, *122* (12), 6996–7004.

(31) Löwe, C.; Weder, C. Oligo(p-Phenylene Vinylene) Excimers as Molecular Probes: Deformation-Induced Color Changes in Photoluminescent Polymer Blends. *Adv. Mater.* **2002**, *14* (22), 1625–1629.

(32) Imato, K.; Kanehara, T.; Ohishi, T.; Nishihara, M.; Yajima, H.; Ito, M.; Takahara, A.; Otsuka, H. Mechanochromic Dynamic Covalent Elastomers: Quantitative Stress Evaluation and Autonomous Recovery. *ACS Macro Lett.* **2015**, *4* (11), 1307–1311.

(33) Sumi, T.; Goseki, R.; Otsuka, H. Tetraarylsuccinonitriles as Mechanochromophores to Generate Highly Stable Luminescent Carbon-Centered Radicals. *Chem. Commun.* **2017**, *53* (87), 11885–11888.

(34) Ishizuki, K.; Oka, H.; Aoki, D.; Goseki, R.; Otsuka, H. Mechanochromic Polymers That Turn Green Upon the Dissociation of Diarylbibenzothiophenonyl: The Missing Piece toward Rainbow Mechanochromism. *Chem. - Eur. J.* **2018**, *24* (13), 3170–3173.

(35) Sakai, H.; Sumi, T.; Aoki, D.; Goseki, R.; Otsuka, H. Thermally Stable Radical-Type Mechanochromic Polymers Based on Difluorenylsuccinonitrile. *ACS Macro Lett.* **2018**, *7* (11), 1359–1363.

(36) Kean, Z. S.; Hawk, J. L.; Lin, S.; Zhao, X.; Sijbesma, R. P.; Craig, S. L. Increasing the Maximum Achievable Strain of a Covalent Polymer Gel Through the Addition of Mechanically Invisible Cross-Links. *Adv. Mater.* **2014**, *26* (34), 6013–6018.

(37) Clough, J. M.; Creton, C.; Craig, S. L.; Sijbesma, R. P. Covalent Bond Scission in the Mullins Effect of a Filled Elastomer: Real-Time Visualization with Mechanoluminescence. *Adv. Funct. Mater.* **2016**, *26* (48), 9063–9074.

(38) Konda, S. S. M.; Brantley, J. N.; Varghese, B. T.; Wiggins, K. M.; Bielawski, C. W.; Makarov, D. E. Molecular Catch Bonds and the Anti-Hammond Effect in Polymer Mechanochemistry. *J. Am. Chem. Soc.* **2013**, *135* (34), 12722–12729.

(39) Church, D. C.; Peterson, G. I.; Boydston, A. J. Comparison of Mechanochemical Chain Scission Rates for Linear versus Three-Arm Star Polymers in Strong Acoustic Fields. *ACS Macro Lett.* **2014**, *3* (7), 648–651.

(40) Li, J.; Shiraki, T.; Hu, B.; Wright, R. A. E.; Zhao, B.; Moore, J. S. Mechanophore Activation at Heterointerfaces. *J. Am. Chem. Soc.* **2014**, *136* (45), 15925–15928.

(41) Larsen, M. B.; Boydston, A. J. "Flex-Activated" Mechanophores: Using Polymer Mechanochemistry To Direct Bond Bending Activation. *J. Am. Chem. Soc.* **2013**, *135* (22), 8189–8192.

(42) Lyu, B.; Cha, W.; Mao, T.; Wu, Y.; Qian, H.; Zhou, Y.; Chen, X.; Zhang, S.; Liu, L.; Yang, G.; Lu, Z.; Zhu, Q.; Ma, H. Surface Confined Retro Diels–Alder Reaction Driven by the Swelling of Weak Polyelectrolytes. *ACS Appl. Mater. Interfaces* **2015**, *7* (11), 6254–6259.

(43) Min, Y.; Huang, S.; Wang, Y.; Zhang, Z.; Du, B.; Zhang, X.; Fan, Z. Sonochemical Transformation of Epoxy–Amine Thermoset into Soluble and Reusable Polymers. *Macromolecules* **2015**, *48* (2), 316–322.

(44) Duan, H.-Y.; Wang, Y.-X.; Wang, L.-J.; Min, Y.-Q.; Zhang, X.-H.; Du, B.-Y. An Investigation of the Selective Chain Scission at Centered Diels–Alder Mechanophore under Ultrasonication. *Macromolecules* **2017**, *50* (4), 1353–1361.

(45) Stevenson, R.; De Bo, G. Controlling Reactivity by Geometry in Retro-Diels–Alder Reactions under Tension. *J. Am. Chem. Soc.* **2017**, *139* (46), 16768–16771.

(46) Wang, J.; Kouznetsova, T. B.; Boulatov, R.; Craig, S. L. Mechanical Gating of a Mechanochemical Reaction Cascade. *Nat. Commun.* **2016**, *7* (1), 13433.

(47) Kida, J.; Imato, K.; Goseki, R.; Morimoto, M.; Otsuka, H. Photoregulation of Retro-Diels–Alder Reaction at the Center of Polymer Chains. *Chem. Lett.* **2017**, *46* (7), 992–994.

(48) Kida, J.; Imato, K.; Goseki, R.; Aoki, D.; Morimoto, M.; Otsuka, H. The Photoregulation of a Mechanochemical Polymer Scission. *Nat. Commun.* **2018**, *9* (1), 3504.

(49) Lemieux, V.; Gauthier, S.; Branda, N. R. Selective and Sequential Photorelease Using Molecular Switches. *Angew. Chem. Int. Ed.* **2006**, *45* (41), 6820–6824.

(50) Hu, X.; McFadden, M. E.; Barber, R. W.; Robb, M. J. Mechanochemical Regulation of a Photochemical Reaction. *J. Am. Chem. Soc.* **2018**, *140* (43), 14073–14077.

(51) Harvey, S. C. Maleimide as a Dienophile. *J. Am. Chem. Soc.* **1949**, *71* (3), 1121–1122.

(52) Beyer, M. K. The Mechanical Strength of a Covalent Bond Calculated by Density Functional Theory. *J. Chem. Phys.* **2000**, *112* (17), 7307–7312.

(53) Kryger, M. J.; Munaretto, A. M.; Moore, J. S. Structure–Mechanochemical Activity Relationships for Cyclobutane Mechanophores. *J. Am. Chem. Soc.* **2011**, *133* (46), 18992–18998.

(54) Lucas, L. N.; van Esch, J.; Kellogg, R. M.; Feringa, B. L. A New Class of Photochromic 1,2-Diarylethenes; Synthesis and Switching Properties of Bis(3-Thienyl)Cyclopentenes. *Chem. Commun.* **1998**, No. 21, 2313–2314.

(55) Kobatake, S.; Terakawa, Y. Acid-Induced Photochromic System Switching of Diarylethene Derivatives between P- and T-Types. *Chem. Commun.* **2007**, No. 17, 1698.

Chapter 2

A Modular Approach to Mechanically Gated Photoswitching with Color-Tunable Force Probes

Adapted with permission from Barber, R. W. and Robb, M. J.

Chem. Sci. **2021**, *12*, 11703–11709.

Copyright 2021, Royal Society of Chemistry

Abstract

Molecular force probes conveniently report on mechanical stress and/or strain in polymers through straightforward visual cues. Unlike conventional mechanochromic mechanophores, the mechanically gated photoswitching strategy decouples mechanochemical activation from the ultimate chromogenic response, enabling the mechanical history of a material to be recorded and read on-demand using light. Here we report a completely redesigned, highly modular mechanophore platform for mechanically gated photoswitching that offers a robust, accessible synthesis and late-stage diversification through Pd-catalyzed cross-coupling reactions to precisely tune the photophysical properties of the masked diarylethene (DAE) photoswitch. Using solution-phase ultrasonication, the reactivity of a small library of functionally diverse mechanophores is demonstrated to be exceptionally selective, producing a chromogenic response under UV irradiation only after mechanochemical activation, revealing colored DAE isomers with absorption spectra that span the visible region of the electromagnetic spectrum. Notably, mechanically gated photoswitching is successfully translated to solid polymeric materials for the first time, demonstrating the potential of the masked diarylethene mechanophore for a variety of applications in force-responsive polymeric materials.

Introduction

The development of stress-sensitive molecules called mechanophores has advanced the scope and functionality of stimuli-responsive polymers.[1,2] Mechanical stress typically leads to nonspecific homolytic scission of polymer chains; however, mechanophores covalently incorporated into polymers harness these normally destructive forces to effect productive chemical transformations.[3] Mechanical force is both ubiquitous and straightforward to apply

using a range of different methods that provide temporal and spatial control,[4–9] making it an appealing stimulus for responsive materials. A wide variety of mechanophores have been developed that produce functional changes in polymers subjected to mechanical force including catalyst activation,[10,11] conductivity switching,[12–14] small molecule release,[15–17] fluorescence changes,[18–21] and chemiluminescence,[22] among others. Mechanophores that generate a change in color are particularly useful due to their ability to act as molecular force beacons, providing straightforward visual identification of the locations of stress and/or strain in polymeric materials.[23] Nevertheless, the reversibility of typical mechanochromic mechanophores like spiropyran,[6] naphthopyran,[24] rhodamine,[25] and diarylbibenzofuranone,[26] for example, limits the mechanical history of a material from being recorded for future detection.[27] Moreover, many mechanochromic mechanophores also lack mechanochemical specificity, as the same reactions that produce the chromogenic response can be promoted by alternative stimuli such as heat, light, or chemical reagents in the absence of mechanical force.[6,24,25,28]

Inspired by the work of Craig and Boulatov on mechanical gating,[29] our group introduced the concept of mechanically gated photoswitching to address, in part, some of the limitations of mechanochromic mechanophores in stress reporting materials.[30] In our original design, mechanical force induces the formal retro-[4+2] cycloaddition reaction of a cyclopentadiene–maleimide Diels–Alder adduct to reveal a diarylethene (DAE) photoswitch, which is subsequently transformed to the conjugated colored isomer under UV light via a 6π electrocyclic ring-closing reaction (**Scheme 2.1a**). In this case, color generation only occurs under UV irradiation if mechanical force has first unmasked the DAE photoswitch, and thus the photochemical ring-closing reaction is gated by the mechanochemical retro-[4+2]

cycloaddition reaction. An important feature of this general molecular design strategy is that mechanochemical activation of the mechanophore is decoupled from the ultimate functional response of the masked intermediate. In principle, this approach enables independent control over each reaction through structural variation, imparting a high degree of modularity to the system. Additionally, the DAE photoswitch generates color reversibly once unmasked by mechanical force, generally with excellent fatigue resistance.[31] While the ring-closed isomer reverts to its colorless form under visible light, irradiation with UV light regenerates the colored isomer and the process can be repeated over many cycles, ensuring that evidence of mechanical activation is preserved.[30]

Despite the promising molecular design strategy, our initial mechanophore is hampered by an inefficient and onerous synthesis and a lack of chemical modularity, which restrict its application and further development. Moreover, unresolved issues of selectivity that manifest as slight coloration under UV light prior to mechanical activation[30] and unsuccessful

Scheme 2.1. Molecular design strategies for mechanically gated photoswitching.

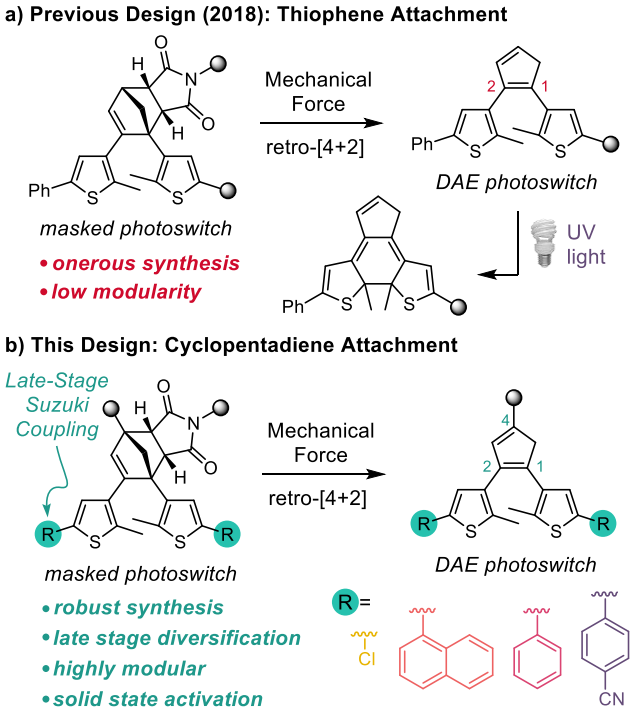

attempts to realize mechanically gated photoswitching in solid polymeric materials have prompted us to completely redesign the mechanophore. Here we present a second-generation platform for mechanically gated photoswitching that relies on a robust synthesis and, critically, enables late-stage diversification to provide a library of color-tunable, masked DAE mechanophores (**Scheme 2.1b**). The reactivity of the mechanophores is demonstrated to be incredibly selective, with no detectable coloration under UV light prior to mechanical activation. Notably, mechanically gated photoswitching is also successfully translated to solid polymeric materials, opening the door to promising potential applications in stress sensing, encryption, and patterning.

Results and Discussion

In our original synthesis of the masked DAE mechanophore, a key step involved the Diels–Alder reaction between a maleimide dienophile and an asymmetric 1,2-disubstituted cyclopentadiene that exists as a mixture of three inseparable tautomers. The reaction produces six constitutional isomers from which the desired Diels–Alder adduct, with *endo* stereochemistry and polymer attachment located on one of the thiophene rings *proximal* to the cyclopentadiene–maleimide junction, was isolated in just 20% yield (see **Scheme 2.1a**).[30] This particular isomer was targeted on the basis of investigations by Stevenson and De Bo on analogous furan–maleimide Diels–Alder adducts that demonstrated the greatest mechanochemical activity for this combination of regiochemistry and stereochemistry.[32] Furthermore, separation of the target cyclopentadiene–maleimide Diels–Alder adduct was only achieved using supercritical fluid chromatography, which limits the accessibility of the chemistry. Finally, the lack of modularity inherent to the original synthesis restricts the ease

with which the mechanochemical properties of the mechanophore and the photochemical properties of the masked DAE photoswitch are modified.

We hypothesized that relocating the polymer attachment position from one of the thiophene substituents to the 4- position of the cyclopentadiene ring would not only enable access to a Diels–Alder adduct with the desired *proximal* regiochemistry, but the increased symmetry of the 1,2,4-trisubstitution pattern would obviate the synthetic challenges encountered previously (see **Scheme 2.1b**). Trisubstituted cyclopentadienes exist preferentially as the two tautomers with maximal substitution of the double bonds;[33] in this case, at the 1- and 3-positions. If the identity of the thienyl substituents at the 1- and 2-positions of the cyclopentadiene is the same, the two tautomers are identical. Thus, reaction with the maleimide dienophile is expected to produce only two Diels–Alder adducts possessing either *endo* or *exo* stereochemistry, the distribution of which can be controlled by varying the reaction conditions. Moreover, substitution of the thiophene rings with chlorine at the 5-positions would provide functional handles for substrate diversification by Pd-catalyzed cross-coupling reactions later in the synthesis, allowing the photophysical properties of the photoswitch to be conveniently modulated. The predisposition of this structural design toward mechanochemical transformation was validated with density functional theory (DFT) calc ulations using the constrained geometries simulate external force (CoGEF) method,[34,35] which predict the desired formal retro-[4+2] cycloaddition

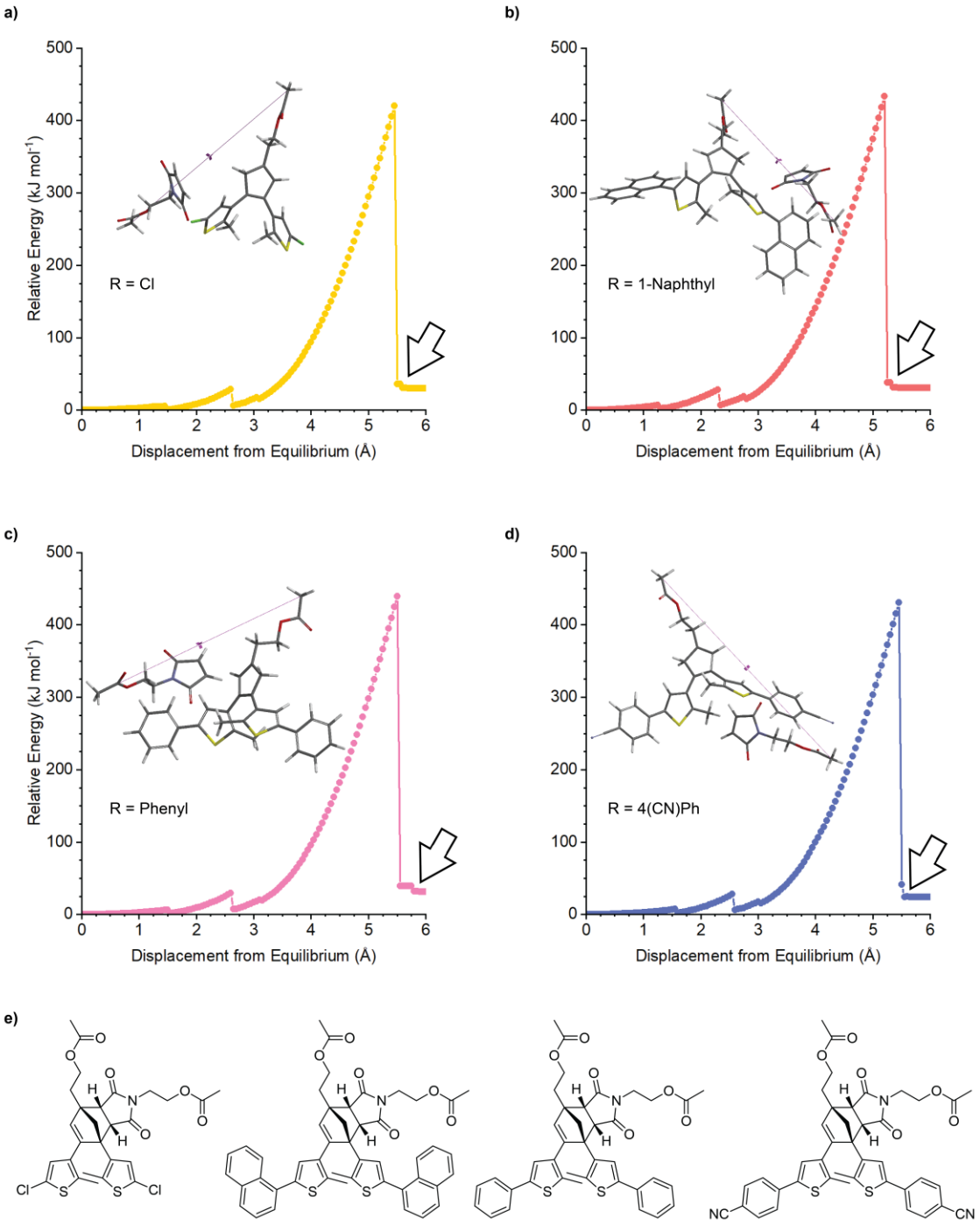

Figure 2.1. DFT calculations using the constrained geometries simulate external force (CoGEF) method at the B3LYP/6-31G* level of theory for (a) chloro-substituted, (b) naphthyl-substituted, (c) phenyl-substituted, and (d) 4-cyanophenyl-substituted cyclopentadiene–maleimide mechanophores. The computed structures of products following the mechanochemical reaction are shown, which correspond to the position on the CoGEF profile indicated by an arrow. e) Structures of truncated models used for CoGEF calculations. The reaction is predicted to occur with a maximum force (F_{max}) of 4.9 nN for all four compounds.

reactions upon molecular elongation to successfully unmask the cyclopentadiene-based DAE photoswitch (**Figure 2.1**). The mechanochemical reaction is predicted to occur wit h a maximum force (F_{max}) of 4.9 nN, which is similar to the predicted F_{max} value of 4.6 nN calculated for the first-generation mechanophore.[30]

With our new molecular design in sight, we set out to synthesize the cyclopentadiene–maleimide Diels–Alder adduct (**Scheme 2.2**). Protection of 4-(2-hydroxyethyl)cyclopentene **2.1** by esterification with benzoyl chloride yielded cyclopentene **2.2**, which was then cleaved by ozonolysis followed by oxidative workup to provide dicarboxylic acid **2.3** in excellent yield. Next, conversion to the diacyl chloride was enacted with oxalyl chloride and catalytic DMF. Reaction times longer than 12 h were necessary to ensure good conversion, as shorter times yielded a significant amount of the corresponding cyclic anhydride. Reaction of the crude diacyl chloride with 2-chloro-5-methyl thiophene and $AlCl_3$ afforded dithienyl diketone **2.4** in 56% yield over the two steps. We note that similar reactions performed on an alternative substrate containing a methylene linker between the benzoate ester and glutaric acid backbone instead of the ethylene tether in **2.3** resulted in the formation of a significant amount of a dihydropyran rearrangement side product. With **2.4** in hand, our attention turned to the

Scheme 2.2. Synthesis of cyclopentadiene–maleimide Diels–Alder adduct diol **2.7.**

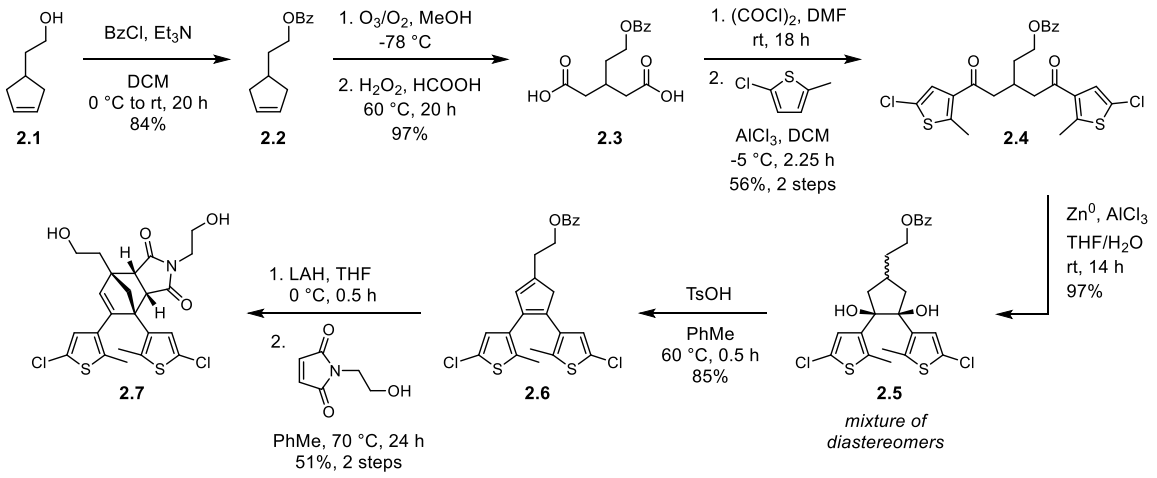

formation of the 5-membered ring that would eventually become the cyclopentadiene core. DAE photoswitches are commonly formed from 1,2-disubstituted cyclopentenes by the reductive coupling of 1,5-diaryl diketones under McMurry conditions.[36] We expected that subjecting **2.4** to these conditions would afford a 1,2,4-trisubstituted cyclopentene that could be oxidized to the corresponding cyclopentadiene (**2.6**) with molecular bromine, as reported by Branda[37] and successfully employed in the synthesis of our first-generation mechanophore.[30] While McMurry coupling afforded the desired cyclopentene in approximately 75% yield, oxidation to the cyclopentadiene proved fruitless with molecular bromine as well as several other oxidants tested under a variety of conditions. Instead, we ultimately explored the use of a reductive pinacol coupling to produce cyclopentanediol **2.5** with a total oxidation state identical to that of the target cyclopentadiene **2.6**, conveniently avoiding additional redox manipulations necessitated by the McMurry sequence. The pinacol coupling proceeded in nearly quantitative conversion to cyclopentanediol **2.5**, which was isolated as a mixture of diastereomers. This mixture was then dehydrated under acidic conditions to generate cyclopentadiene **2.6** in 85% yield. Analysis by ^{1}H NMR spectroscopy confirmed that cyclopentadiene **2.6** exists as a single tautomer, which DFT calculations predict to be the most energetically favorable by nearly 5.6 kcal/mol (**Scheme 2.3**). Removal of the benzoate protecting group with LAH produced the transiently stable alcohol, which was treated in rapid succession with N-(2-hydroxyethyl)maleimide and heated at 70 °C for 24 h to

Scheme 2.3. Structures of cyclopentadiene tautomers and calculated relative ΔG values.

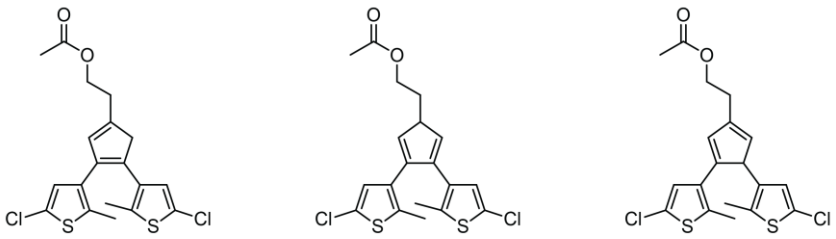

provide *endo* Diels–Alder adduct diol **2.7** in 51% yield over the two steps. Diol **2.7** is readily separated from the *exo* stereoisomer by reverse phase column chromatography, or alternatively, simply by recrystallization. Importantly, refluxing a diester derivative of cyclopentadiene–maleimide adduct **2.7** in toluene for 24 h results in negligible retro-Diels-Alder reaction, confirming the thermal stability of the core structure (**Figure 2.2**).

Diversification of Diels–Alder adduct diol **2.7** into several different masked DAE photoswitches with varied photophysical properties was effected by Suzuki–Miyaura cross-coupling using several commercially available aryl boronic acids to demonstrate the modularity of the scaffold (**Scheme 2.4a**).Despite the generally low reactivity of unactivated aryl chlorides toward oxidative addition, we found that transformation of **2.7** could be successfully executed to produce derivatives **2.8a**–**c** in fair to very good yields with a variety of aryl boronic acids using the Buchwald third generation XPhos precatalyst.[38] The specific aryl boronic acids employed were chosen to provide ring-closed DAE isomers that exhibit absorption maxima across a wide range of the visible spectrum, in addition to the parent 5-chlorothiophene substrate that was expected to produce a yellow- colored ring-closed DAE isomer upon mechanochemical unmasking and subsequent irradiation with UV light.[36,39,40] Next, esterification of each of the four diols with α-bromoisobutyryl bromide afforded **2.9a**–**d**, which were employed as bis-initiators in the controlled radical polymerization of methyl acrylate to yield poly(methyl acrylate) (PMA) polymers centrally functionalized with each Diels–Alder adduct mechanophore. Characterization of polymers **2.10a**–**d** by gel permeation chromatography (GPC) equipped

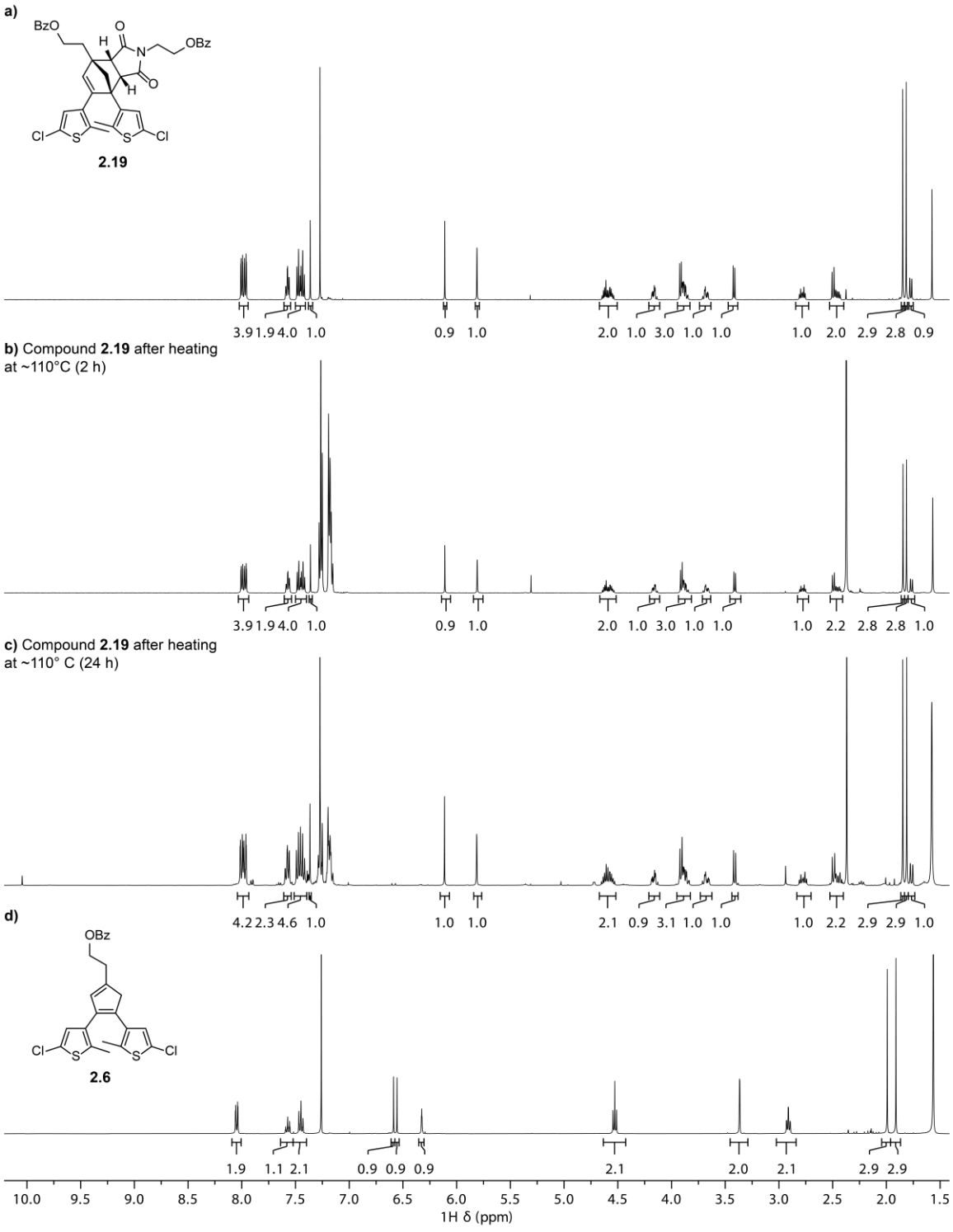

Figure 2.2. ^{1}H NMR (500 MHz, $CDCl_3$) spectra of cyclopentadiene–maleimide Diels–Alder adduct **2.19** (a) before, and after heating in refluxing toluene for (b) 2 h and (c) 24 h, demonstrating the thermal stability of the adduct. (d) The ^{1}H NMR spectrum (400 MHz, $CDCl_3$) of cyclopentadiene **2.6** is included for reference.

Scheme 2.4. a) Synthesis of polymers **2.10a–d** containing a chain-centered mechanophore with varied substitution, and b) unveiling of DAE photoswitches by ultrasound-induced mechanical force and subsequent photoswitching.

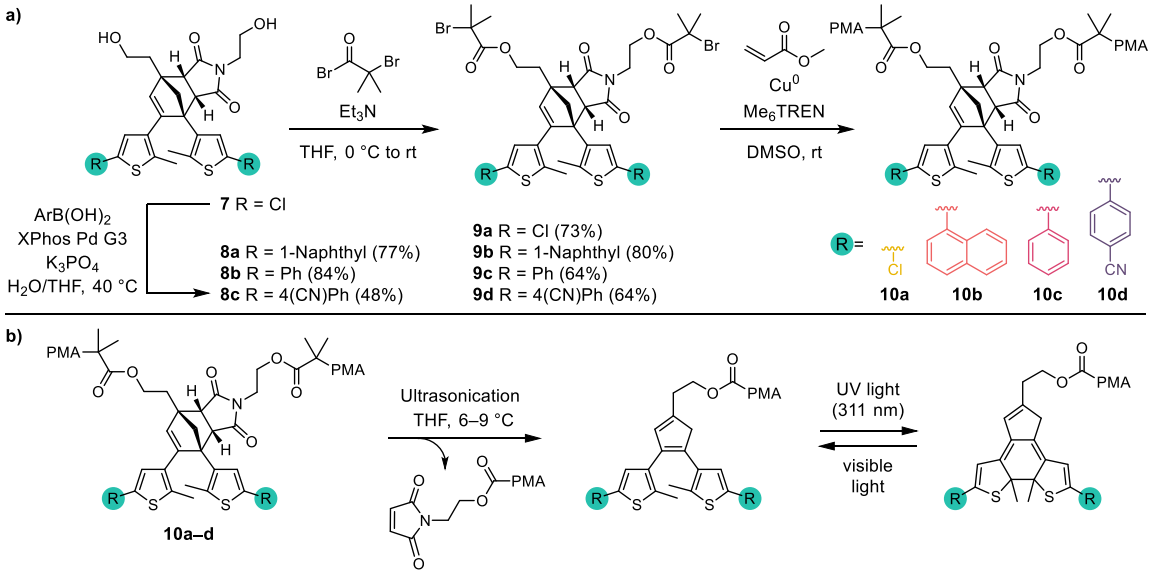

with multi-angle light scattering and refractive index (RI) detectors confirmed that the polymers have similar molecular weight and narrow dispersity, with M_n = 96–112 kg/mol and $Đ$ = 1.05–1.07 (**see experimental details**). Overall, the preparation of chain-centered polymers incorporating a diverse range of functional masked DAE mechanophores requires no more than three steps from diol **2.7**. Late stage mechanophore diversification by Pd-catalyzed cross-coupling reactions, supported by the ready availability of a wide variety of aryl boronic acids, makes **2.7** a highly modular intermediate for the implementation of mechanically gated photoswitching.

The reactivity of the masked DAE mechanophores was initially investigated experimentally by subjecting solutions of each polymer (2 mg/mL in THF) to combinations of pulsed ult rasonication (6–9 °C, 1 s on/2 s off, 11.6 W/cm^2) and UV irradiation as illustrated in **Scheme 2.4b**. Ultrasonication generates mechanical forces on polymers maximized near the chain midpoint where the mechanophores are installed, enabling convenient evaluation of mechanochemical reactivity.[41] The untreated polymer solutions are colorless, and moreover,

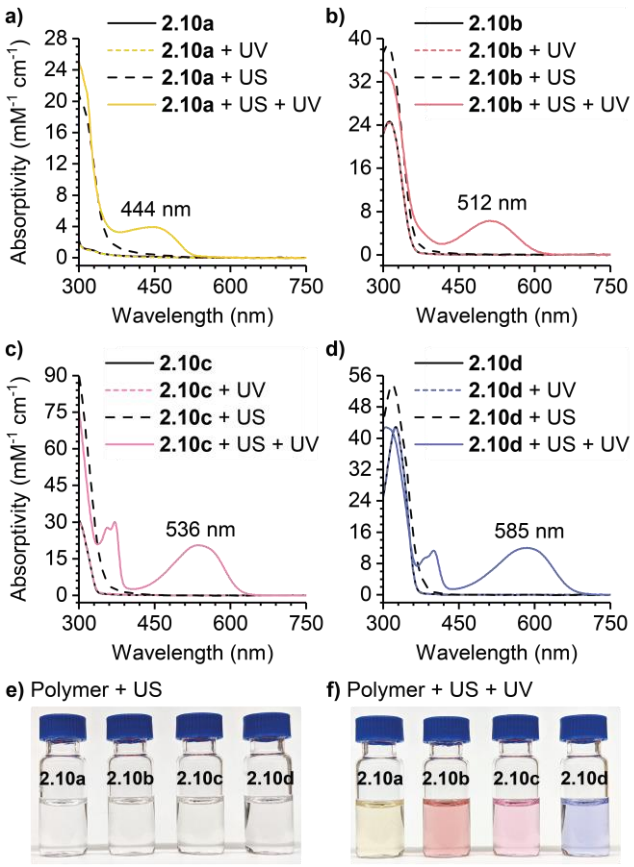

Figure 2.3. Characterization of mechanically gated photoswitching. (a–d) UV-vis absorption spectra of polymers **2.10a–d** (2 mg mL^{-1} in THF) before and after 120 min of ultrasonication (US) and/or irradiation with UV light (311 nm, 60 s). Photographs of the polymer solutions (e) after ultrasonication, and (f) the same solutions after irradiation with UV light (311 nm, 120 s). The solutions of polymers **2.10a** and **2.10b** were concentrated 5x after ultrasonication for the photographs.

completely unresponsive to UV irradiation (311 nm for 60 s) as evidenced by the absence of any perceptible changes in UV-vis absorption after exposure to UV light (**Figure 2.3**). The polymer solutions also remain completely colorless after ultrasonication for 120 min. However, when the polymers previously subjected to ultrasound-induced mechanical activation are irradiated with UV light under the same conditions as above, the solutions become intensely colored with absorption maxima ranging from 444 nm to 585 nm depending on the substitution of the thienyl groups on the cyclopentadiene–maleimide mechanophores.

Monitoring the mechanochemical transformations over the course of each sonication experiment by subjecting the polymer solutions to UV irradiation at various time points reveals a progressive increase in optical density in the visible region with increasing duration of

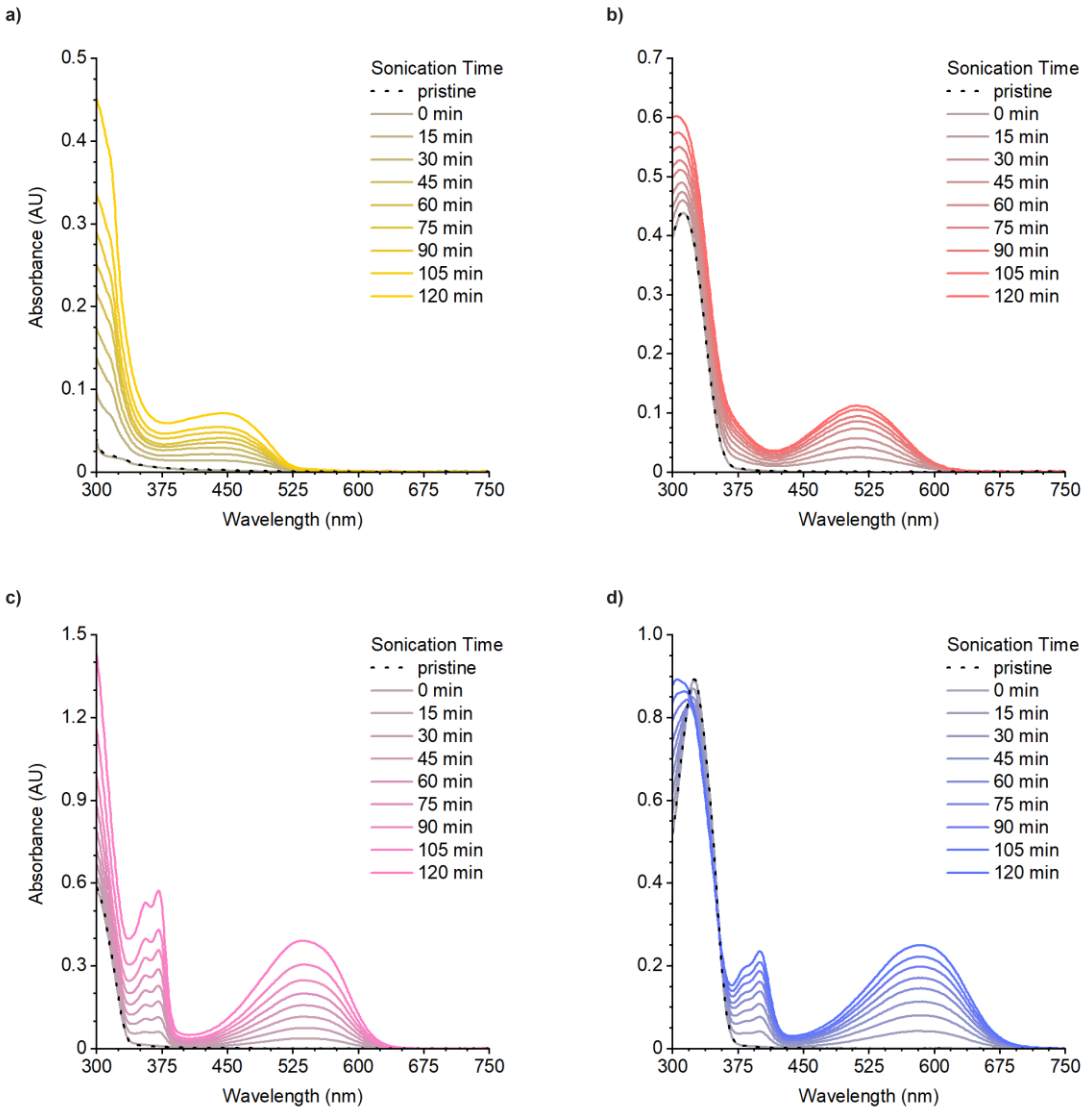

Figure 2.4. UV-vis absorption spectra of (a) **2.10a**, (b) **2.10b**, (c) **2.10c**, and (d) **2.10d** (2 mg/mL in THF) as a function of ultrasonication time and after irradiation with UV light. Spectra of pristine polymers were acquired before UV irradiation or ultrasonication. All other spectra were acquired after the indicated duration of ultrasonication, and after irradiation with a 311 nm UV lamp for 60 s. The increasing absorbance in the visible region of the spectra is indicative of progressively greater mechanophore conversion with increasing sonication time, resulting in increasing concentration of the diarylethene photoswitches.

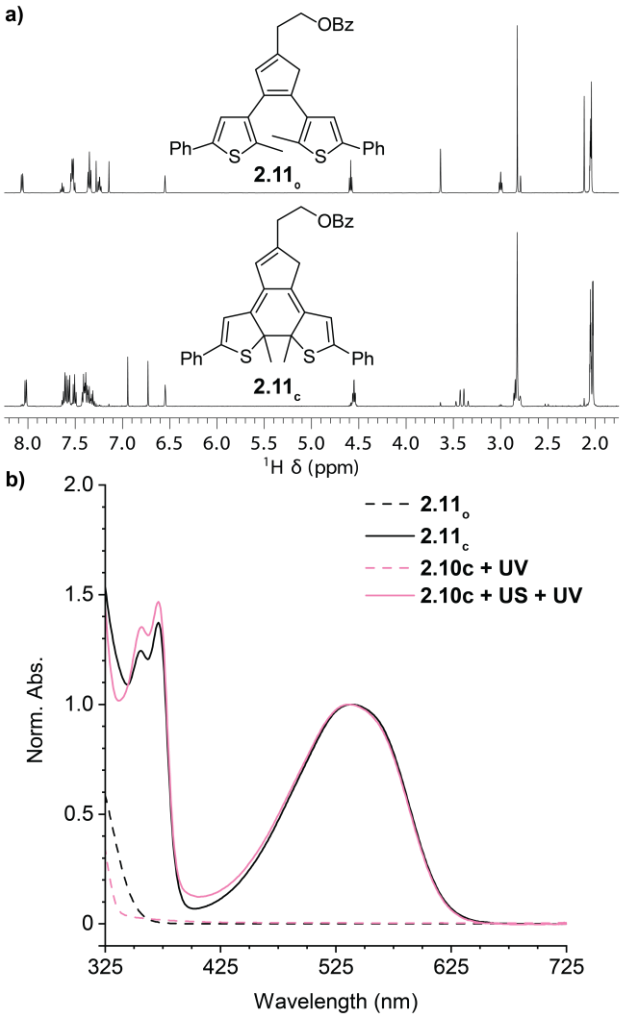

Figure 2.5. (a) Partial ^{1}H NMR spectra (500 MHz, acetone-d_6) of model small molecule **2.11$_o$** (top) and the ring-closed isomer **2.11$_c$** (bottom) generated nearly quantitatively upon irradiation with UV light (311 nm, 60 min). (b) UV-vis absorption spectra of **2.11$_o$** and **2.11$_c$** compared to polymer **2.10c** in THF before and after ultrasonication (US) and irradiation with UV light. The matching absorption spectra indicate that the same ring-closed DAE structure exemplified by small molecule **2.11$_c$** is generated from mechanochemical activation and subsequent UV photoirradiation of polymer **2.10c**.

ultrasonication (**Figure 2.4**). The sequence of mechanical activation followed by UV irradiation is critical for color formation, consistent with the mechanophore design in which the retro-[4+2] cycloaddition reaction of the cyclopentadiene–maleimide Diels–Alder adduct gates the photoinduced 6π electrocyclic ring-closing reaction of the unmasked DAE photoswitch. The results of the solution-phase experiments expose two important points about

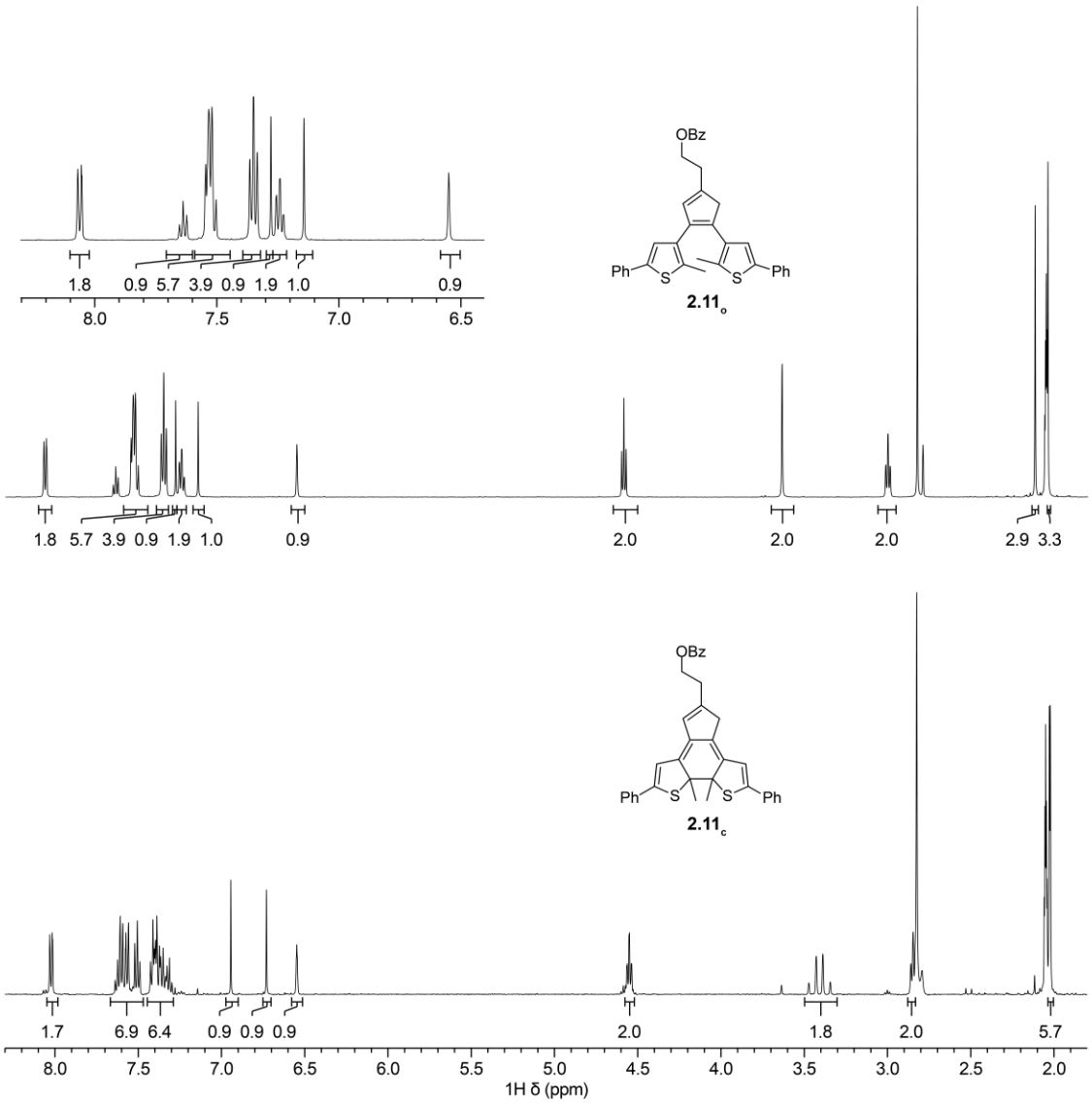

Figure 2.6. ^{1}H NMR spectra (500 MHz, acetone-d$_6$) of **2.11$_o$** (top) and the same sample after irradiation with 311 nm light for 60 min (bottom) displaying nearly complete conversion to **2.11$_c$** (**2.11$_c$**:**2.11$_o$** = 18:1).

the mechanophore design. First, the specificity observed in the reaction sequence as illustrated by the UV-vis absorption spectra acquired after various mechanochemical and photochemical treatments of the polymers demonstrates a clear advance over our prior mechanophore design.[30] Second, the modularity of the masked DAE photoswitch is evident in the range of absorption achieved that spans the visible spectrum, enabled by late-stage functionalization of

the mechanophore and leveraging the extensive structure–property relationships developed for DAE molecules.[31]

A series of control experiments was performed to further characterize the reactivity of the cyclopentadiene–maleimide mechanophore. In order to further support the structural identity of the colored species generated after sequential ultrasonication and UV photoirradiation of the polymers above, we synthesized small molecule model compound **2.11$_o$** to serve as an analog of the photoswitch implicated in the mechanical activation of polymer **2.10c** containing a phenyl-substituted masked DAE mechanophore. Irradiation of model compound **2.11$_o$** in acetone-d_6 with 311 nm light for 60 min produces an intensely purple-colored solution that was analyzed by ^{1}H NMR spectroscopy (**Figure 2.5a**). The ^{1}H NMR spectrum obtained after photoirradiation is consistent with nearly quantitative

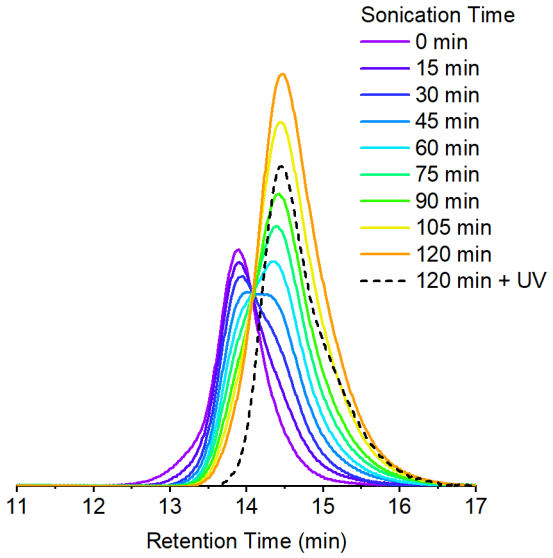

Figure 2.7. GPC traces (RI response) of aliquots of **2.10c** collected over the course of ultrasound-induced mechanical activation demonstrating features characteristic of mid-chain scission. A GPC measurement monitored using a UV-vis detector (491– 581 nm) performed on the sample after 120 min of ultrasonication and UV irradiation (λ = 311 nm, 60 s) reveals a peak with a retention time corresponding to that of the polymer fragments, indicating the formation of a polymer-bound photoswitch upon polymer chain scission.

conversion of **2.11$_o$** to ring-closed isomer **2.11$_c$** (**Figure 2.6**). Critically, the UV-vis absorption spectrum of **2.11$_c$** in THF closely matches the spectrum of polymer **2.10c** obtained after ultrasonication and UV irradiation (**Figure 2.5b**). Furthermore, additional GPC measurements using an in-line UV-vis detector were performed on polymer **2.10c** after being subjected to ultrasonication and UV photoirradiation. A peak monitored at 491–581 nm, encompassing the

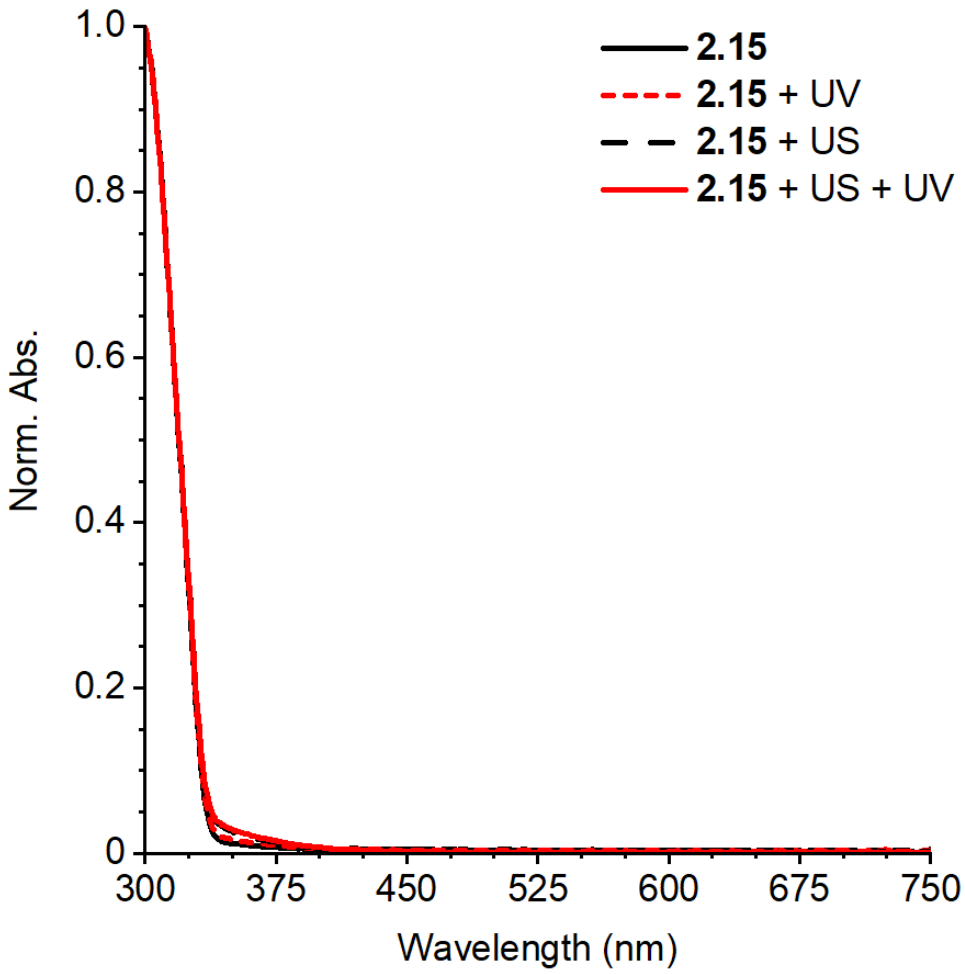

Figure 2.8. UV-vis absorption spectra of chain-end functional control polymer **2.15** (2 mg/mL in THF) before and after being subjected to combinations of ultrasonication (120 min) and UV photoirradiation (λ = 311 nm, 60 s). Negligible changes in the absorption spectra are observed supporting that the activation of polymers **2.10a–d** is mechanochemical in nature.

λ_{max} of the anticipated ring-closed DAE isomer, is observed with a retention time that coincides with the low molecular weight polymer peak in the RI traces, indicating that polymer chain scission is accompanied by the generation of a polymer-bound photoswitch, consistent with the expected reactivity (**Figure 2.7**). Finally, the same sequential ultrasonication and UV irradiation treatment was applied to a control polymer analogous to **2.10c** but containing the Diels–Alder adduct at the end of the polymer chain, which is not subjected to mechanical force during ultrasonication.[3] No change in visible absorption is detected under these conditions (**Figure 2.8**), confirming the mechanical origin of the reactivity observed for polymers **2.10a**–**d** containing a chain-centered mechanophore.

Encouraged by the solution-phase reactivity of the mechanophores, we sought to investigate mechanically gated photoswitching in solid polymeric materials. A PMA network

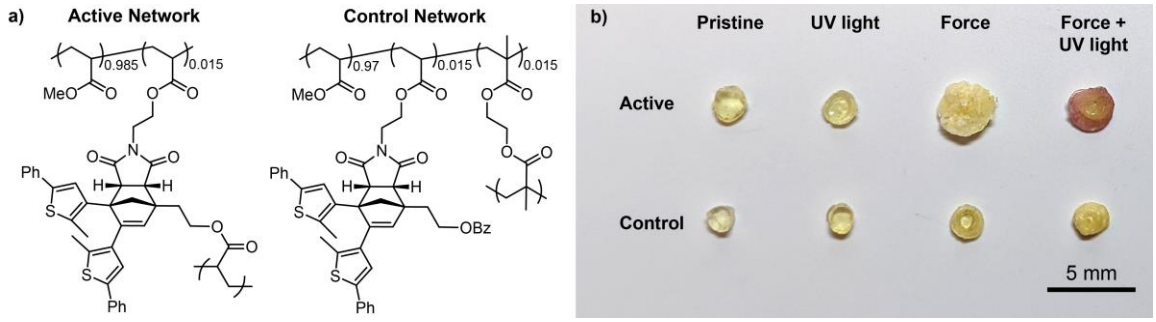

Figure 2.9. (a) Structures of the active and control PMA networks containing 1.5 mol% of a mechanophore crosslinker and pendant group, respectively. The control network was crosslinked with 1.5 mol% of a mechanochemically inactive ethylene glycol dimethacrylate crosslinker. (b) Photographs of the active and control PMA networks before and after being subjected to combinations of mechanical force and UV light irradiation. From left to right: pristine samples, after irradiation with 311 nm light (5 min), after uniaxial compression (10 tons for 5 min), and samples after uniaxial compression (10 tons for 5 min) and subsequent irradiation with 311 nm light (5 min). Color is only produced in the active network following the sequence of compression followed by UV irradiation, indicating that the DAE photoswitch is successfully revealed under mechanical force. The control samples display no change in color in response to any stimuli, indicating that force must be transferred across the cyclopentadiene–maleimide junction to activate the mechanophore. Greater deformation is observed for the active network compared to the control network, suggesting that the mechanochemical sensitivity of the mechanophore crosslinker influences macroscopic fracture behavior.

incorporating 1.5 mol% of a cyclopentadiene–maleimide mechanophore crosslinker analogous to the structure in **2.10c** was synthesized via free radical polymerization. Likewise, a control PMA network was synthesized similarly using 1.5 mol% of a mechanochemically inactive ethylene glycol dimethacrylate crosslinker and 1.5 mol% of a monoacrylate-functionalized mechanophore comonomer (**Figure 2.9a,** see experimental details). Compression of both polymeric materials for 5 min with a hydraulic press followed by irradiation with 311 nm light for 5 min produces a purple color in the active, mechanophore crosslinked material indicating successful generation of the ring- closed DAE photoswitch (**Figure 2.9b**). The photochromic behavior of the mechanically activated material was still evident one week after the original compression experiment (**Figure 2.10**). Consistent with the solution-phase experiments, no color change was observed in the active network upon irradiation with UV light without first applying mechanical force (**Figure 2.9b**). On the other hand, no color was produced by the control network after subjecting it to the same sequence of compression and UV photoirradiation, indicating that transfer of mechanical force across the cyclopentadiene–

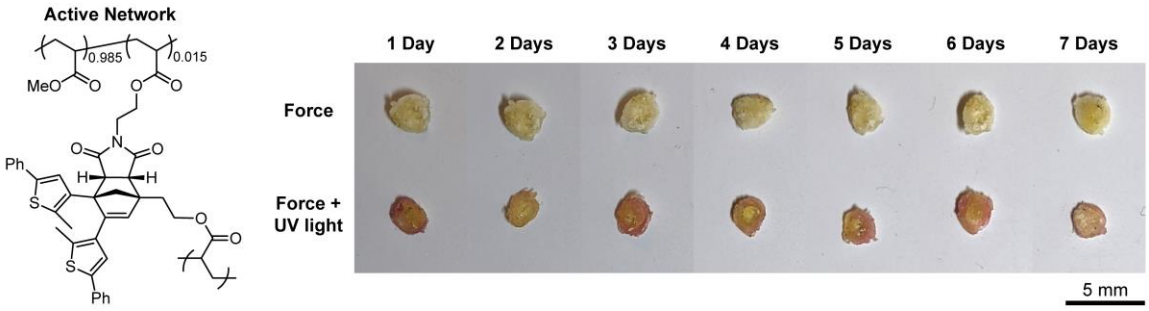

Figure 2.10. Structure of the active PMA network containing 1.5 mol% of a mechanophore crosslinker and photographs of samples of the polymer network after being subjected to combinations of compressive force and UV irradiation. Each sample was subjected to uniaxial compression (10 tons, 5 min) on the same day and subsequently stored in the dark at room temperature under air. The photochromic behavior of the samples was then analyzed on successive days following the initial compression experiment. Top row: a polymer sample subjected to compressive force that was not irradiated with UV light, as a reference. Bottom row: polymer samples irradiated with UV light (311 nm, 5 min) on the indicated day after the initial compression. The photochromic behavior of the mechanically activated material is evident for one week, demonstrating the persistence of the mechanically gated photoswitching response.

maleimide junction of the mechanophore is necessary to induce the retro-[4+2] cycloaddition reaction and reveal the DAE photoswitch.

Conclusions

We have designed a masked diarylethene (DAE) mechanophore for mechanically gated photoswitching that overcomes significant prior limitations and presents a highly modular platform for accessing color-tunable molecular force probes. Mechanical activation of the cyclopentadiene–maleimide Diels–Alder adduct facilitates a formal retro-[4+2] cycloaddition reaction to reveal a latent DAE photoswitch, which is transformed via a 6π electrocyclic ring-closing reaction under UV light to generate an intensely colored isomer. Unlike many conventional mechanochromic mechanophores, the mechanically gated photoswitching strategy enables the mechanical history of a material to be recorded and read on demand using light. Moreover, by decoupling the mechanochemical reaction from the chromogenic response, the design overcomes limitations of mechanochemical specificity encountered by other mechanophores, which in many cases produce the same visual signal upon exposure to alternative stimuli. We present a robust synthetic strategy that enables straightforward access to the cyclopentadiene–maleimide mechanophore, which is diversified via late stage Pd-catalyzed cross-coupling reactions to modulate the photophysical properties of the masked DAE photoswitch. Solution-phase ultrasonication experiments performed on a small library of functionally diverse mechanophores showcase the excellent selectivity of the compounds upon exposure to combinations of mechanical force and UV light. A chromogenic response is only observed upon sequential mechanochemical activation followed by UV photoirradiation, revealing colored DAE isomers with absorption spectra that span the visible region of the electromagnetic spectrum. We also demonstrate mechanically gated

photoswitching in solid polymeric materials for the first time, illustrating the potential of this mechanophore platform for a variety of stress reporting/recording, encryption, and pattering applications.

Experimental Details

General Experimental Details

Reagents from commercial sources were used without further purification unless otherwise stated. Methyl acrylate was passed through a short plug of basic alumina to remove inhibitor immediately prior to use. Copper wire was cleaned prior to use by soaking in 1 M HCl for 15 min, and then rinsed thoroughly with deionized water and dried. Dry solvents were obtained from a Pure Process Technology solvent purification system. All reactions were performed under a N_2 or Ar atmosphere unless specified otherwise. Column chromatography was performed manually using Silicycle SiliaFlash F60 silica gel or on a Biotage Isolera system using SiliCycle SiliaSep HP flash cartridges or Buchi FlashPure C18 30 μm spherical reverse phase cartridges.

NMR spectra were recorded using a 400 MHz Bruker Avance III HD with Prodigy Cryoprobe, a 400 MHz Bruker Avance Neo, a 500 MHz Varian Inova, or a 300 MHz Varian spectrometer. All ^{1}H NMR spectra are reported in δ units, parts per million (ppm), and were measured relative to the signals for residual chloroform (7.26 ppm), acetone (2.05 ppm), or methanol (3.31 ppm) in deuterated solvent. All ^{13}C NMR spectra were measured in deuterated solvents and are reported in ppm relative to the signals for chloroform (77.16 ppm), acetone (29.84 or 206.26 ppm), or methanol (49.00 ppm). Multiplicity and qualifier abbreviations are as follows: s = singlet, d = doublet, t = triplet, q = quartet, quint = quintet, m = multiplet, br = broad, app = apparent.

High resolution mass spectra (HRMS) were obtained from a Waters LCT Premier XE time-of-flight mass spectrometer equipped with an electrospray ionization source (ESI+) or a JEOL JMS-600H magnetic sector spectrometer equipped with a fast atom bombardment (FAB) ionization source.

Analytical gel permeation chromatography (GPC) was performed using an Agilent 1260 series pump equipped with two Agilent PLgel MIXED-B columns (7.5 x 300 mm), an Agilent 1200 series diode array detector, a Wyatt 18-angle DAWN HELEOS light scattering detector, and an Optilab rEX differential refractive index detector. The mobile phase was THF at a flow rate of 1 mL/min. Molecular weights and molecular weight distributions were calculated by light scattering using a dn/dc value of 0.062 mL/g (25 °C) for poly(methyl acrylate).

UV-vis absorption spectra were recorded on a Thermo Scientific Evolution 220 spectrometer.

Ultrasound experiments were performed inside a sound abating enclosure using a Vibra Cell 505 liquid processor equipped with a 0.5-inch diameter solid probe (part #630-0217), sonochemical adapter (part #830-00014), and a Suslick reaction vessel made by the Caltech glass shop (analogous to vessel #830- 00014 from Sonics and Materials). UV irradiation was performed using a Philips PL-S 9W/01/2P UVB bulb with a narrow emission of 305–315 nm and a peak at 311 nm under ambient conditions unless indicated otherwise.

Crosslinked polymer samples with a thickness of approximately 1 mm were cut with a 2 mm hammer-driven hole punch. Compression experiments were performed using a hydraulic press under a force of 10 tons. Photographs were captured using a Google Pixel 5 and corrected for exposure in Adobe Photoshop.

Synthetic Details

Scheme S2.5. Synthesis of mechanophore diol **2.7**

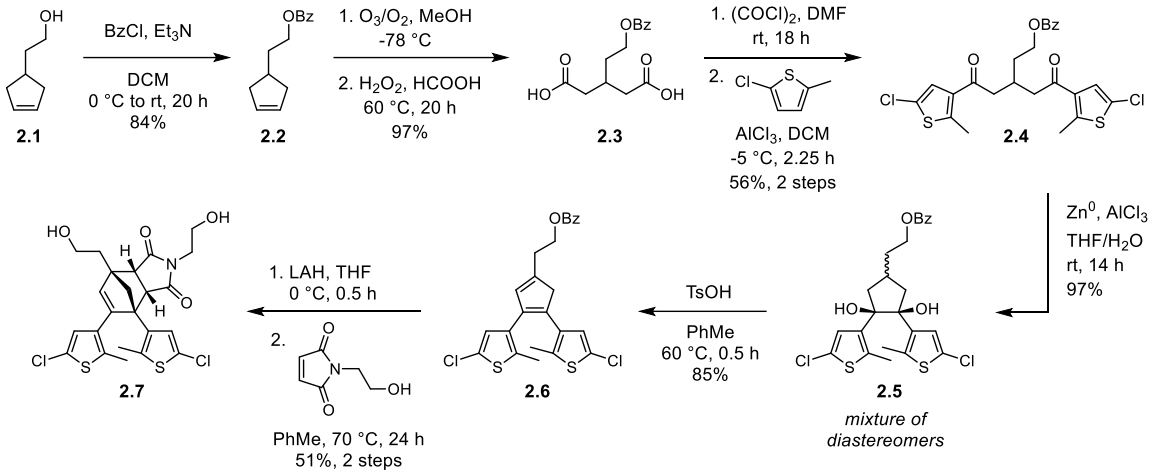

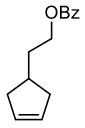

2.2

2-(cyclopent-3-en-1-yl)ethyl benzoate (2.2). A flame-dried round bottom flask equipped with a stir bar was charged with 2-(cyclopent-3-en-1-yl)ethan-1-ol **1**[42] (8.13 g, 72.5 mmol), triethylamine (50.0 mL, 359 mmol), and dry DCM (200 mL). The solution was cooled to 0 °C in an ice/water bath and benzoyl chloride (25.0 mL, 215 mmol) was added slowly with stirring. Immediately after the addition was complete, the reaction was removed from the ice bath and warmed to room temperature over 20 h. The organic layer was washed with saturated $NaHCO_3$ (3 x 100 mL) and once with brine (100 mL). The organics were dried with Na_2SO_4, filtered, and concentrated under vacuum. The crude mixture was purified by silica gel chromatography (0–15% EtOAc/hexanes) to provide the title compound as colorless oil (13.2 g, 84%).

TLC (10% EtOAc/hexanes): R_f = 0.45

^{1}H NMR (500 MHz, $CDCl_3$) δ: 8.20 – 7.90 (m, 2H), 7.61 – 7.52 (m, 1H), 7.49 – 7.39 (m, 2H), 5.69 (s, 2H), 4.36 (t, *J* = 6.7 Hz, 2H), 2.72 – 2.49 (m, 2H), 2.49 – 2.37 (m, 1H), 2.16 – 2.01 (m, 2H), 1.89 (q, *J* = 6.9 Hz, 2H) ppm.

^{13}C{^{1}H} NMR (126 MHz, $CDCl_3$) δ: 166.9, 133.0, 130.6, 130.0, 129.7, 128.5, 64.4, 39.0, 35.3, 34.8 ppm.

HRMS (FAB, *m/z*): calc'd for $[C_{14}H_{17}O_2]^+$ $(M+H)^+$ 217.1223, found 217.1227.

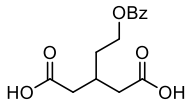

2.3

3-(2-(benzoyloxy)ethyl)pentanedioic acid (2.3). A round bottom flask equipped with a stir bar was charged with **2.2** (1.62 g, 7.49 mmol) and methanol (50 mL). The solution was cooled to −78 °C in a dry ice/acetone bath and a stream of O_2/O_3 was bubbled through the solution until it became blue. To remove excess ozone, O_2 was bubbled through the solution until the blue color disappeared. After warming to room temperature, the solution was diluted with formic acid (50 mL) and concentrated partially under vacuum to remove methanol. This process was repeated 2×, after which the residue was dissolved in formic acid (50 mL) in a round bottom flask equipped with a reflux condenser. Hydrogen peroxide (35 wt% in water, 6.50 mL, 75.6 mmol) was added and the reaction, which was then heated to 60 °C. After 20 h the solution tested negative for peroxides and was cooled to room temperature. The products were extracted into EtOAc (5 x 50 mL), and the combined organics were washed once with brine (50 mL), dried with Na_2SO_4, filtered, and concentrated to provide the title compound as a white solid (2.04 g, 97%).

TLC (5 % MeOH/DCM): R_f = 0.13

^{1}H NMR (400 MHz, CD_3OD) δ: 8.10 – 7.97 (m, 2H), 7.64 – 7.54 (m, 1H), 7.47 (ddt, *J* = 8.0, 6.7, 1.2 Hz, 2H), 4.40 (t, *J* = 6.4 Hz, 2H), 2.65 – 2.39 (m, 5H), 1.90 (app q, *J* = 6.4 Hz, 2H) ppm.

^{13}C{^{1}H} NMR (101 MHz, CD_3OD) δ: 176.1, 168.0, 134.2, 131.5, 130.6, 129.5, 63.9, 39.2, 33.7, 30.6 ppm.

HRMS (FAB, *m/z*): calc'd for $[C_{14}H_{17}O_6]^+$ $(M+H)^+$ 281.1020, found 281.1049.

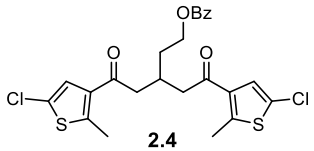

2.4

5-(5-chloro-2-methylthiophen-3-yl)-3-(2-(5-chloro-2-methylthiophen-3-yl)-2-oxoethyl)-5-oxopentyl benzoate (2.4). A flame-dried round bottom flask equipped with a magnetic stir bar was charged with **2.3** (1.72 g, 6.14 mmol). The atmosphere was evacuated and refilled with N_2 3×. Dry DCM (100 mL) was added, followed by dry DMF (10 drops, cat.). Oxalyl chloride (5.30 mL, 61.8 mmol) was added slowly, after which the reaction stirred at room temperature. After 15 h, it was concentrated under vacuum and re-dissolved in a minimal amount of dry DCM. The catalyst was removed by syringe filtration, after which the products were concentrated under vacuum to provide the crude material as a brown oil that was used in the next step without further purification.

A flame-dried round bottom flask equipped with a magnetic stir bar was charged with $AlCl_3$ (1.88 g, 14.1 mmol). The atmosphere was evacuated and refilled with N_2 3×. Anhydrous DCM (110 mL) was added and the flask was cooled to -5 °C in an ice/brine bath. The acyl chloride was added as a solution in DCM (10 mL), followed by 2-chloro-5-methylthiophene[43] (1.30 mL, 11.86 mmol). The reaction stirred at -5 °C for 2.25 h, after which it was quenched with deionized water (50 mL). The aqueous layer was washed with DCM (3 x 30 mL), and the

combined organics were washed with brine (30 mL), dried with Na_2SO_4, and filtered. The products were separated by silica gel chromatography (0–20% EtOAc/hexanes), yielding the title compound as a light yellow oil (1.53 g, 56% over 2 steps).

TLC (10% EtOAc/hexanes): R_f = 0.70

^{1}H NMR (400 MHz, $CDCl_3$) δ: 8.02 – 7.88 (m, 2H), 7.54 (ddt, *J* = 8.8, 7.0, 1.3 Hz, 1H), 7.40 (ddt, *J* = 7.8, 6.6, 1.1 Hz, 2H), 7.19 (s, 2H), 4.39 (t, *J* = 6.3 Hz, 2H), 3.11 – 2.77 (m, 5H), 2.63 (s, 5H), 1.95 (app q, *J* = 6.2 Hz, 2H) ppm.

^{13}C{^{1}H} NMR (101 MHz, $CDCl_3$) δ: 194.4, 166.6, 148.3, 135.0, 133.1, 130.2, 129.6, 128.5, 126.9, 125.5, 63.0, 45.7, 32.9, 28.2, 16.2 ppm.

HRMS (FAB, *m/z*): calc'd for $[C_{24}H_{23}Cl_2O_4S_2]^+$ $(M+H)^+$ 509.0410, found 509.0414.

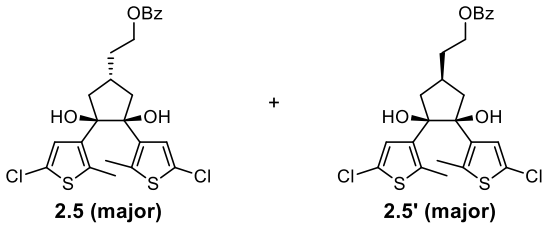

2.5 (major) **2.5' (major)**

2-((1r,3R,4S)-3,4-bis(5-chloro-2-methylthiophen-3-yl)-3,4-dihydroxycyclopentyl)ethyl benzoate (2.5 and diastereomer 2.5′). An oven-dried round bottom flask was charged with Zn^0 powder (4.85 g, 74.2 mmol) in the glovebox. The flask was sealed and removed from the box. $AlCl_3$ (6.11 g, 45.8 mmol) was added to the flask and the atmosphere was evacuated and refilled with N_2 3×. The flask was placed in a room temperature water bath and H_2O (50 mL) was added slowly, followed by **2.4** in a solution of dry THF (50 mL). The reaction was allowed to stir at room temperature for 14 h, after which the solids were removed by filtration through celite. The celite was flushed with EtOAc (200 mL) and the organics were washed with $NaHCO_3$ (3 x 100 mL) and once with brine (100 mL). The organics were dried with Na_2SO_4, filtered, and concentrated to provide the title compounds as a white solid (4.72 g, 97%). The

product was retrieved as a mixture of diastereomers that were not separated before the next step.

TLC (25% EtOAc/hexanes): R_f = 0.50

^{1}H NMR (400 MHz, $CDCl_3$, major diastereomer): 8.05 – 7.98 (m, 2H), 7.59 – 7.53 (m, 1H), 7.46 – 7.39 (m, 2H), 6.38 (s, 2H), 4.34 (t, 2H, *J* = 6.6 Hz), 3.51 (s, 2H, -OH), 2.75 (app quint, 1H, *J* = 8.1 Hz), 2.29 – 2.05 (m, 10 H), 2.03 – 1.94 (m, 2H) ppm.

$^{13}C\{^1H\}$ NMR (101 MHz, $CDCl_3$, major diastereomer) δ: 166.9, 137.3, 136.2, 133.2, 130.1, 129.7, 128.5, 127.5, 123.5, 86.5, 64.3, 46.4, 34.0, 31.7, 15.0 ppm.

HRMS (FAB, *m/z*): calc'd for $[C_{24}H_{24}\ Cl_2O_4S_2]^{+\cdot}$ $(M)^{+\cdot}$ 510.0493, found 510.0506.

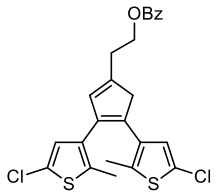

2.6

2-(3,4-bis(5-chloro-2-methylthiophen-3-yl)cyclopenta-1,3-dien-1-yl)ethyl benzoate (2.6). A round bottom flask equipped with a magnetic stir bar was charged with **2.5** (588 mg, 1.15 mmol). Dry toluene (40 mL) was added and the solution was heated to 60 °C. p-Toluenesulfonic acid monohydrate (40.0 mg, 0.210 mmol) was added in one portion and the reaction stirred for 30 min open to the atmosphere. The reaction was then cooled to room temperature and washed with saturated $NaHCO_3$ (3 x 15 mL) and brine (15 mL). The organics were dried with Na_2SO_4, filtered, and concentrated. The products were purified by silica gel chromatography (0–10% EtOAc/hexanes), yielding the title compound as an orange solid (464 mg, 85%).

TLC (25% EtOAc/hexanes): R_f = 0.78

^{1}H NMR (400 MHz, $CDCl_3$) δ: 8.14 – 7.98 (m, 2H), 7.65 – 7.51 (ddt, *J* = 7.9, 6.9, 1.3 Hz 1H), 7.45 (m, 2H), 6.60 (s, 1H), 6.57 (s, 1H), 6.33 (app quint, *J* = 1.3 Hz, 1H), 4.53 (t, *J* = 6.7 Hz, 2H), 3.37 (d, *J* = 1.1 Hz, 2H), 2.91 (td, *J* = 6.7, 1.4 Hz, 2H), 1.99 (s, 3H), 1.91 (s, 3H) ppm.

^{13}C{^{1}H} NMR (101 MHz, $CDCl_3$) δ: 166.6, 143.9, 136.8, 135.0, 134.1, 133.9, 133.7, 133.1, 133.0, 131.9, 130.3, 129.7, 128.5, 127.4, 127.1, 125.6, 125.4, 64.3, 47.8, 30.2, 14.4, 14.2 ppm.

HRMS (FAB, *m/z*): calc'd for $[C_{24}H_{20}Cl_2O_2S_2]^{+\cdot}$ $(M)^{+\cdot}$ 474.0282, found 474.0301.

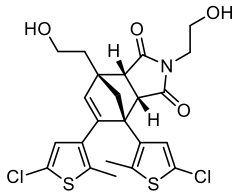

2.7

(3aS,4S,7S,7aR)-4,5-bis(5-chloro-2-methylthiophen-3-yl)-2,7-bis(2-hydroxyethyl)-3a,4,7,7a-tetrahydro-1H-4,7-methanoisoindole-1,3(2H)-dione (2.7). A flame-dried round bottom flask was charged with LAH (19.9 mg, 0.524 mmol) and the atmosphere was evacuated and backfilled with N_2 3×. THF (2 mL) was added and the mixture was cooled to 0 °C. A solution of **2.6** (251 mg, 0.528 mmol) in THF (1 mL) was added slowly, after which the reaction was allowed to stir at 0 °C for 30 min. It was quenched with saturated NH_4Cl (3 mL) and the products were extracted into Et_2O (3 x 5 mL). During each extraction, the combined organic and aqueous layers were sonicated for approximately 30 s in a bath sonicator in order to liberate the reduced product from Al salt aggregates. The combined organics were washed with brine (5 mL), dried with Na_2SO_4, and filtered. The products were purified by silica gel chromatography (0–50% EtOAc/hexanes), yielding 2-(3,4-bis(5-chloro-2-methylthiophen-3-yl)cyclopenta-1,3-dien-1-yl)ethan-1-ol as a light yellow oil contaminated with a roughly equimolar amount of benzyl alcohol. It was used directly in the next step without further purification to avoid decomposition.

A flame-dried round bottom flask was charged with *N*-(2-hydroxyethyl)maleimide[44] (748 mg, 5.30 mmol) and the atmosphere was evacuated and refilled with N_2 3×. 2-(3,4-bis(5-chloro-2-methylthiophen-3-yl)cyclopenta-1,3-dien-1-yl)ethan-1-ol was added as a solution in dry toluene (5.0 mL) and the reaction was stirred at 70 °C for 24 h. The reaction was cooled to room temperature and concentrated. The crude mixture was separated by reverse phase chromatography on a C18 column (45–60% MeCN/H_2O) to provide the title compound as a white solid (148 mg, 51% over 2 steps). Alternatively, silica gel chromatography (0–10% MeOH/DCM) followed by recrystallization from toluene also afforded the pure *endo* product.

TLC (5% MeOH/DCM): R_f = 0.43

^{1}H NMR (500 MHz, $(CD_3)_2CO$) δ: 7.47 (s, 1H), 6.20 (s, 1H), 6.13 (s, 1H), 4.15 (d, *J* = 7.7 Hz), 3.86 (td, *J* = 6.5, 0.9 Hz), 3.83 – 3.79 (m, 1H, -OH), 3.60 (t, 1H, J = 6.0 Hz, -OH), 3.54 (d, *J* = 7.7 Hz), 3.41 – 3.29 (m, 2H), 3.25 – 3.14 (m, 2H), 2.58 (d, *J* = 9.0 Hz), 2.47 – 2.35 (m, 4H), 2.17 (dt, *J* = 14.3, 6.5 Hz), 2.01 (s, 3H), 1.88 (dd, *J* = 9.0, 1.1 Hz) ppm.

^{13}C{^{1}H} NMR (101 MHz, $(CD_3)_2CO$) δ: 177.9, 177.6, 143.6, 136.2, 136.1, 135.9, 135.8, 132.4, 130.4, 127.7, 124.0, 123.4, 62.1, 61.8, 60.0, 58.9, 56.1, 52.0, 51.3, 41.1, 35.5, 15.1, 14.4 ppm.

HRMS (ESI, *m/z*): calc'd for $[C_{23}H_{24}Cl_2NO_4S_2]^+$ $(M+H)^+$ 512.0519, found 512.0524.

Scheme S2.6. Differentiation of **2.7** and Synthesis of Mechanophore-Centered Polymers

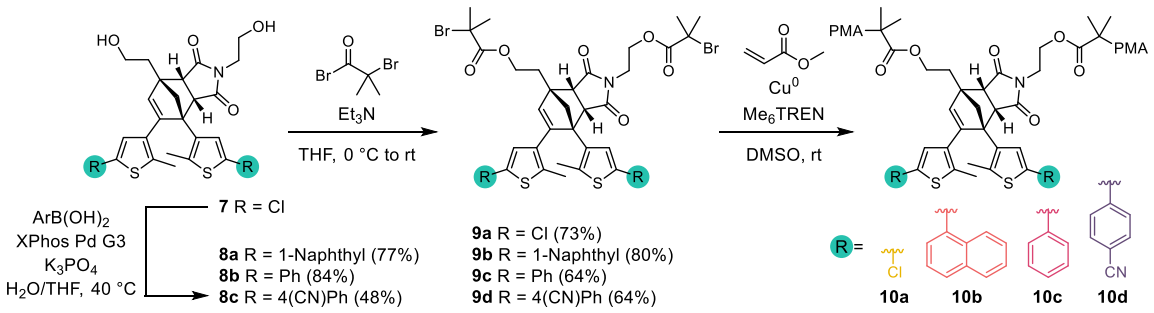

General Procedure A for Suzuki–Miyaura Cross-Coupling of Thienyl Chlorides with Aryl Boronic Acids. A round bottom flask was charged with the appropriate thienyl chloride (1.0 equiv), XPhos Pd G3 (0.1 equiv), K_3PO_4 (6 equiv), and the appropriate aryl boronic acid (4 equiv). The atmosphere was evacuated and refilled with N_2 3×. Degassed water was added, followed by dry THF, and the reaction was stirred at the indicated temperature for the indicated amount of time. Upon completion, the reaction was cooled to room temperature (if applicable) and diluted with EtOAc (10 mL). The organics were washed with 1 M NaOH (3 x 5 mL), then the combined aqueous layer was extracted once with EtOAc (5 mL). The organic layers were combined and washed with brine (5 mL), dried over Na_2SO_4, filtered, and concentrated under reduced pressure.

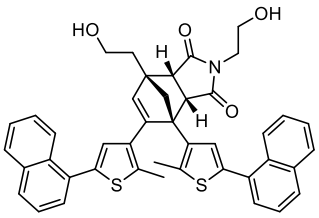

2.8a

(3aS,4S,7S,7aR)-2,7-bis(2-hydroxyethyl)-4,5-bis(2-methyl-5-(naphthalen-1-yl)thiophen-3-yl)-3a,4,7,7a-tetrahydro-1H-4,7-methanoisoindole-1,3(2H)-dione (2.8a). Synthesized according to general procedure A with **2.7** (100 mg, 0.195 mmol), XPhos Pd G3 (16.5 mg, 0.0195 mmol), K_3PO_4 (250 mg, 1.18 mmol), and 1-naphthaleneboronic acid (134 mg, 0.779 mmol). It was purified by silica gel chromatography (0–10% MeOH/DCM) to yield the title compound as a light brown solid (105 mg, 77%).

TLC (5% MeOH/DCM): R_f = 0.37

^{1}H NMR (400 MHz, CD_3OD) δ: 8.10 (m, 1H), 7.89 – 7.78 (m, 3H), 7.73 (m, 2H), 7.69 (s, 1H), 7.43 – 7.39 (m, 2H), 7.37 – 7.28 (m, 3H), 7.17 – 7.08 (m, 2H), 6.95 (ddd, 1H, *J* = 8.3, 6.8, 1.3 Hz), 6.80 (s, 1H), 6.17 (s, 1H), 4.19 (d, 1H, *J* = 7.7 Hz), 3.93 (td, 2H, *J* = 6.7, 1.1 Hz), 3.47 (d, 1H, *J* = 7.7 Hz), 3.43 – 3.37 (m, 2H), 3.24 (t, 2H, *J* = 6.6 Hz), 2.66 (d, 1H, *J* = 8.9 Hz), 2.61 (s, 3H), 2.50 (dt, 1H, *J* = 13.8, 6.7 Hz), 2.30 – 2.15 (m, 4H), 1.90 (dd, 1H, *J* = 8.9, 1.0 Hz) ppm.

^{13}C{^{1}H} NMR (101 MHz, CD_3OD) δ: 179.1, 178.9, 145.9, 138.0, 137.9, 137.4, 137.1, 136.9, 135.4, 135.3, 135.0, 133.7, 133.6, 133.4, 132.64, 132.62, 132.0, 129.8, 129.13, 129.10, 129.06, 129.0, 128.7, 128.6, 127.9, 127.3, 127.0, 126.8, 126.7, 126.6, 126.12, 126.06, 63.0, 62.6, 60.6, 59.4, 56.3, 52.9, 51.7, 41.1, 35.9, 15.4, 14.6 ppm.

HRMS (ESI, *m/z*): calc'd for $[C_{43}H_{38}NO_4S_2]^+$ $(M+H)^+$ 696.2237, found 696.2250.

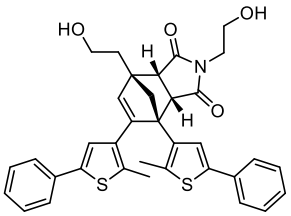

2.8b

(3aS,4S,7S,7aR)-2,7-bis(2-hydroxyethyl)-4,5-bis(2-methyl-5-phenylthiophen-3-yl)-3a,4,7,7a-tetrahydro-1H-4,7-methanoisoindole-1,3(2H)-dione (2.8b). Synthesized according to general procedure A with **2.7** (200 mg, 0.390 mmol), XPhos Pd G3 (33 mg, 0.039 mmol), K_3PO_4 (495 mg, 2.33 mmol), and phenylboronic acid (190 mg, 1.56 mmol). It was purified by silica gel chromatography (0–10% MeOH/DCM) to yield the title compound as a light brown solid (195 mg, 84%).

TLC (5% MeOH/DCM): R_f = 0.39

^{1}H NMR (400 MHz, $(CD_3)_2CO$) δ: 8.07 (s, 1H), 7.68 – 7.64 (m, 2H), 7.44 (t, 2H, *J* = 7.8 Hz), 7.31 (td, 1H, *J* = 7.3, 1.2 Hz), 7.22 (dd, 2H, *J* = 8.0, 1.6 Hz), 7.17 – 7.08 (m, 3H), 6.72 (s, 1H),

6.16 (s, 1H), 4.31 (d, 1H, *J* = 7.7 Hz), 3.92 (ddd, 2H, *J* = 10.4, 7.6, 5.0 Hz), 3.81 (t, 1H, *J* = 5.2 Hz, -OH), 3.58 (d, 1H, *J* = 7.6 Hz), 3.51 (t, 1H, *J* = 6.0 Hz, -OH), 3.34 (dd, 2H, *J* = 7.1, 5.9 Hz), 3.18 (qd, 2H, *J* = 6.7, 2.1 Hz), 2.67 (d, 1H, *J* = 8.9 Hz), 2.53 (s, 3H), 2.46 (dt, 1H, *J* = 13.5, 6.5 Hz), 2.23 (dt, 1H, *J* = 14.4, 6.5 Hz), 2.09 (s, 3H), 1.94 (dd, 1H, *J* = 9.0, 1.0 Hz) ppm.

$^{13}C\{^{1}H\}$ NMR (101 MHz, $(CD_3)_2CO$) δ: 178.0, 177.8, 144.6, 139.4, 138.0, 137.8, 136.8, 136.6, 135.6, 135.4, 134.7, 133.5, 129.9, 129.6, 128.2, 128.0, 127.7, 126.2, 125.8, 125.7, 62.4, 61.7, 60.2, 59.0, 56.1, 52.2, 51.5, 41.1, 35.8, 15.5, 14.7 ppm.

HRMS (ESI, *m/z*): calc'd for $[C_{35}H_{34}NO_4S_2]^+$ $(M+H)^+$ 596.1924, found 596.1931.

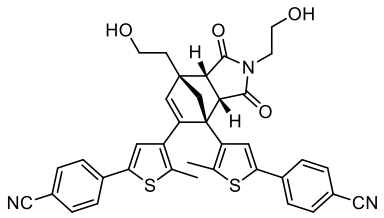

2.8c

4,4'-(((3aS,4S,7S,7aR)-2,7-bis(2-hydroxyethyl)-1,3-dioxo-1,2,3,3a,7,7a-hexahydro-4H-4,7-methanoisoindole-4,5-diyl)bis(5-methylthiophene-4,2-diyl))dibenzonitrile (2.8c). Synthesized according to general procedure A with **2.7** (100 mg, 0.195 mmol), XPhos Pd G3 (16.2 mg, 0.0191 mmol), K_3PO_4 (246 mg, 1.16 mmol), and 4-(cyanophenyl)boronic acid (115 mg, 0.783 mmol). It was purified by silica gel chromatography (0–10% MeOH/DCM) to yield the title compound as a white solid (60 mg, 48%).

TLC (5% MeOH/DCM): R_f = 0.37

^{1}H NMR (500 MHz, $(CD_3)_2CO$) δ: 8.27 (s, 1H), 7.85 (s, 4H), 7.56 (d, 2H, *J* = 8.2 Hz), 7.35 (d, 2H, *J* = 8.2 Hz), 6.82 (s, 1H), 6.22 (s, 1H), 4.38 (d, 1H, *J* = 7.7 Hz), 3.94 – 3.87 (m, 2H), 3.83 (t, 1H, *J* = 5.1 Hz, -OH), 3.61 (d, 1H, *J* = 7.7 Hz), 3.54 (t, 1H, *J* = 6.0 Hz, -OH), 3.35 (t, 2H, *J* = 6.6 Hz), 3.18 (app q, 2H, *J* = 6.8 Hz), 2.69 (d, 1H, *J* = 9.0 Hz), 2.57 (s, 3H), 2.47 (dt,

1H, *J* = 13.6, 6.7 Hz), 2.23 (dt, 1H, *J* = 13.6, 6.4 Hz), 2,13 (s, 3H), 1.97 (d, 1H, *J* = 9.0 Hz) ppm.

$^{13}C\{^{1}H\}$ NMR (101 MHz, $(CD_3)_2CO$) δ: 178.2, 177.7, 144.0, 139.7, 139.6, 139.52, 139.50, 138.5, 137.3, 136.0, 135.7, 134.1, 133.9, 133.6, 130.4, 127.6, 126.5, 126.0, 119.4, 119.2, 111.1, 110.8, 62.3, 61.6, 60.2, 60.0, 59.0, 58.9, 56.3, 52.1, 51.5, 41.1, 35.7, 15.5, 14.8 ppm.

HRMS (ESI, *m/z*): calc'd for $[C_{37}H_{31}N_3O_4S_2]^+$ $(M+H)^+$ 646.1829, found 646.1846.

General Procedure B for the Synthesis of Polymerization Initiators and Crosslinkers by Esterification. A flame-dried round bottom flask was charged with the appropriate diol (1.0 equiv) and the atmosphere was evacuated and refilled 3× with N_2. Dry THF (1.5 mL) was added and the solution was cooled to 0 °C in an ice/water bath. Triethylamine (7.0 equiv) was added, followed by either α-bromoisobutyryl bromide or acryloyl chloride (5.0 equiv). Immediately after the addition, the reaction was removed from the bath to warm to room temperature and stirred for the indicated amount of time. The reaction mixture was then diluted with EtOAc (5 mL) and the solution was washed with saturated $NaHCO_3$ (3 x 5 mL) and then brine (5 mL), dried over Na_2SO_4, filtered, and concentrated under reduced pressure.

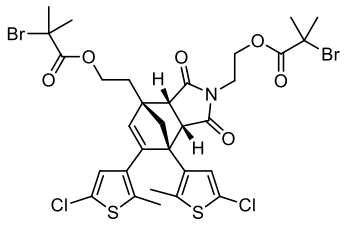

2.9a

((3aR,4S,7S,7aS)-6,7-bis(5-chloro-2-methylthiophen-3-yl)-1,3-dioxo-3,3a,7,7a-tetrahydro-1H-4,7-methanoisoindole-2,4-diyl)bis(ethane-2,1-diyl) bis(2-bromo-2-methylpropanoate) (2.9a). Synthesized according to general procedure B with **2.7** (80 mg,

0.16 mmol), triethylamine (150 μL, 1.08 mmol), and α-bromoisobutyryl bromide (100 μL, 0.811 mmol). It stirred for 17 h before being worked up and purified by silica gel chromatography (0–50% EtOAc/hexanes) and the title compound was retrieved as a light yellow solid (92 mg, 73%).

TLC (25% EtOAc/hexanes): R_f = 0.36

^{1}H NMR (500 MHz, $CDCl_3$) δ: 7.33 (s, 1H), 6.13 (s, 1H), 5.98 (s, 1H), 4.51 – 4.36 (m, 2H), 4.16 (dt, 1H, *J* = 11.5, 5.0 Hz), 3.96 – 3.85 (m, 2H), 3.60 (t, 2H, *J* = 5.4 Hz), 3.39 (d, 1H, *J* = 7.8 Hz), 2.59 (dt, 1H, *J* = 15.0, 5.6 Hz), 2.51 (d, *J* = 9.1 Hz), 2.44 – 2.35 (m, 4H), 1.96 – 1.91 (m, 9H), 1.91 (s, 3H), 1.89 (s, 3H), 1.80 (dd, 1H, *J* = 9.1, 1.1 Hz) ppm.

^{13}C{^{1}H} NMR (126 MHz, $CDCl_3$) δ: 176.1, 176.0, 171.7, 171.4, 144.9, 135.2, 134.9, 133.6, 132.7, 130.4, 128.7, 126.3, 125.0, 124.6, 63.8, 62.6, 61.9, 61.5, 55.8, 55.7, 54.9, 51.3, 50.7, 37.4, 30.88, 30.87, 30.85, 30.8, 30.6, 15.4, 14.4 ppm.

HRMS (ESI, *m/z*): calc'd for $[C_{31}H_{34}Br_2Cl_2NO_6S_2]^+$ $(M+H)^+$ 809.9546, found 809.9565.

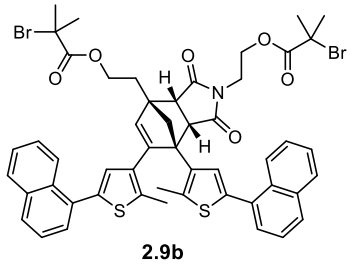

2.9b

((3aR,4S,7S,7aS)-6,7-bis(2-methyl-5-(naphthalen-1-yl)thiophen-3-yl)-1,3-dioxo-3,3a,7,7a-tetrahydro-1H-4,7-methanoisoindole-2,4-diyl)bis(ethane-2,1-diyl) bis(2-bromo-2-methylpropanoate) (2.9b). Synthesized according to general procedure B with **2.8a** (80 mg, 0.12 mmol), triethylamine (112 μL, 0.804 mmol), and α-bromoisobutyryl bromide (71 μL, 0.57 mmol). Stirred for 15 h before being worked up and purified by silica gel

chromatography (10–40% EtOAc/hexanes) and the title compound was retrieved as a light yellow solid (91 mg, 80%).

TLC (25% EtOAc/hexanes): R_f = 0.38

^{1}H NMR (500 MHz, $(CD_3)_2CO$) δ: 8.21 (d, 1H, *J* = 8.6 Hz), 7.99 – 7.93 (m, 1H), 7.92 – 7.85 (m, 2H), 7.85 – 7.77 (m, 2H), 7.73 (s, 1H), 7.50 – 7.33 (m, 5H), 7.27 (tt, 2H, *J* = 6.8, 5.1 Hz), 7.12 (ddd, 1H, *J* = 8.3, 6.8, 1.3 Hz), 6.86 (s, 1H), 6.33 (s, 1H), 4.63 – 4.51 (m, 2H), 4.38 (d, 1H, *J* = 7.8 Hz), 4.07 (dt, 1H, *J* = 11.5, 5.0 Hz), 3.86 (ddd, 1H, *J* = 11.7, 7.5, 5.0 Hz), 3.68 – 3.53 (m, 3H), 2.79 (d, 1H, *J* = 8.8 Hz), 2.73 – 2.64 (m, 4H), 2.46 (ddd, 1H, *J* = 14.1, 7.8, 6.3 Hz), 2.35 (s, 2H), 2.11 (d, 1H, *J* = 8.7 Hz), 1.97 (s, 6H), 1.89 – 1.85 (m, 6H) ppm.

^{13}C{^{1}H} NMR (101 MHz, $(CD_3)_2CO$) δ: 177.9, 177.1, 171.9, 171.6, 146.2, 137.7, 137.1, 137.0, 136.7, 136.5, 135.0, 134.9, 134.2, 133.22, 133.19, 133.1, 132.3, 132.12, 132.09, 129.3, 129.1, 129.02, 128.97, 128.9, 128.5, 128.4, 127.7, 127.3, 126.8, 126.7, 126.5, 126.3, 126.11, 126.06, 64.7, 63.3, 62.8, 62.6, 57.4, 57.1, 55.8, 52.5, 51.3, 37.6, 31.5, 31.04, 31.03, 30.99, 15.5, 14.7 ppm.

HRMS (ESI, *m/z*): calc'd for $[C_{51}H_{48}Br_2NO_6S_2]^+$ $(M+H)^+$ 992.1285, found 922.1307.

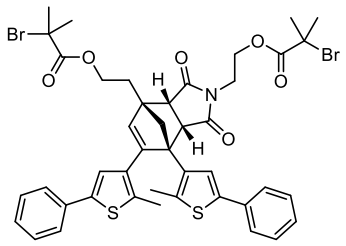

2.9c

((3aR,4S,7S,7aS)-6,7-bis(2-methyl-5-phenylthiophen-3-yl)-1,3-dioxo-3,3a,7,7a-tetrahydro-1H-4,7-methanoisoindole-2,4-diyl)bis(ethane-2,1-diyl) bis(2-bromo-2-methylpropanoate) (2.9c). Synthesized according to general procedure B with **2.8b** (50 mg, 0.084 mmol), triethylamine (82 μL, 0.59 mmol), and α-bromoisobutyryl bromide (52 μL, 0.42

mmol). It stirred for 15 h before being worked up and purified by silica gel chromatography (0–35% EtOAc/hexanes) and the title compound was retrieved as a light yellow solid (48 mg, 64%).

TLC (25% EtOAc/hexanes): R_f = 0.36

^{1}H NMR (500 MHz, $CDCl_3$) δ: 7.92 (s, 1H), 7.66 – 7.61 (m, 2H), 7.41 (t, 2H, *J* = 7.6 Hz), 7.30 (t, 1H, *J* = 7.4 Hz), 7.22 – 7.17 (m, 2H), 7.15 – 7.06 (m, 2H), 6.59 (s, 1H), 6.05 (s, 1H), 4.57 – 4.41 (m, 2H), 4.17 – 4.08 (m, 2H), 3.87 (ddd, 1H, *J* = 11.4 Hz, 6.7 Hz, 4.5 Hz), 3.66 – 3.53 (m, 2H), 3.45 (d, 1H, *J* = 7.8 Hz), 2.71 – 2.61 (m, 2H), 2.51 (s, 3H), 2.45 (ddd, 1H, J = 14.4, 8.1, 6.0 Hz), 2.06 (s, 3H), 1.96 (s, 6H), 1.93 – 1.87 (m, 7H) ppm.

^{13}C{^{1}H} NMR (126 MHz, $CDCl_3$) δ: 176.4, 176.3, 171.8, 171.5, 145.7, 139.7, 138.3, 136.6, 136.5, 135.5, 134.7, 134.3, 131.6, 131.4, 129.0, 128.8, 127.3, 126.9, 126.7, 125.9, 125.4, 124.2, 63.9, 62.7, 62.0, 61.4, 55.9, 55.7, 55.1, 51.6, 51.0, 37.3, 30.92, 30.91, 30.86, 30.85, 30.8, 15.8, 14.7 ppm.

HRMS (ESI, *m/z*): calc'd for $[C_{43}H_{44}Br_2NO_6S_2]^+$ $(M+H)^+$ 892.0972, found 892.0981.

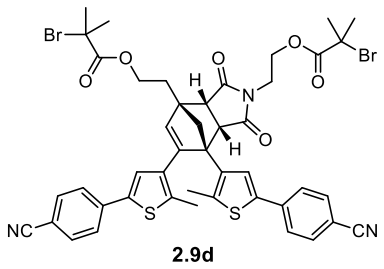

2.9d

((3aR,4S,7S,7aS)-6,7-bis(5-(4-cyanophenyl)-2-methylthiophen-3-yl)-1,3-dioxo-3,3a,7,7a-tetrahydro-1H-4,7-methanoisoindole-2,4-diyl)bis(ethane-2,1-diyl) bis(2-bromo-2-methylpropanoate) (2.9d). Synthesized according to general procedure B with **2.8c** (40 mg, 0.062 mmol), triethylamine (60 μL, 0.430 mmol), and α-bromoisobutyryl bromide (38 μL, 0.31 mmol). It stirred for 15 h before it was worked up and purified by silica gel

chromatography (30–70% EtOAc/hexanes) and the title compound was retrieved as a light yellow solid (37 mg, 64%).

TLC (25% EtOAc/hexanes): R_f = 0.13

^{1}H NMR (500 MHz, $CDCl_3$) δ: 8.02 (s, 1H), 7.69 (s, 4H), 7.39 (d, 2H, *J* = 8.5 Hz), 7.25 – 7.21 (m, 2H), 6.65 (s, 1H), 6.10 (s, 1H), 4.56 – 4.41 (m, 2H), 4.18 – 4.09 (m, 2H), 3.87 (ddd, 1H, *J* = 11.4, 6.8, 4.4 Hz), 3.67 – 3.53 (m, 2H), 3.49 (d, 1H, *J* = 7.8 Hz), 2.71 – 2.61 (m, 2H), 2.53 (s, 3H), 2.47 (ddd, 1H, *J* = 13.9, 8.0, 5.6 Hz), 2.08 (s, 3H), 1.95 (s, 6H), 1.93 – 1.86 (m, 7H) ppm.

^{13}C{^{1}H} NMR (126 MHz, $CDCl_3$) δ: 176.6, 176.0, 171.7, 171.5, 144.9, 139.2, 139.1, 138.6, 138.5, 137.3, 136.3, 136.2, 133.0, 132.7, 132.6, 132.1, 128.5, 126.0, 125.7, 125.4, 118.9, 110.6, 110.1, 63.8, 62.5, 61.8, 61.5, 55.83, 55.78 55.2, 51.4, 51.0, 37.4, 30.92, 30.90, 30.86, 30.8, 30.7, 15.9, 14.9 ppm.

HRMS (ESI, *m/z*): calc'd for $[C_{45}H_{42}Br_2N_3O_6S_2]^+$ $(M+H)^+$ 942.0877, found 942.0883.

General Procedure C for the Synthesis of Poly(Methyl Acrylate) (PMA) Polymers Incorporating a Cyclopentadiene–Maleimide Mechanophore. Polymers were synthesized by controlled radical polymerization following the procedure by Nguyen *et al*.[45] A flame-dried Schlenk flask was charged with freshly cut 20 G copper wire (2 cm), initiator, DMSO, and methyl acrylate. The flask was sealed and the solution was degassed via three freeze-pump-thaw cycles, then backfilled with N_2 and warmed to room temperature. Me_6TREN was added via microsyringe and the reaction was stirred at room temperature for the indicated amount of time. Following completion of the polymerization, the flask was opened to atmosphere and

diluted with a minimal amount of DCM. The polymer was precipitated 3× into methanol cooled with dry ice and then dried under vacuum to afford the polymer.

Polymer 2.10a. Synthesized using general procedure C with **2.9a** (10.0 mg, 0.0123 mmol), methyl acrylate (1.56 mL, 17.2 mmol), DMSO (1.56 mL), and Me_6TREN (13.0 μL, 0.0486 mmol). Polymerization for 55 min provided the title polymer as a tacky white solid (837 mg, 56%). M_n = 111 kg/mol; $Đ$ = 1.05.

Polymer 2.10b. Synthesized using general procedure C with **2.9b** (6.7 mg, 0.0067 mmol), methyl acrylate (850 μL, 9.38 mmol), DMSO (850 μL), and Me_6TREN (6.2 μL, 0.023 mmol). Polymerization for 35 min provided the title polymer as a tacky white solid (427 mg, 52%). M_n = 112 kg/mol; $Đ$ = 1.07.

Polymer 2.10c. Synthesized using general procedure C with **2.9c** (10.0 mg, 0.0112 mmol), methyl acrylate (1.42 mL, 15.7 mmol), DMSO (1.42 mL), and Me_6TREN (12.0 μL, 0.0449 mmol). Polymerization for 55 min provided the title polymer as a tacky white solid (639 mg, 47%). M_n = 105 kg/mol; $Đ$ = 1.06.

Polymer 2.10d. Synthesized using general procedure C with **2.9d** (10.2 mg, 0.0108 mmol), methyl acrylate (1.37 mL, 15.1 mmol), DMSO (1.37 mL), and Me_6TREN (9.9 μL, 0.037

Scheme S2.7. Synthesis of Chain-End Functional Control PMA Polymer **2.15**

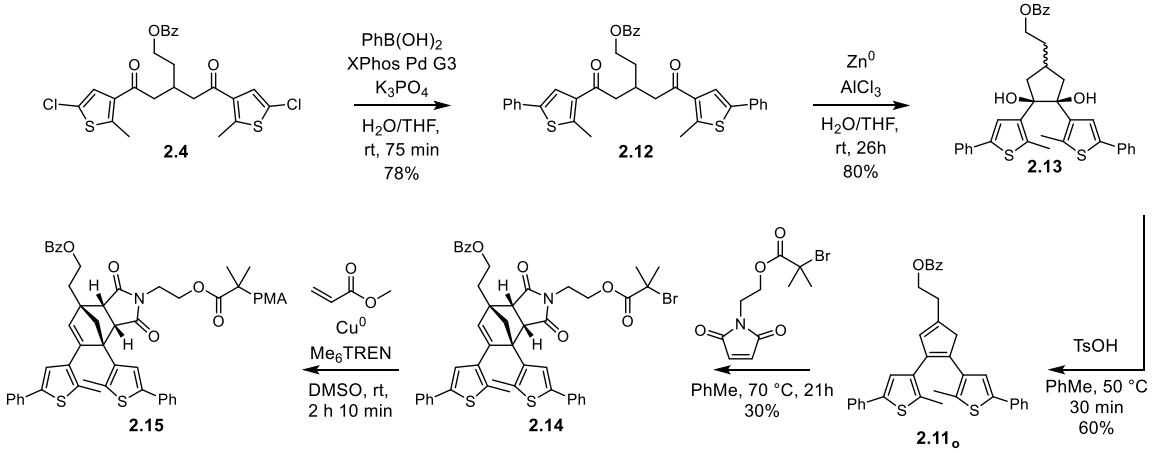

mmol). Polymerization for 35 min provided the title polymer as a tacky white solid (663 mg, 51%). M_n = 96 kg/mol; $Đ$ = 1.06.

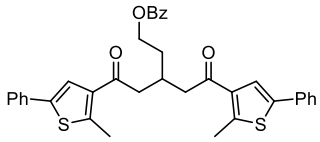

2.12

5-(2-methyl-5-phenylthiophen-3-yl)-3-(2-(2-methyl-5-phenylthiophen-3-yl)-2-oxoethyl)-5-oxopentyl benzoate (2.12). Synthesized according to general procedure A using **2.4** (1.00 g, 1.69 mmol), XPhos Pd G3 (166 mg, 0.196 mmol), K_3PO_4 (2.49 g, 11.7 mmol), and phenylboronic acid (957 mg, 7.85 mmol) in H_2O (12.0 mL) and THF (6.0 mL) at room temperature for 75 min. Purified by silica gel chromatography (0–25% EtOAc/hexanes) and the title compound was retrieved as a brown solid (909 mg, 78%).

TLC (25% EtOAc/hexanes): R_f = 0.58

^{1}H NMR (500 MHz, $CDCl_3$) δ: 7.95 (dd, 2H, *J* = 8.3, 1.3 Hz), 7.65 (s, 2H), 7.53 (dd, 4H, *J* = 8.2, 1.3 Hz), 7.47 (ddt, 1H, *J* = 8.7, 7.4, 1.3 Hz), 7.36 (t, 4H, *J* = 7.7 Hz), 7.34 – 7.27 (m, 4H), 4.45 (t, 2H, *J* = 6.3 Hz), 3.20 – 3.10 (m, 3H), 2.75 (s, 6H), 2.04 (app q, 2H, *J* = 6.1 Hz) ppm.

^{13}C{^{1}H} NMR (126 MHz, $CDCl_3$) δ: 195.6, 166.7, 149.2, 139.8, 136.5, 133.6, 133.0, 130.2, 129.6, 129.1, 128.5, 127.9, 125.8, 123.9, 63.1, 46.0, 32.9, 28.6, 16.5 ppm.

HRMS (FAB, *m/z*): calc'd for $[C_{36}H_{32}O_4S_2]^{+\cdot}$ $(M)^{+\cdot}$ 593.1815, found 593.1829.

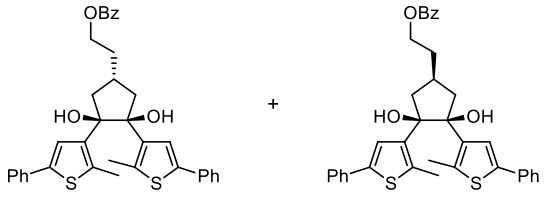

2.13 (major) **2.13'** (minor)

2-(3,4-dihydroxy-3,4-bis(2-methyl-5-phenylthiophen-3-yl)cyclopentyl)ethyl benzoate (2.13 and diastereomer 2.13′). An oven-dried round bottom flask was charged with Zn^0 powder (134 mg, 2.05 mmol) in the glovebox. The flask was sealed and removed from the box. $AlCl_3$ (244 mg, 1.83 mmol) was added to the flask and the atmosphere was evacuated and refilled with N_2 3×. The flask was placed in a room temperature water bath and H_2O (2.0 mL) was added slowly, followed by **2.12** (114 mg, 0.192 mmol) in a solution of dry THF (2.0 mL). The reaction was allowed to stir at room temperature for 26 h, after which the solids were removed by filtration through celite. The celite was flushed with EtOAc (15 mL) and the organics were washed with $NaHCO_3$ (3 x 5 mL) and once with brine (5 mL). The organics were dried with Na_2SO_4, filtered, and concentrated. The products were separated by silica gel chromatography (0–50% EtOAc/hexanes), yielding the title compounds as white solid (91 mg, 80%). The product was isolated as a mixture of diastereomers which were not separated before the next step.

TLC (25% EtOAc/hexanes): R_f = 0.48

^{1}H NMR (500 MHz, $(CD_3)_2CO$) δ: 8.07 – 8.04 (m, 2H), 7.64 – 7.59 (m, 1H), 7.52 – 7.46 (m, 2H), 7.36 –7.41 (m, 4H), 7.30 – 7.24 (m, 4H), 7.23 – 7.17 (m, 2H), 7.02 (s, 2H), 4.86 (s, 2H), 4.47 (t, 2H, *J* = 6.5 Hz), 2.93 (app quint, 1H, *J* = 8.6 Hz), 2.53 – 2.44 (m, 2H), 2.43 – 2.35 (m, 8H), 2.18 (app q, 2H, *J* = 6.9 Hz) ppm.

^{13}C{^{1}H} (101 MHz, $(CD_3)_2CO$) δ: 166.8, 141.2, 137.7, 137.4, 135.5, 133.9, 131.5, 130.2, 129.6, 129.4, 127.7, 126.5, 126.0, 87.1, 65.1, 47.6, 34.7, 32.8, 15.6 ppm.

HRMS (FAB, *m/z*): calc'd for $[C_{36}H_{34}O_4S_2]^{+\cdot}$ $(M)^{+\cdot}$ 594.1899, found 594.1904.

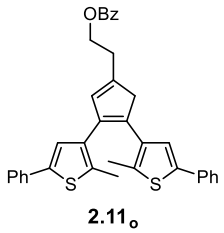

2.11$_o$

2-(3,4-bis(2-methyl-5-phenylthiophen-3-yl)cyclopenta-1,3-dien-1-yl)ethyl benzoate (2.11$_o$). A round bottom flask equipped with a magnetic stir bar was charged with **2.13** (150 mg, 0.252 mmol). Dry toluene (7.5 mL) was added and the solution was heated to 50 °C. *p*-Toluenesulfonic acid monohydrate (9.5 mg, 0.050 mmol) was added in one portion and the reaction stirred for 30 min open to the atmosphere. The reaction was then cooled to room temperature and washed with saturated $NaHCO_3$ (3 x 5 mL) and brine (5 mL). The organics were dried with Na_2SO_4, filtered, and concentrated. The products were purified by C18 reverse phase chromatography (80–100% MeCN/H_2O), yielding the title compound as a purple solid (84 mg, 60%).

TLC (25% EtOAc/hexanes): R_f = 0.73

^{1}H NMR (500 MHz, $(CD_3)_2CO$) δ: 8.06 (m, 2H), 7.63 (m, 1H), 7.57 – 7.49 (m, 6H), 7.35 (t, 4H, *J* = 7.6 Hz), 7.28 (s, 1H), 7.24 (td, 2H, *J* = 7.3, 1.4 Hz), 7.14 (s, 1H), 6.56 (s, 1H), 4.59 (t, 2H, *J* = 6.6 Hz), 3.64 (d, 2H, *J* = 1.2 Hz), 3.00 (td, 2H, *J* = 6.7, 1.3 Hz), 2.12 (s, 3H), 2.04 (s, 3H) ppm.

^{13}C{^{1}H} NMR (126 MHz, $(CD_3)_2CO$) δ: 166.7, 145.0, 140.7, 140.3, 137.9, 137.1, 136.9, 136.6, 135.5, 135.3, 135.2, 134.4, 133.9, 132.8, 131.4, 130.2, 129.8, 129.4, 128.1, 128.0, 126.0, 125.88, 125.86, 125.4, 64.9, 48.3, 30.8, 14.7, 14.4 ppm.

HRMS (FAB, *m/z*): calc'd for $[C_{36}H_{30}O_2S_2]^{+\cdot}$ $(M)^{+\cdot}$ 558.1687, found 558.1694.

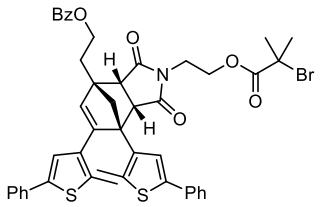

2.14

2-((3aR,4S,7S,7aS)-2-(2-((2-bromo-2-methylpropanoyl)oxy)ethyl)-6,7-bis(2-methyl-5-phenylthiophen-3-yl)-1,3-dioxo-1,2,3,3a,7,7a-hexahydro-4H-4,7-methanoisoindol-4-yl)ethyl benzoate (2.14). A flame-dried round bottom flask was charged with 2-(2,5-dioxo-2,5-dihydro-1H-pyrrol-1-yl)ethyl 2-bromo-2-methylpropanoate[32] (121 mg, 0.417 mmol) and the atmosphere was evacuated and refilled with N_2 3×. A solution of **2.11$_o$** (121 mg, 0.217 mmol) in dry toluene (3.0 mL) was added and the reaction was stirred at 70 °C for 21 h. The reaction was cooled to room temperature and concentrated. The products were separated by C18 reverse phase chromatography (80–100% MeCN/H_2O). The resulting light brown solid was recrystallized from acetone, yielding the title compound as a white solid (55 mg, 30%).

TLC (25% EtOAc/hexanes): R_f = 0.32

^{1}H NMR (500 MHz, $CDCl_3$) δ: 8.08 – 8.03 (m, 2H), 7.91 (s, 1H), 7.66 – 7.61 (m, 2H), 7.58 (dt, 1H, *J* = 7.3, 1.3 Hz), 7.45 (t, 2H, *J* = 7.8 Hz), 7.41 (t, 2H, *J* = 7.7 Hz), 7.32 – 7.28 (m, 1H), 7.19 (dd, 2H, *J* = 7.9, 1.7 Hz), 7.14 – 7.06 (m, 3H), 6.59 (s, 1H), 6.09 (s, 1H), 4.72 – 4.61 (m, 2H), 4.18 – 4.09 (m, 2H), 3.85 (ddd, 1H, *J* = 11.4, 6.7, 4.5 Hz), 3.66 – 3.54 (m, 2H), 3.44 (d, 1H, *J* = 7.8 Hz), 2.82 (dt, 1H, *J* = 14.9, 5.9 Hz), 2.68 (d, 1H, *J* = 9.0 Hz), 2.49 (dt, 1H, *J* = 15.0, 6.6 Hz), 2.41 (s, 3H), 1.98 (s, 3H), 1.91 (s, 3H), 1.90 – 1.85 (m, 4H) ppm.

^{13}C{^{1}H} NMR (126 MHz, $CDCl_3$) δ: 176.4, 176.3, 171.5, 166.7, 145.5, 139.7, 138.3, 136.6, 136.5, 135.6, 134.7, 134.4, 133.3, 131.64, 131.58, 130.2, 129.7, 129.0, 128.8, 128.7, 127.3, 126.9, 126.7, 125.9, 125.4, 124.2, 62.8, 62.7, 62.0, 61.2, 55.9, 55.3, 51.9, 50.9, 37.4, 31.2, 30.9, 15.6, 14.6 ppm.

HRMS (ESI, *m/z*): calc'd for $[C_{46}H_{32}BrNO_6S_2]^+$ $(M+H)^+$ 848.1710, found 848.1728.

Synthesis of Chain-End Functional Control Polymer 15. Synthesized using general procedure C with **14** (10.0 mg, 0.0118 mmol), methyl acrylate (1.50 mL, 16.6 mmol), DMSO (1.50 mL), and Me_6TREN (6.3 μL, 0.024 mmol). Polymerization for 130 min provided the title polymer as a tacky white solid (689 mg, 48%). M_n = 96 kg/mol; $Đ$ = 1.04.

Scheme S2.8. Synthesis of diester cyclopentadiene–maleimide Diels–Alder adduct **2.19.**

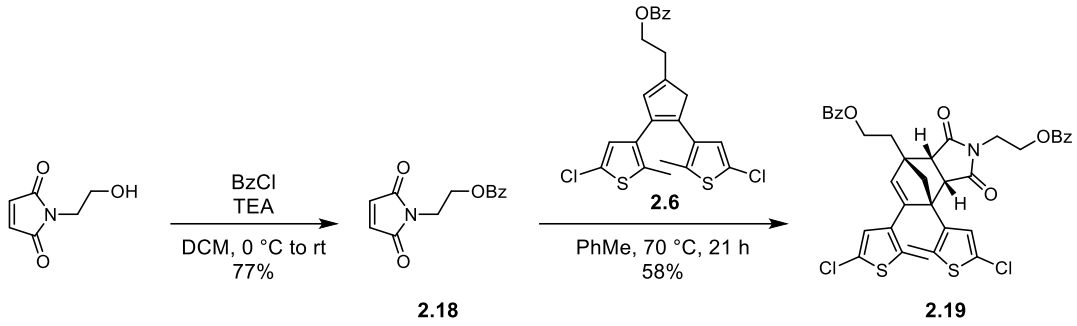

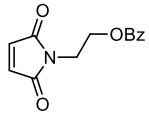

2.18

2-(2,5-dioxo-2,5-dihydro-1H-pyrrol-1-yl)ethyl benzoate (2.18). A flame-dried round bottom flask equipped with an addition funnel was charged with *N*-(2-hydroxyethyl)maleimide (996 mg, 7.06 mmol), DCM (24 mL) and triethylamine (5.00 mL, 35.9 mmol) were added and the solution was cooled to 0 °C in an ice bath. A solution of benzoyl chloride (1.65 mL, 14.2 mmol) in DCM (24 mL) was added dropwise via addition funnel. Immediately following the addition, the reaction was removed from the ice bath and allowed to warm to room temperature. After stirring for 18 h, the organic layer was washed with saturated $NaHCO_3$ (3 x 30 mL) and brine (30 mL). The organic phase was dried with

Na_2SO_4, filtered, and concentrated under vacuum. The crude mixture was purified by silica gel chromatography (0–25% EtOAc/hexanes) to provide the title compound as a light yellow solid (1.33 g, 77%).

TLC (25% EtOAc/hexanes): R_f = 0.41

^{1}H NMR (300 MHz, $CDCl_3$) δ: 8.02–7.94 (m, 2H), 7.59–7.51 (m, 1H), 7.47–7.39 (m, 2H), 6.73 (s, 2H), 4.48–4.41 (m, 2H), 3.99–3.92 (m, 2H) ppm.

$^{13}C\{^1H\}$ NMR (126 MHz, $CDCl_3$) δ: 170.5, 166.5, 134.4, 133.3, 129.8, 129.7, 128.6, 62.3, 37.0 ppm.

HRMS (FAB, *m/z*): calc'd for $[C_{13}H_{12}NO_4]^+$ $(M+H)^+$ 246.0761, found 246.0761

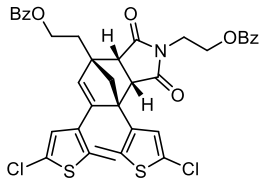

2.19

((3aR,4S,7S,7aS)-6,7-bis(5-chloro-2-methylthiophen-3-yl)-1,3-dioxo-3,3a,7,7a-tetrahydro-1H-4,7-methanoisoindole-2,4-diyl)bis(ethane-2,1-diyl) dibenzoate (19). A flame-dried round bottom flask was charged with **2.18** (59 mg, 0.241 mmol) and then sealed and evacuated and refilled with N_2 3×. A solution of **2.6** (101 mg, 0.212 mmol) in toluene (2.0 mL) was added and the reaction was heated to 70 °C for 21 h. After cooling to room temperature, the reaction was filtered and the collected solids were washed with toluene to yield the title compound as a white solid. A second crop was isolated from the filtrate and recrystallized from toluene to provide additional product as a white solid (88 mg combined, 58%).

TLC (25% EtOAc/hexanes): R_f = 0.16

^{1}H NMR (500 MHz, $CDCl_3$) δ: 7.97 (ddd, 4H, *J* = 16.4, 8.4, 1.4 Hz), 7.59–7.53 (m, 2H), 7.49–7.39 (m, 4H), 7.35 (s, 1H), 6.10 (s, 1H), 5.80 (s, 1H), 4.66–4.50 (m, 2H), 4.19–4.11 (m, 1H), 3.94–3.81 (m, 3H), 3.72–3.63 (m, 1H), 3.41 (d, 1H, *J* = 7.8 Hz), 2.82–2.73 (dt, 1H, *J* = 14.9, 6.0 Hz), 2.52–2.40 (m, 2H), 1.84 (s, 3H), 1.80 (s, 1H), 1.76 (dd, 1H, *J* = 9.0, 1.1 Hz) ppm.

^{13}C{^{1}H} NMR (101 MHz, $CDCl_3$) δ: 176.3, 176.1, 166.5, 165.6, 144.3, 135.1, 134.8, 133.6, 133.3, 133.0, 130.2, 130.0, 129.8, 129.62, 129.58, 128.58, 128.55, 125.8, 124.9, 124.8, 62.4, 61.9, 61.6, 61.5, 55.0, 51.7, 50.3, 37.4, 31.1, 14.4, 14.2 ppm.

HRMS (FAB, *m/z*): calc'd for $[C_{37}H_{31}Cl_2NO_6S_2]^{+\cdot}$ $(M)^{+\cdot}$ 719.0970, found 719.0991.

Scheme S2.9. Synthesis of mechanophore-crosslinked active PMA network **2.20.**

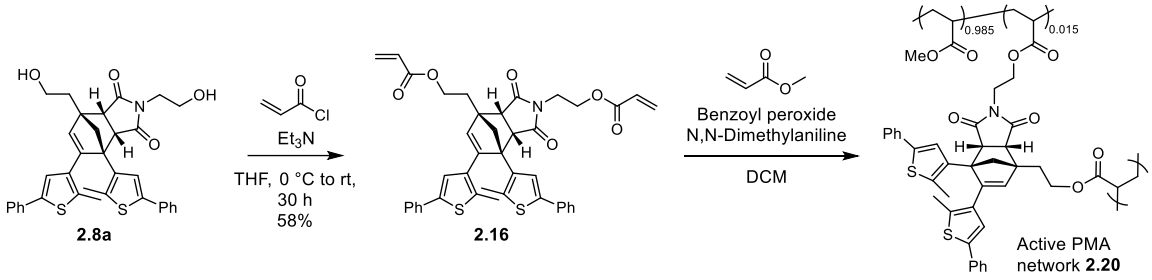

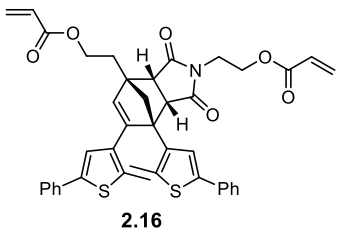

2.16

((3aR,4S,7S,7aS)-6,7-bis(2-methyl-5-phenylthiophen-3-yl)-1,3-dioxo-3,3a,7,7a-tetrahydro-1H-4,7-methanoisoindole-2,4-diyl)bis(ethane-2,1-diyl) diacrylate (2.16). Synthesized using general procedure B with **2.9c** (100 mg, 0.168 mmol), acryloyl chloride (68 μL, 0.84 mmol) and triethylamine (160 μL, 1.15 mmol) in dry THF (2.0 mL). The reaction stirred for 30 h before it was worked up and purified by silica gel chromatography (0–50% EtOAc/hexanes) to yield the title compound as a white solid (69 mg, 58%).

TLC (25% EtOAc/hexanes): R_f = 0.16

^{1}H NMR (500 MHz, $CDCl_3$) δ: 7.92 (s, 1H), 7.64 (dd, 2H, *J* = 8.1, 1.2 Hz), 7.41 (t, 2H, *J* = 7.7 Hz), 7.30 (t, 1H, *J* = 7.3 Hz), 7.20 (dd, 2H, *J* = 7.6, 1.9 Hz), 7.15 – 7.06 (m, 3H), 6.59 (s, 1H), 6.44 (dd, 1H, *J* = 17.3, 1.4 Hz), 6.31 (dd, 1H, *J* = 17.2, 1.5 Hz), 6.14 (dd, 1H, *J* = 17.3, 10.4 Hz), 5.97 (s, 1H), 5.93 – 5.84 (m, 2H), 5.74 (dd, 1H, *J* = 10.4, 1.5 Hz), 4.50 (t, 2H, *J* = 6.4 Hz), 4.12 (d, 1H, *J* = 7.8 Hz), 4.05 – 3.97 (m, 1H), 3.82 – 3.74 (m, 1H), 3.66 – 3.56 (m, 2H), 3.40 (d, 1H, *J* = 7.8 Hz), 2.71 (dt, 1H, *J* = 14.8, 6.3 Hz), 2.59 (d, 1H, *J* = 9.0 Hz), 2.44 (s, 3H), 2.40 (dt, 1H, *J* = 15.1, 6.7 Hz), 2.02 (s, 3H), 1.83 (d, 1H, *J* = 9.0 Hz) ppm.

^{13}C{^{1}H} NMR (126 MHz, $CDCl_3$) δ: 176.5, 176.4, 166.2, 165.6, 145.4, 139.7, 138.4, 136.41, 136.38, 135.6, 134.7, 134.4, 131.7, 131.5, 131.31, 131.28, 129.0, 128.8, 128.4, 128.0, 127.3, 126.9, 126.6, 125.9, 125.4, 124.2, 62.2, 62.0, 61.3, 61.1, 55.1, 51.6, 50.8, 37.5, 31.0, 15.6, 14.6 ppm.

HRMS (ESI, *m/z*): calc'd for $[C_{42}H_{40}BrNO_6S_2Na]^+$ $(M+Na)^+$ 726.1954, found 726.1954.

Synthesis of Active PMA network 2.20. Bis-acrylate functionalized mechanophore crosslinker **2.16** (50 mg, 0.071 mmol, 1.5 mol%) and benzoyl peroxide (3.9 mg, 0.016 mmol) were combined in a scintillation vial with a stir bar. The atmosphere was purged with N_2 for 10 min, after which methyl acrylate (420 μL, 4.63 mmol) was added and the mixture was stirred until homogeneous. N,N-dimethylaniline (4.0 μL, 0.032 mmol) was added via microsyringe and the solution was stirred again for 3 minutes, after which the vial was cooled to 8 °C for 22 h. The material was subsequently dried under vacuum for 2 days to yield a clear, slightly yellow polymer.

Scheme **S2.10.** Synthesis of control PMA network **2.21**

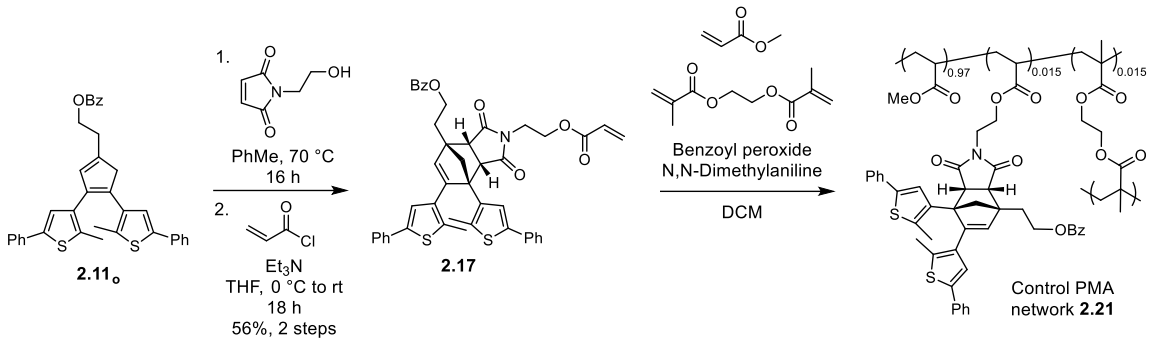

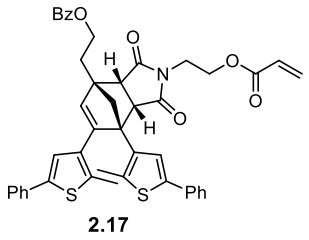

2-((3aR,4S,7S,7aS)-2-(2-(acryloyloxy)ethyl)-6,7-bis(2-methyl-5-phenylthiophen-3-yl)-1,3-dioxo-1,2,3,3a,7,7a-hexahydro-4H-4,7-methanoisoindol-4-yl)ethyl benzoate (2.17). A flame-dried round bottom flask was charged with *N*-(2-hydroxyethyl)maleimide (53 mg, 0.38 mmol) and the atmosphere was evacuated and refilled with N_2 3×. A solution of **2.11o** (93 mg, 0.166 mmol) in dry toluene (3.0 mL)was added and the reaction was stirred at 70 °C for 16 h. The reaction was then cooled to room temperature and concentrated in vacuo. Then, the crude mixture was dissolved in dry THF (3.0 mL) and esterified according to general procedure B with acryloyl chloride (45 μL, 0.56 mmol) and triethylamine (130 μL, 0.933 mmol). It stirred for 18 h before being worked up and purified by silica gel chromatography (0–50% EtOAc/hexanes) to yield a light brown solid. It was recrystallized from acetone to yield the title compound as colorless crystals (73 mg, 56% over 2 steps).

TLC (50% EtOAc/hexanes): R_f = 0.48

^{1}H NMR (500 MHz, $CDCl_3$) δ: 8.09 – 9.03 (m, 2H), 7.92 (s, 1H), 7.66 – 7.61 (m, 2H), 7.60 – 7.55 (m, 1H), 7.45 (t, 2H, *J* = 7.7 Hz), 7.41 (t, 2H, *J* = 7.7 Hz), 7.33 – 7.27 (m, 1H), 7.21 – 7.16 (m, 2H), 7.22 – 7.06 (m, 3H), 6.58 (s, 1H), 6.30 (dd, 1H, *J* = 17.3, 1.5 Hz), 6.01 (s, 1H), 5.88 (dd, 1H, *J* = 17.3, 10.4 Hz), 5.72 (dd, 1H, *J* = 10.5, 1.4 Hz), 4.72 – 4.62 (m, 2H), 4.12 (d, 1H, *J* = 7.8 Hz), 4.05 – 3.98 (m, 1H), 3.78 (ddd, 1H, *J* = 11.4, 6.5, 4.8 Hz), 3.67 – 3.56 (m, 2H), 3.44 (d, 1H, *J* = 7.7 Hz), 2.82 (dt, 1H, *J* = 14.8, 6.0 Hz), 2.67 (d, 1H, *J* = 9.0 Hz), 2.50 (dt, 1H, *J* = 14.3 Hz, 6.6 Hz), 2.38 (s, 3H), 1.97 (s, 3H), 1.88 (d, 1H, *J* = 9.0 Hz) ppm.

$^{13}C\{^{1}H\}$ NMR (126 MHz, $CDCl_3$) δ: 176.5, 176.4, 166.7, 165.6, 145.5, 139.7, 138.3, 136.48, 136.47, 135.6, 134.7, 134.4, 133.3, 131.7, 131.4, 131.3, 130.2, 129.7, 129.0, 128.8, 128.7, 128.0, 127.3, 126.9, 126.7, 126.0, 125.4, 124.2, 62.7, 62.1, 61.3, 61.2, 55.2, 51.8, 50.8, 37.6, 31.2, 15.6, 14.6 ppm.

HRMS (ESI, *m/z*): calc'd for $[C_{45}H_{40}NO_6S_2]^+$ $(M+H)^+$ 754.2292, found 754.2296.

Synthesis of Control PMA network 2.21. A scintillation vial was charged with benzoyl peroxide (2.3 mg, 0.0095 mmol) and the atmosphere was purged with N_2 for 10 min. Ethylene glycol dimethacrylate (11.8 μL, 0.063 mmol, 1.5 mol %) and methyl acrylate (380 mL, 4.19 mmol) were added, followed by **2.17** (47 mg, 0.062 mmol, 1.5 mol %) as a solution in dry DCM (300 μL). The mixture was stirred until homogeneous, then N,N-dimethylaniline (1.6 μL, 0.013 mmol) was added and the solution was stirred for 3 min. The vial was kept at 8 °C for 23 h, after which the material was dried under vacuum for 4 days to yield a clear, light brown polymer.

GPC Chromatograms of All Polymers

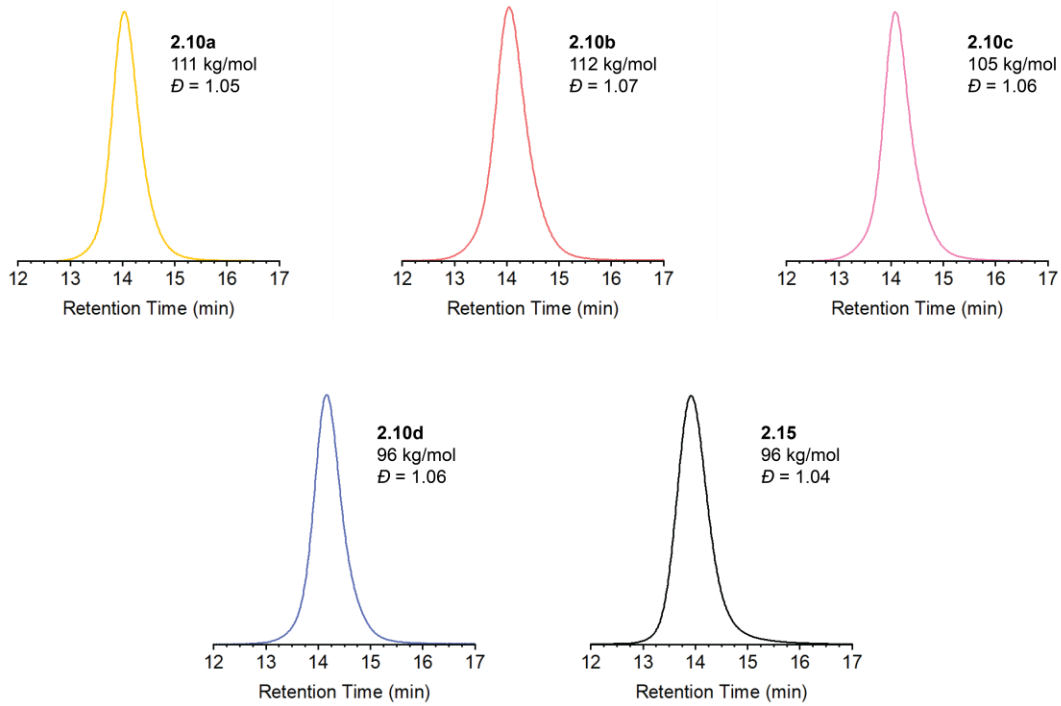

Figure S2.11. GPC traces (refractive index response), M_n, and dispersity ($Đ$) for functional polymers **2.10a–d** and chain-end functional control polymer **2.15**.

DFT Calculations

CoGEF calculations were performed using Spartan ′18 Parallel Suite according to previously reported methods.[34,35] Ground state energies were calculated using DFT at the B3LYP/6-31G* level of theory. For each model, an initial equilibrium conformer calculation was performed using Molecular Mechanics (MMFF), followed by an unconstrained equilibrium geometry calculation. Starting from the equilibrium geometry of the unconstrained molecules (energy = 0 kJ/mol), the distance between the terminal methyl groups of the truncated structures was increased in increments of 0.05 Å and the energy was minimized at each step. Calculations were run until a chemical transformation was predicted to occur, as evidenced by the rupture and reorganization of one or more covalent bonds. The maximum force associated with the mechanochemical reaction was calculated from the slope

of the curve immediately prior to the predicted chemical reaction. For all four truncated structures, a formal retro- [4+2] cycloaddition reaction was predicted with a maximum force of 4.9 nN.

Energy calculations were performed on three possible cyclopentadiene tautomers shown in **Scheme 2.3** using Spartan ′18 Parallel Suite. Simplified structures with benzoate esters replaced by acetate esters were investigated to establish the relative energies of each tautomer. Equilibrium geometries and the corresponding Gibbs free energy for each tautomer were calculated at the M06-2X/6-31G* level of theory.

Details for Sonication/Photoirradiation Experiments

An oven-dried sonication vessel was fitted with a Teflon screw cap sealed with an O-ring and was allowed to cool under a stream of dry Ar. The probe tip was situated 1 cm above the bottom of the sonication vessel. The vessel was charged with a solution of the polymer in dry THF (2.0 mg/mL, 20.0–25.0 mL) and immersed in an ice/water bath. The solution was sparged continuously with Ar beginning 15 min prior to sonication and for the duration of the sonication experiment. Pulsed ultrasound (1 s on/2 s off, 25% amplitude, 20 kHz, 11.6 W/cm^2) was then applied to the system. At 15 minute intervals of sonication time, aliquots were removed from the sonication vessel and analyzed by UV-vis absorption spectroscopy. The solution in the cuvette was then irradiated with 311 nm UV light for 60 s and the sample was reanalyzed by UV-vis spectroscopy. Ultrasonication intensity was calibrated using the method described by Berkowski et al.[41]

Photographs of Solutions of Polymers 2.10a and 2.10b (2 mg/mL)

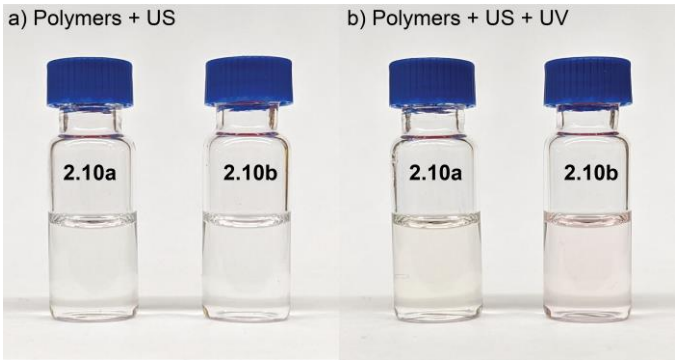

Figure S2.12. (a) Photographs of solutions of polymers **2.10a** and **2.10b** at their original concentrations (2 mg/mL in THF) after being subjected to ultrasonication (120 min), and (b) the same solutions after irradiation with UV light (311 nm, 120 s).

^{1}H and ^{13}C NMR Spectra

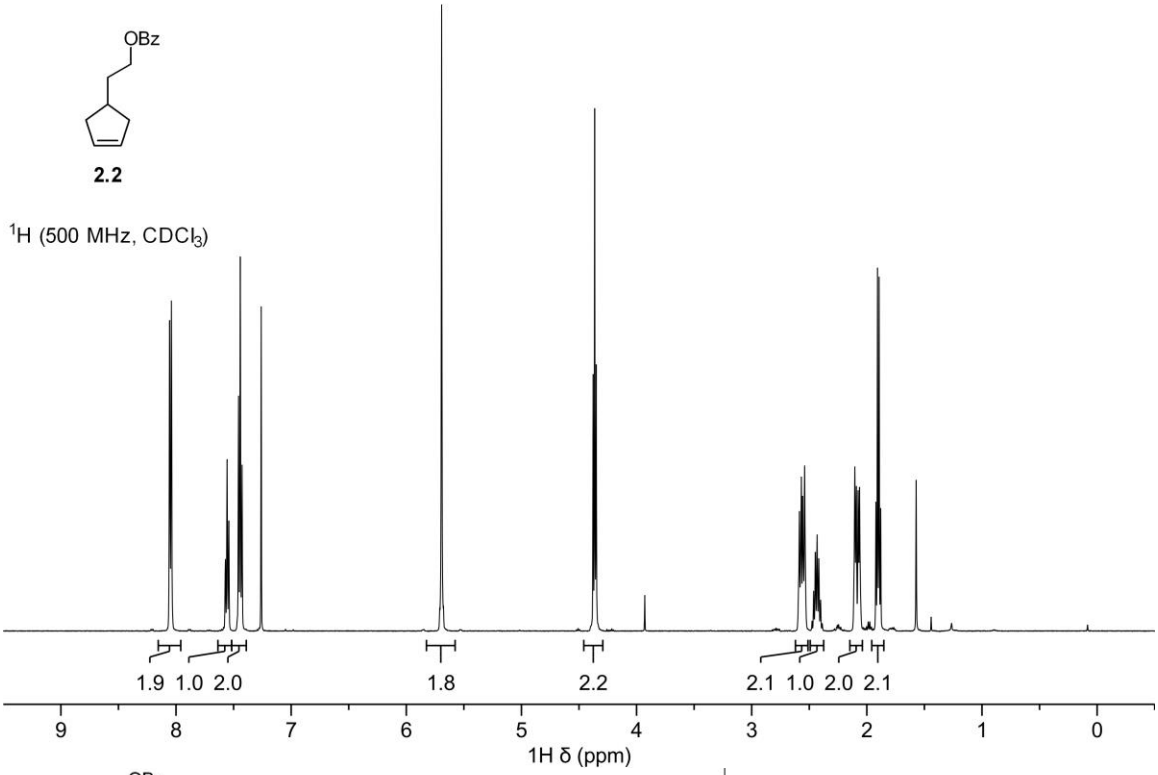

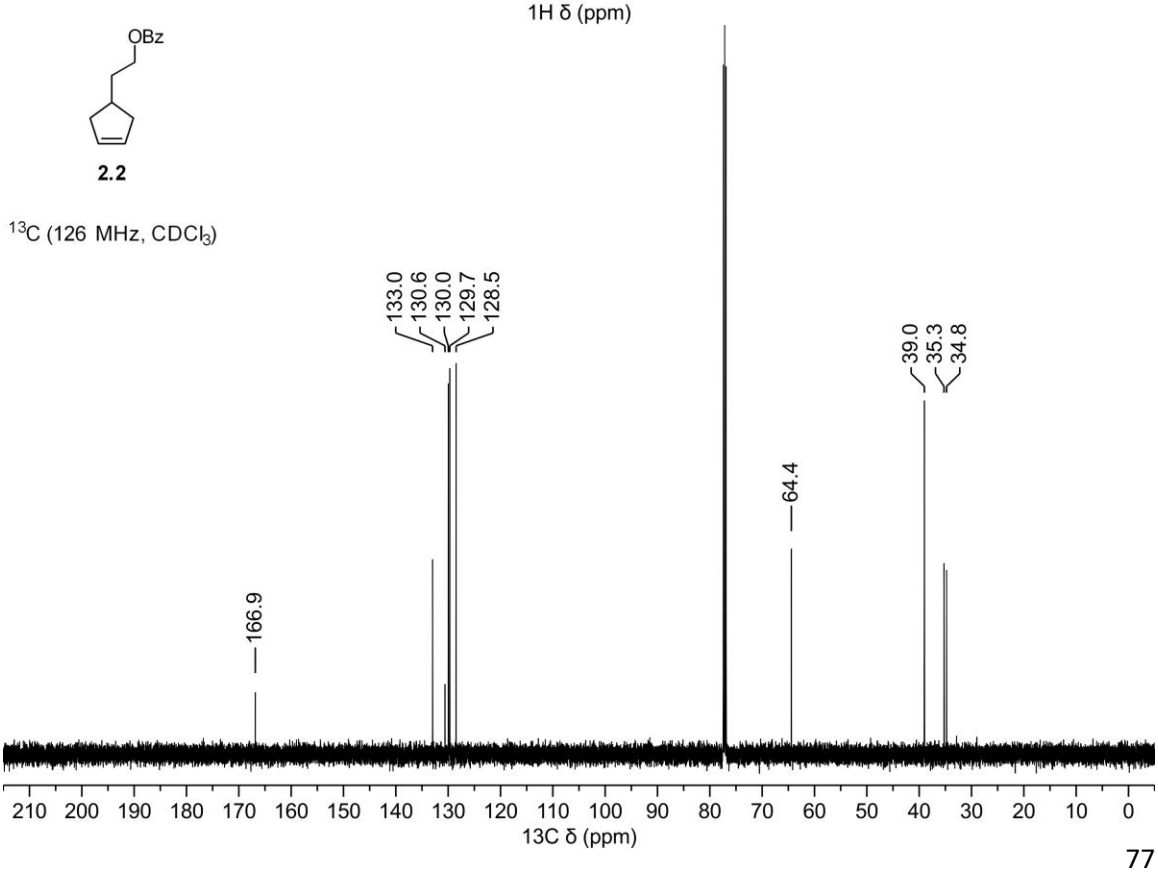

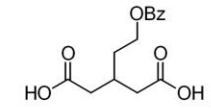

2.3

^{1}H (400 MHz, CD_3OD)

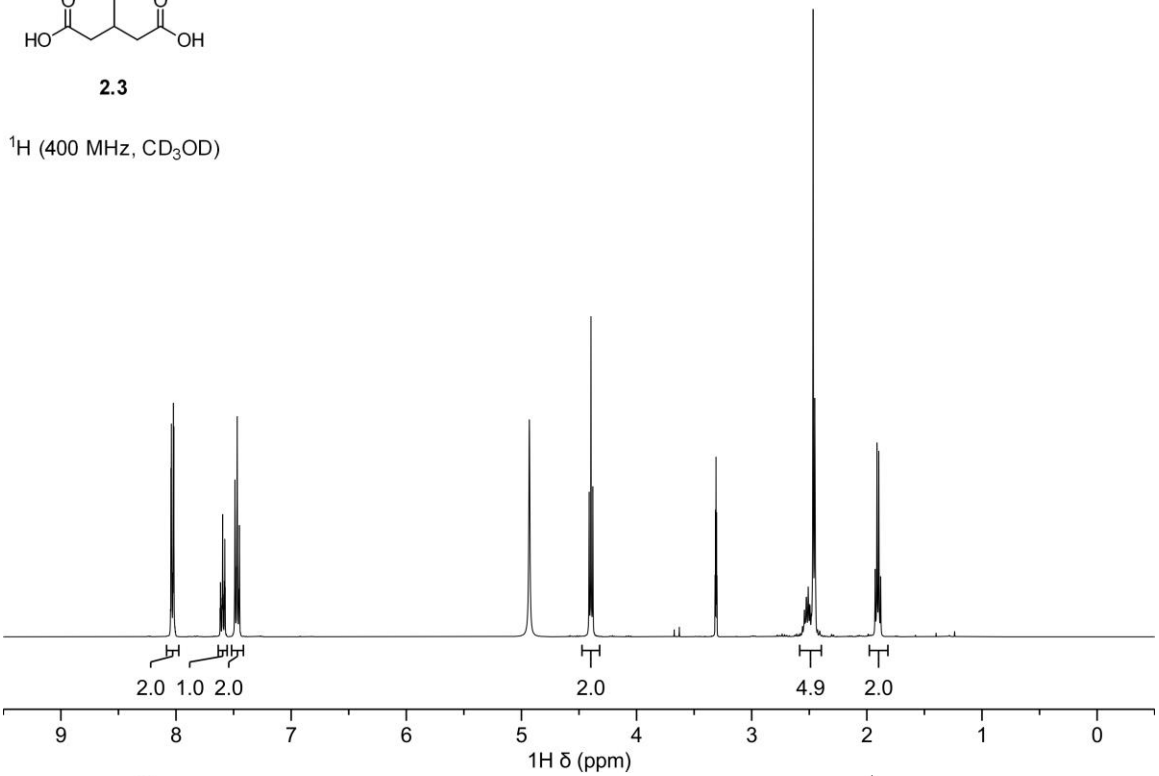

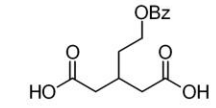

2.3

^{13}C (126 MHz, CD_3OD)

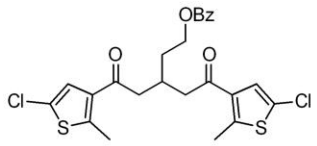

2.4

^{1}H (400 MHz, $CDCl_3$)

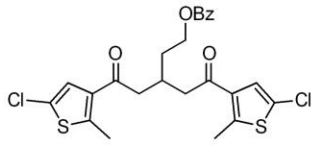

2.4

^{13}C (101 MHz, $CDCl_3$)

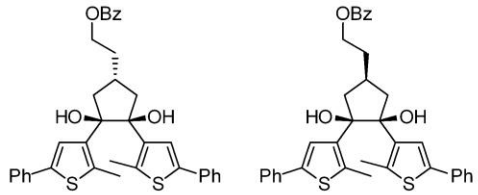

2.5 (major)

2.5' (*minor)

^{1}H (400 MHz, $CDCl_3$)

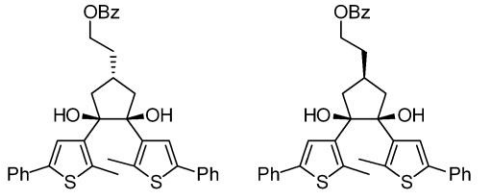

2.5 (major)

2.5' (*minor)

^{13}C (101 MHz, $CDCl_3$)

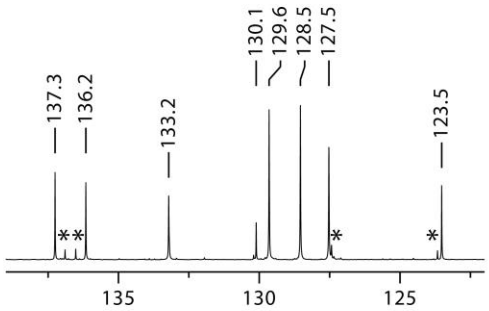

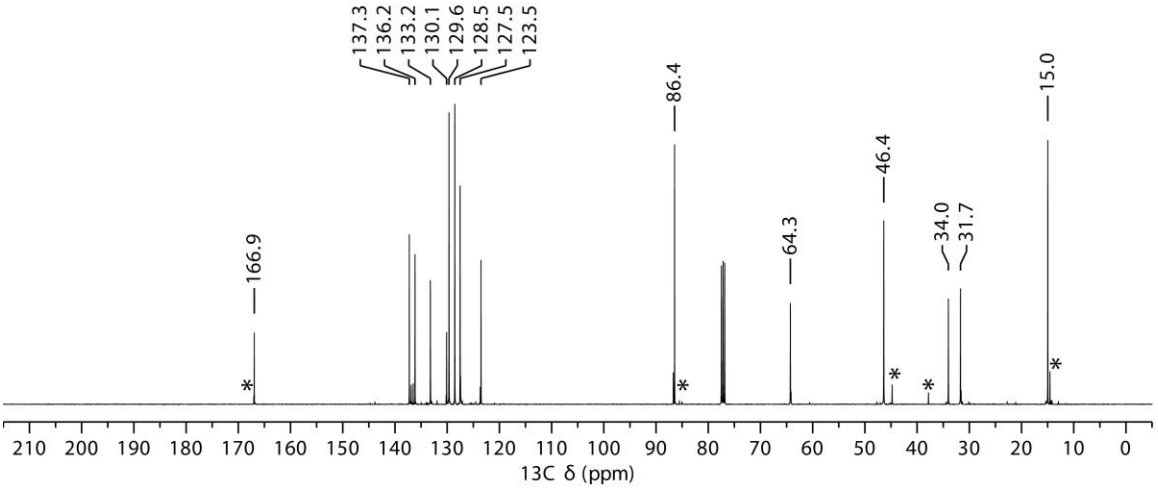

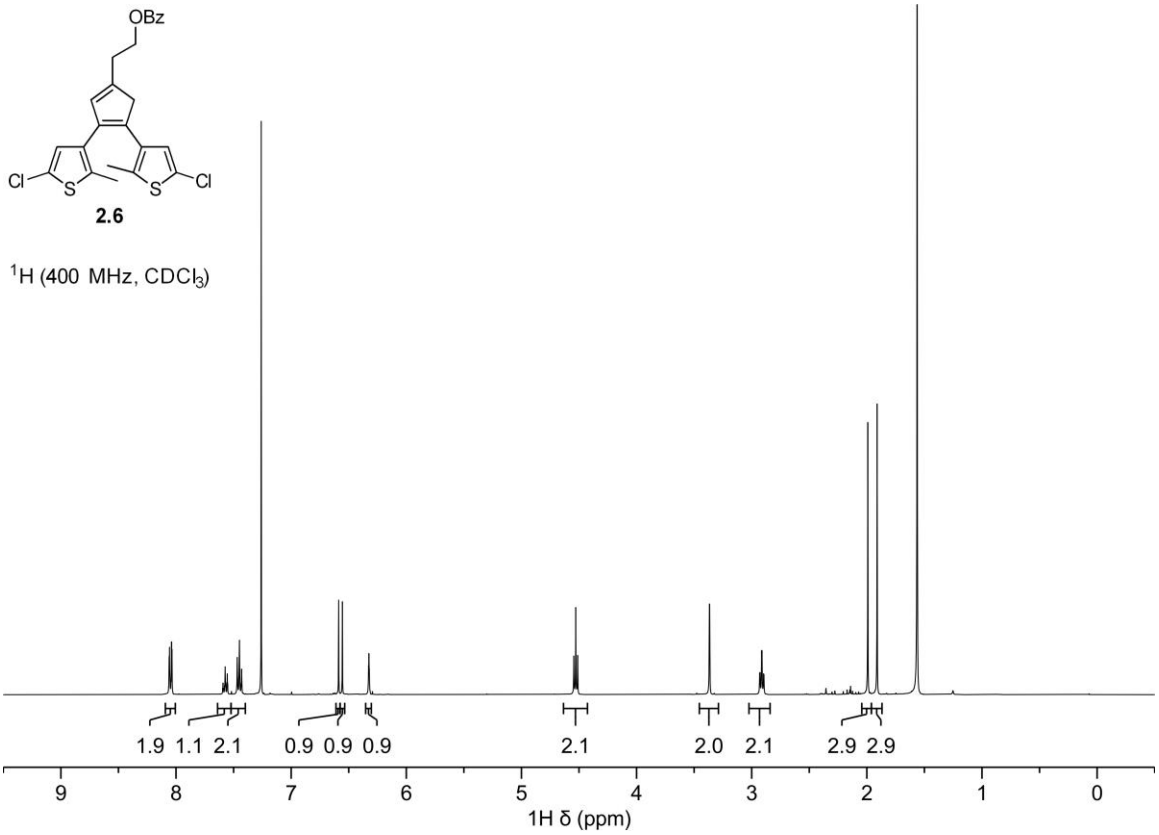
OBz
Cl
S
S
Cl
2.6
1H (400 MHz, CDCl3)
1.9 1.1 2.1 0.9 0.9 0.9 2.1 2.0 2.1 2.9 2.9
9 8 7 6 5 4 3 2 1 0
1H δ (ppm)

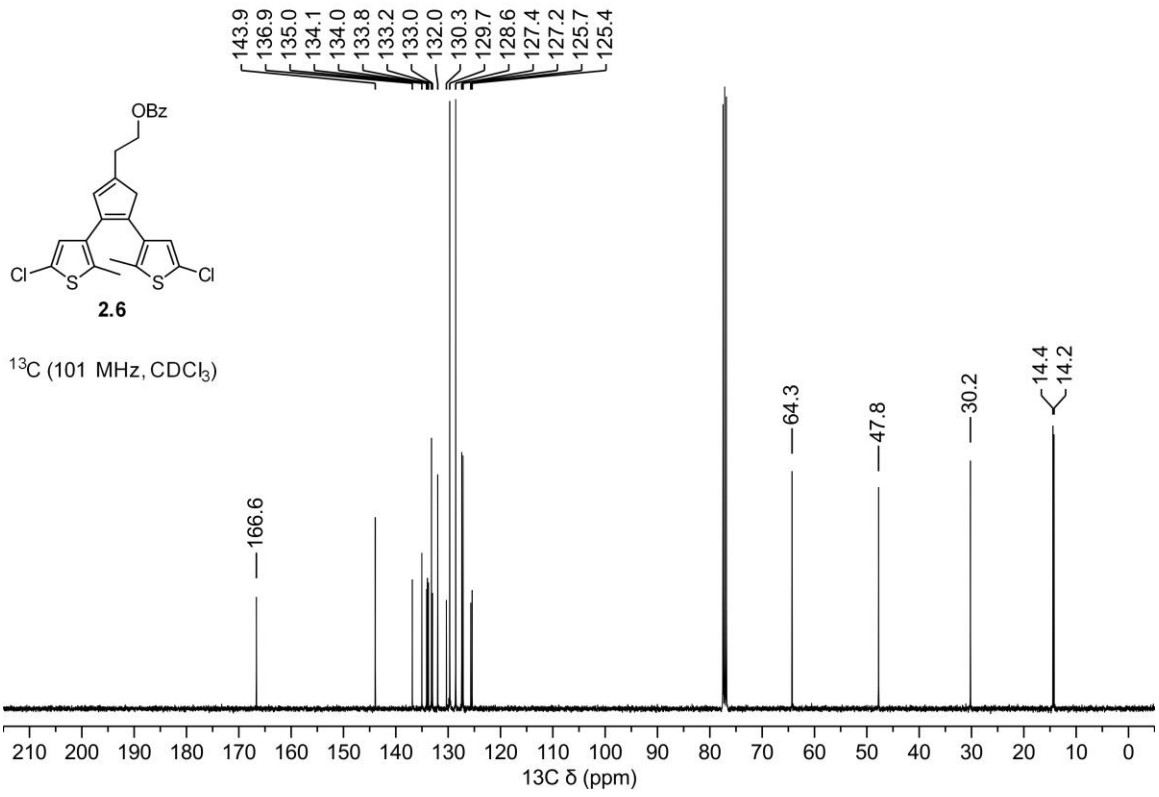
143.9
136.9
135.0
134.1
134.0
133.8
133.2
133.0
132.0
130.3
129.7
128.6
127.4
127.2
125.7
125.4
OBz
Cl
S
S
Cl
2.6
13C (101 MHz, CDCl3)
166.6
64.3
47.8
30.2
14.4
14.2
210 200 190 180 170 160 150 140 130 120 110 100 90 80 70 60 50 40 30 20 10 0
13C δ (ppm)

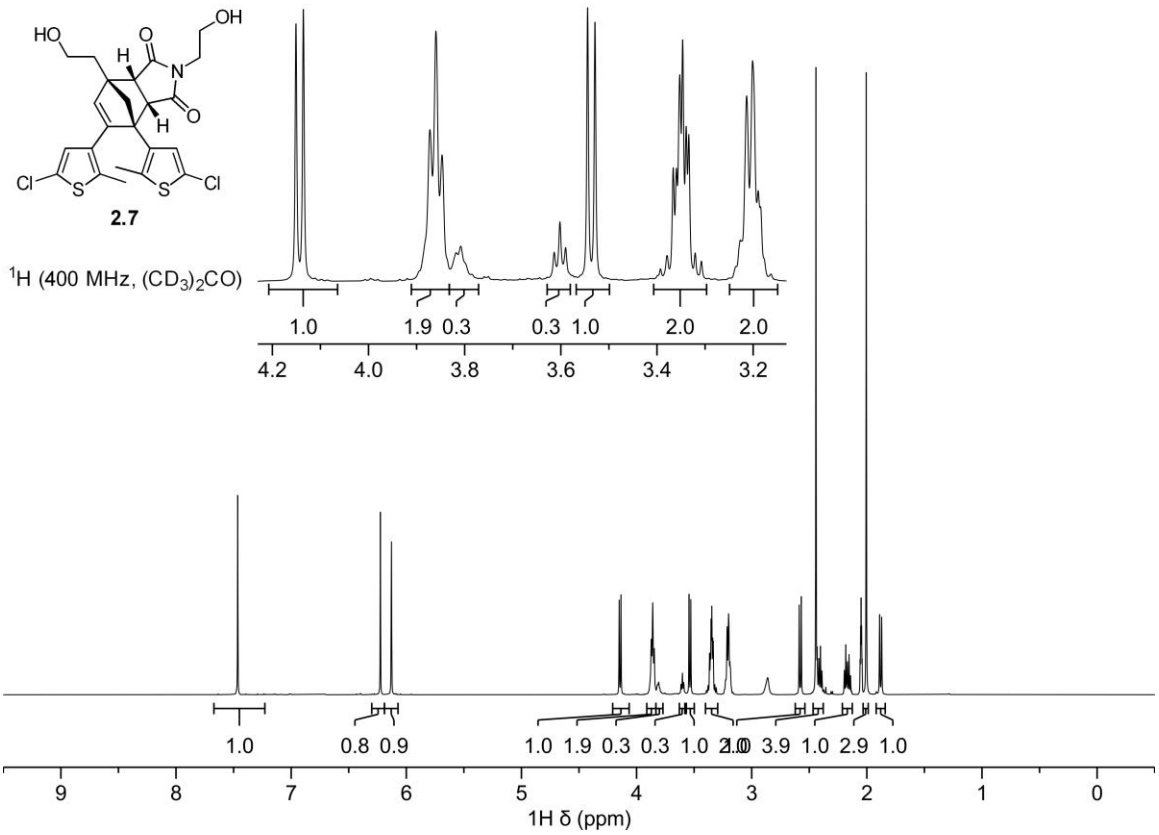
HO
OH
O
H
N
O
H
Cl
S
S
Cl
2.7
1H (400 MHz, (CD3)2CO)
1.0
1.9 0.3
0.3 1.0
2.0
2.0
4.2
4.0
3.8
3.6
3.4
3.2
1.0
0.8 0.9
1.0 1.9 0.3 0.3 1.0 2.0 3.9 1.0 2.9 1.0
9
8
7
6
5
4
3
2
1
0
1H δ (ppm)

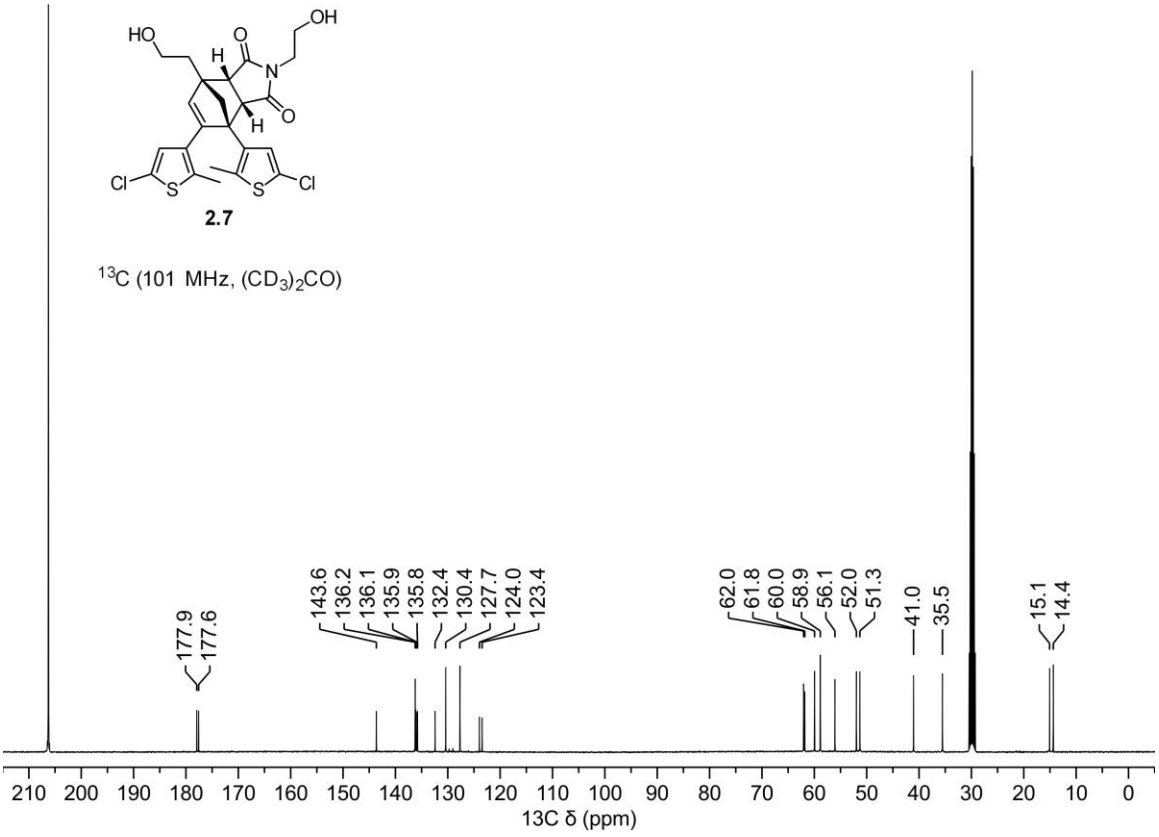
HO
OH
O
H
N
O
H
Cl
S
S
Cl
2.7
13C (101 MHz, (CD3)2CO)
177.9
177.6
143.6
136.2
136.1
135.9
135.8
132.4
130.4
127.7
124.0
123.4
62.0
61.8
60.0
58.9
56.1
52.0
51.3
41.0
35.5
15.1
14.4
210 200 190 180 170 160 150 140 130 120 110 100 90 80 70 60 50 40 30 20 10 0
13C δ (ppm)

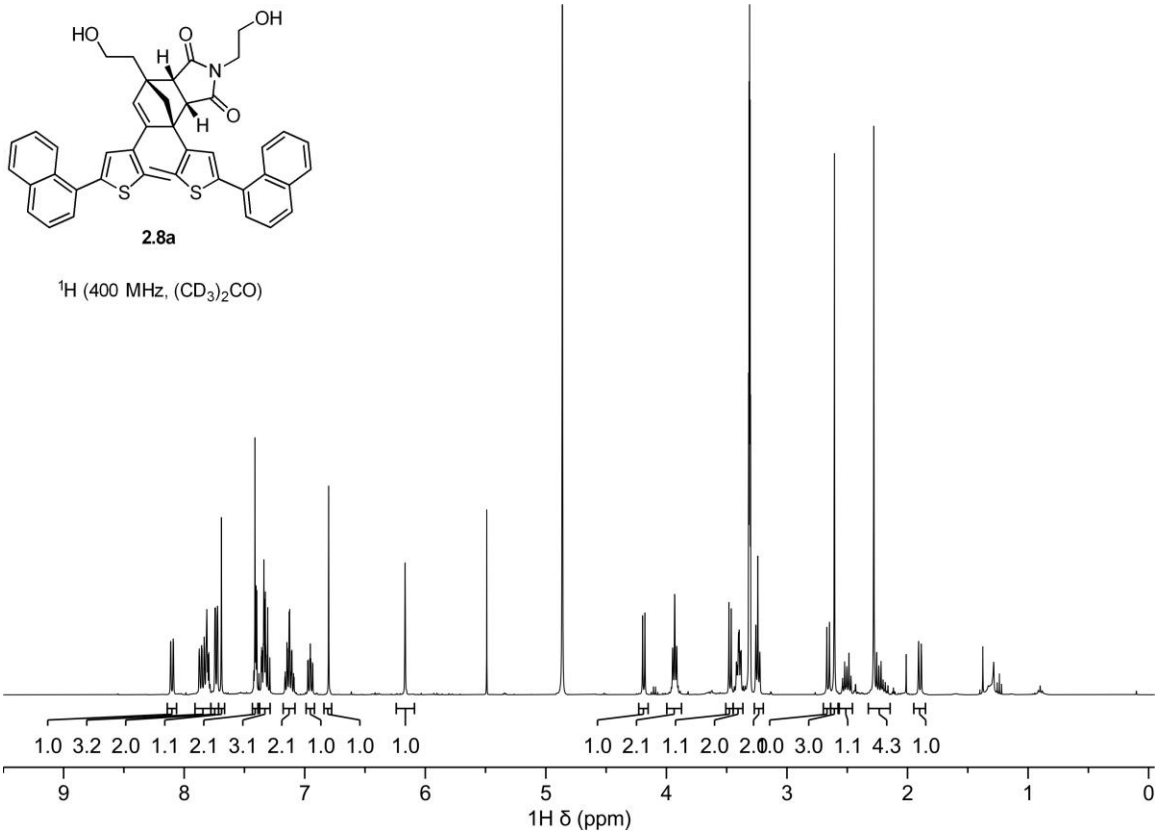
HO
OH
O
N
O
H
H
S
S
2.8a
1H (400 MHz, (CD3)2CO)
1.0 3.2 2.0 1.1 2.1 3.1 2.1 1.0 1.0 1.0
1.0 2.1 1.1 2.0 2.0 3.0 1.1 4.3 1.0
9 8 7 6 5 4 3 2 1 0
1H δ (ppm)

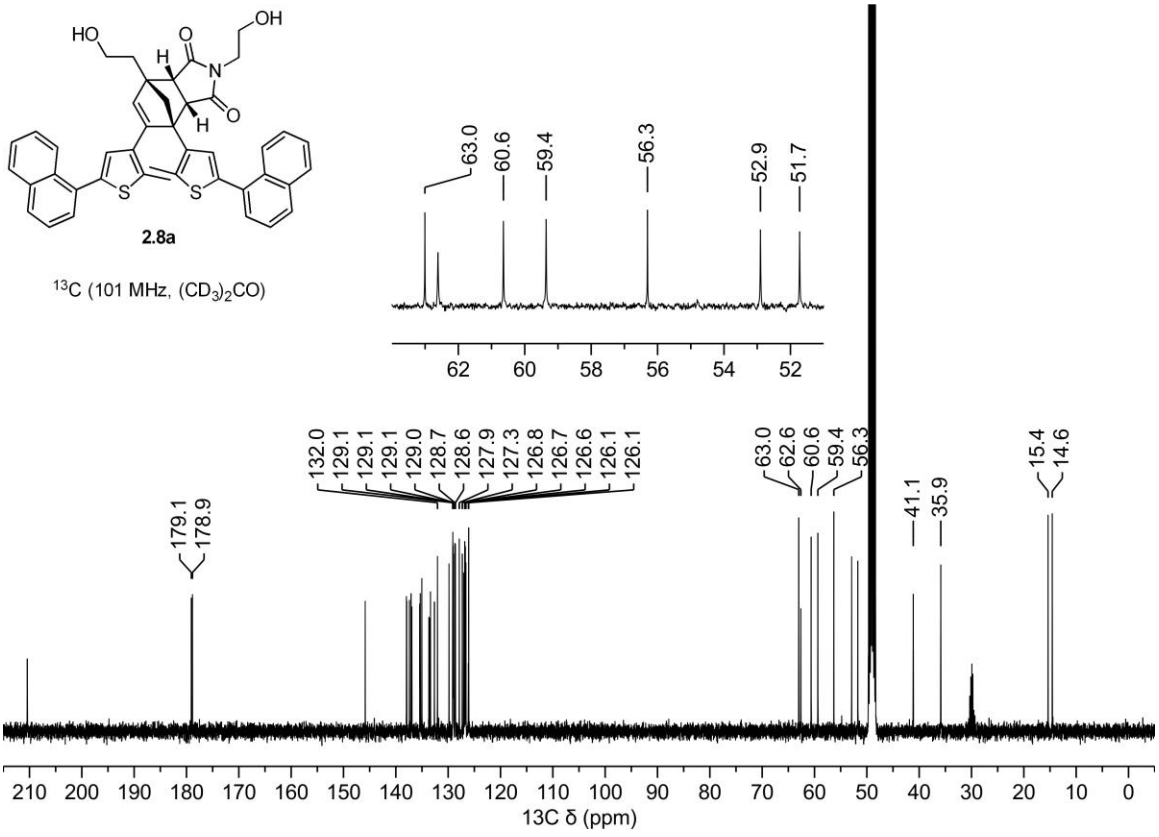
HO
OH
O
N
O
H
H
S
S
2.8a
13C (101 MHz, (CD3)2CO)
63.0
60.6
59.4
56.3
52.9
51.7
62 60 58 56 54 52
132.0
129.1
129.1
129.1
129.0
128.7
128.6
127.9
127.3
126.8
126.7
126.6
126.1
126.1
179.1
178.9
63.0
62.6
60.6
59.4
56.3
41.1
35.9
15.4
14.6
210 200 190 180 170 160 150 140 130 120 110 100 90 80 70 60 50 40 30 20 10 0
13C δ (ppm)

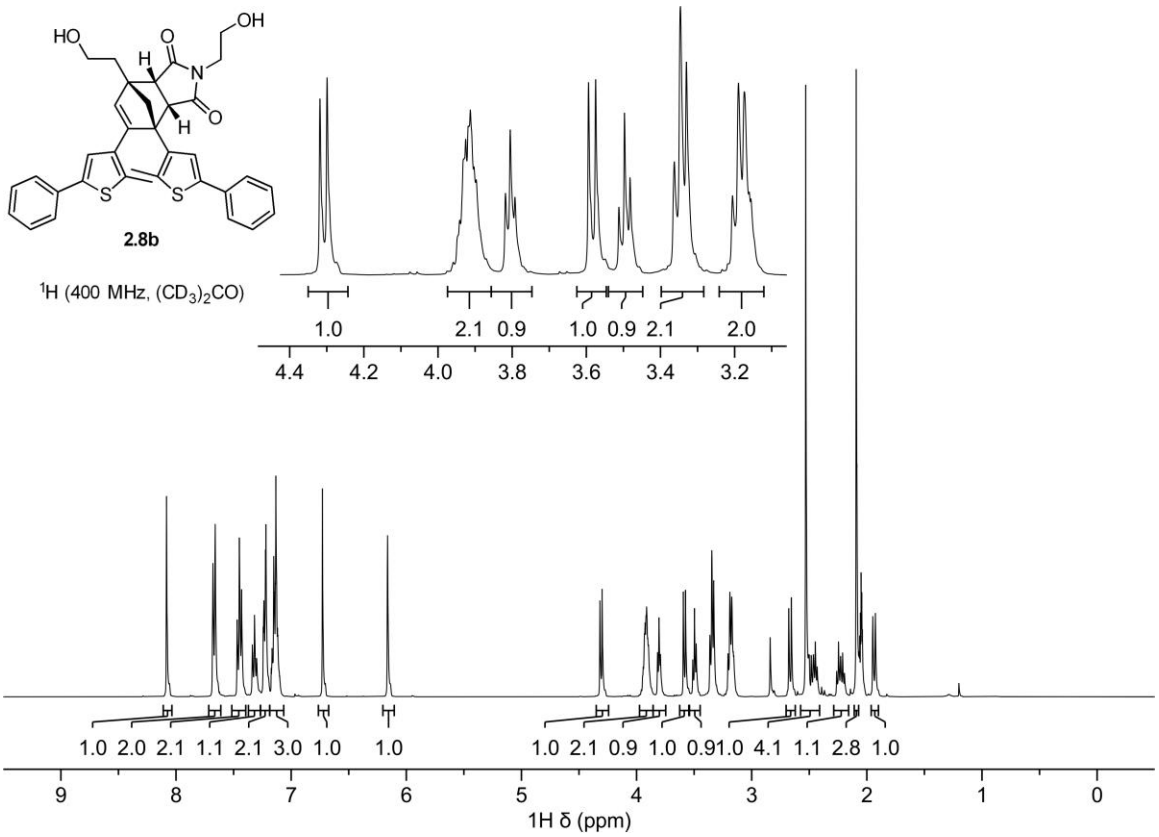
HO
OH
O
N
H
H
S
S
2.8b
^{1}H (400 MHz, $(CD_3)_2CO$)
1.0 2.1 0.9 1.0 0.9 2.1 2.0
4.4 4.2 4.0 3.8 3.6 3.4 3.2
1.0 2.0 2.1 1.1 2.1 3.0 1.0 1.0
1.0 2.1 0.9 1.0 0.91.0 4.1 1.1 2.8 1.0
9 8 7 6 5 4 3 2 1 0
1H δ (ppm)

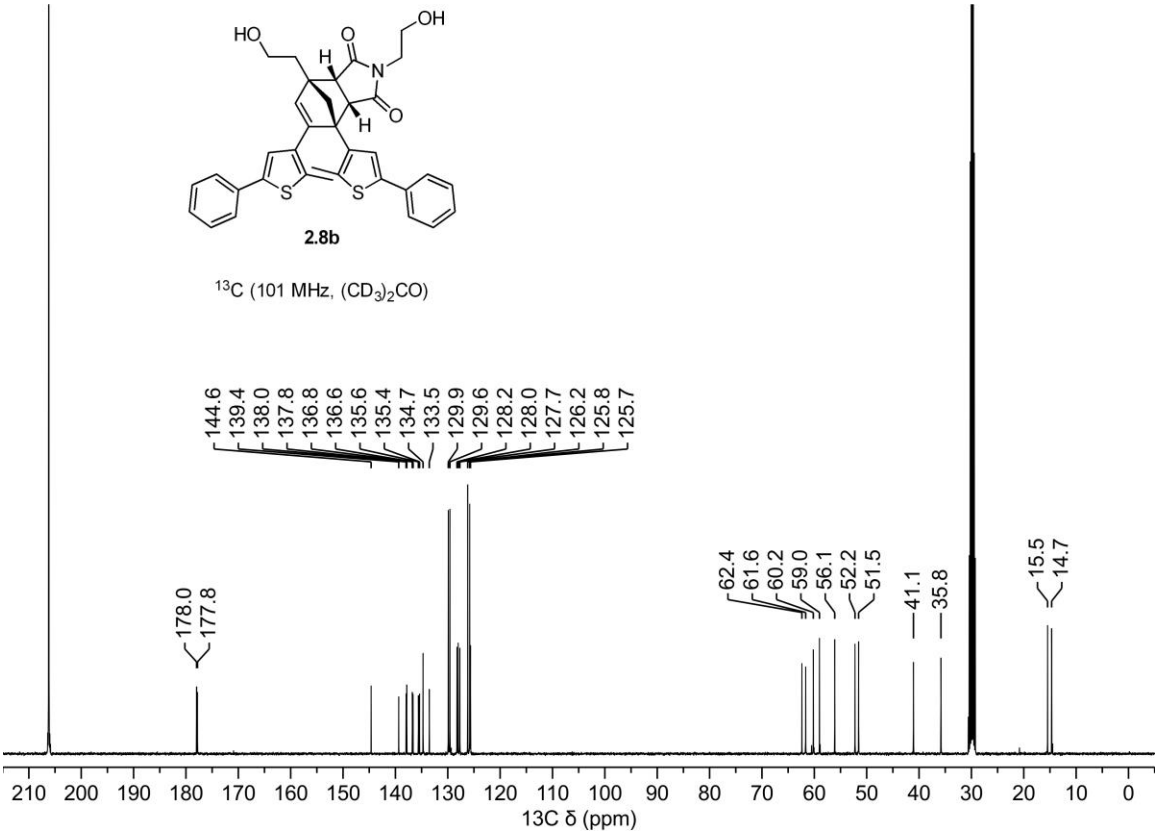
HO
OH
O
N
H
H
S
S
2.8b
^{13}C (101 MHz, $(CD_3)_2CO$)
144.6
139.4
138.0
137.8
136.8
136.6
135.6
135.4
134.7
133.5
129.9
129.6
128.2
128.0
127.7
126.2
125.8
125.7
178.0
177.8
62.4
61.6
60.2
59.0
56.1
52.2
51.5
41.1
35.8
15.5
14.7
210 200 190 180 170 160 150 140 130 120 110 100 90 80 70 60 50 40 30 20 10 0
13C δ (ppm)

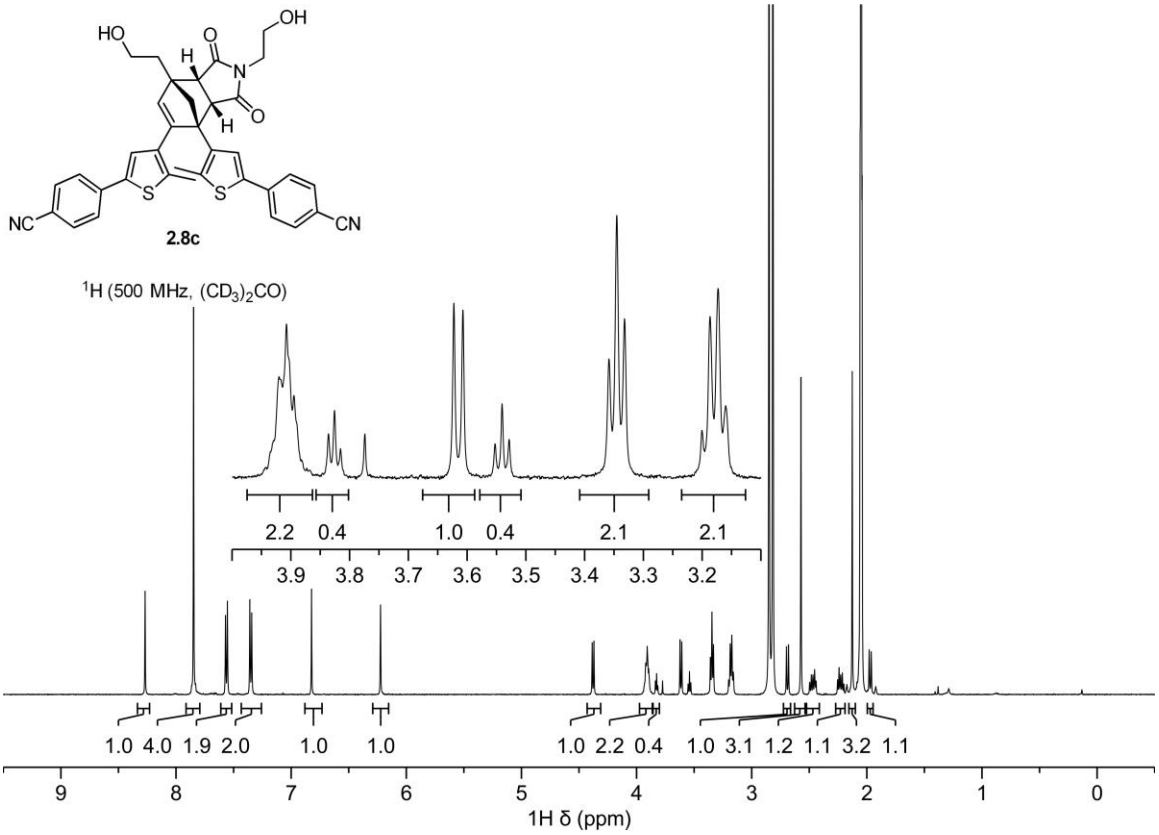
HO
OH
O
H
N
O
H
S
S
NC
CN
2.8c
^{1}H (500 MHz, $(CD_3)_2CO$)
2.2 0.4 1.0 0.4 2.1 2.1
3.9 3.8 3.7 3.6 3.5 3.4 3.3 3.2
1.0 4.0 1.9 2.0 1.0 1.0 1.0 2.2 0.4 1.0 3.1 1.2 1.1 3.2 1.1
9 8 7 6 5 4 3 2 1 0
1H δ (ppm)

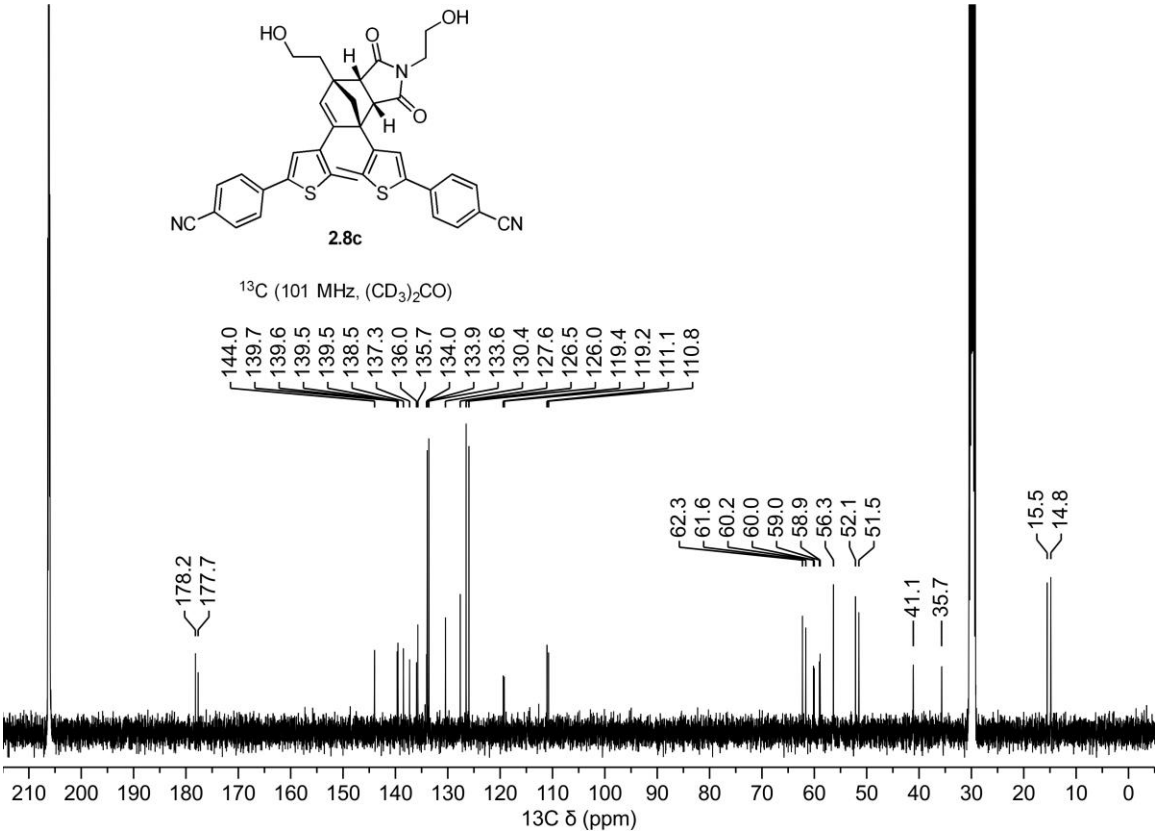
HO
OH
O
H
N
O
H
S
S
NC
CN
2.8c
^{13}C (101 MHz, $(CD_3)_2CO$)
144.0 139.7 139.6 139.5 139.5 138.5 137.3 136.0 135.7 134.0 133.9 133.6 130.4 127.6 126.5 126.0 119.4 119.2 111.1 110.8
178.2 177.7
62.3 61.6 60.2 60.0 59.0 58.9 56.3 52.1 51.5
41.1 35.7
15.5 14.8
210 200 190 180 170 160 150 140 130 120 110 100 90 80 70 60 50 40 30 20 10 0
13C δ (ppm)

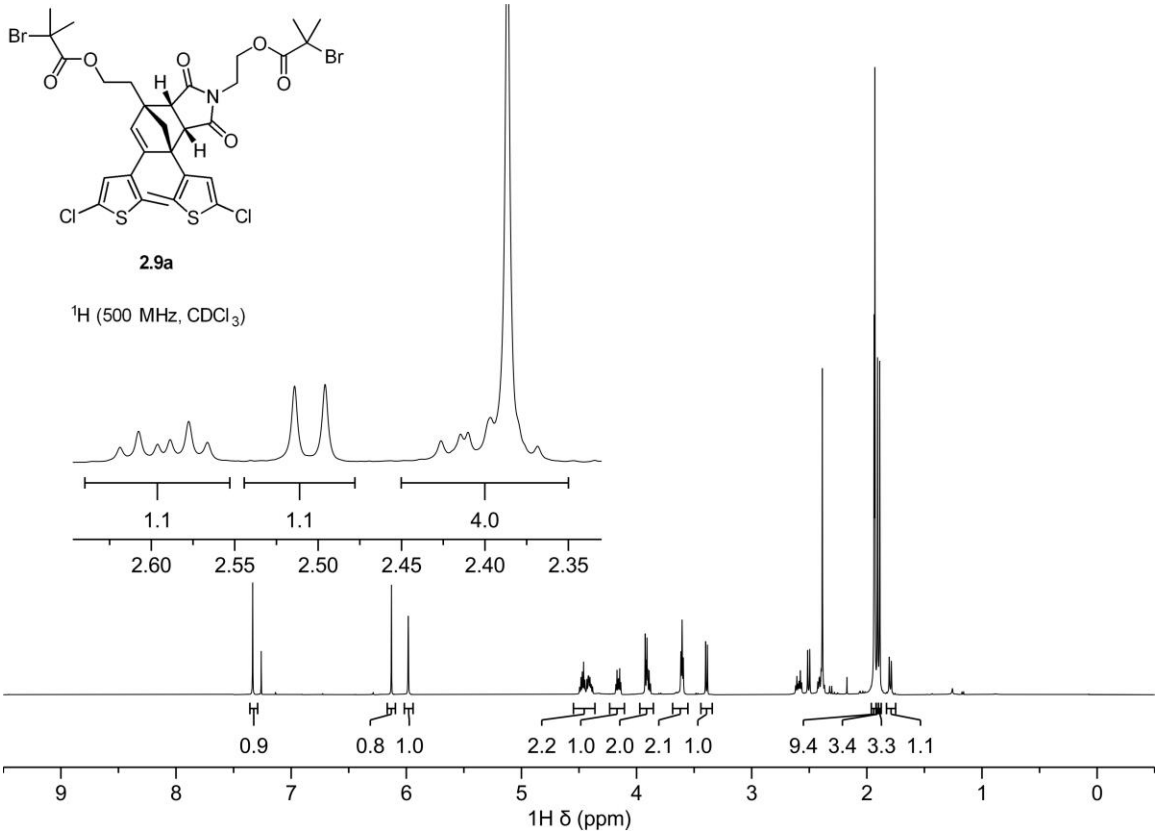
2.9a
1H (500 MHz, CDCl3)
1.1
1.1
4.0
2.60
2.55
2.50
2.45
2.40
2.35
0.9
0.8 1.0
2.2 1.0 2.0 2.1 1.0
9.4 3.4 3.3 1.1
9 8 7 6 5 4 3 2 1 0
1H δ (ppm)

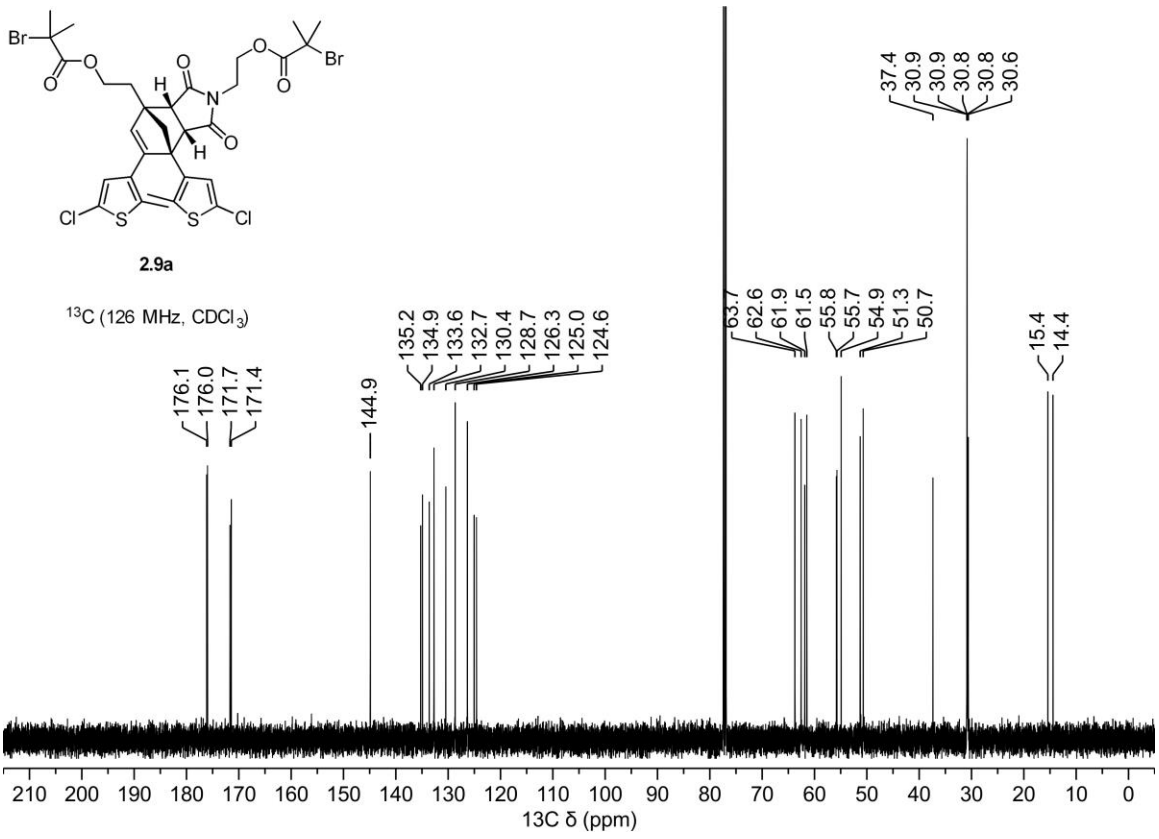
2.9a
13C (126 MHz, CDCl3)
176.1
176.0
171.7
171.4
144.9
135.2
134.9
133.6
132.7
130.4
128.7
126.3
125.0
124.6
63.7
62.6
61.9
61.5
55.8
55.7
54.9
51.3
50.7
37.4
30.9
30.9
30.8
30.8
30.6
15.4
14.4
210 200 190 180 170 160 150 140 130 120 110 100 90 80 70 60 50 40 30 20 10 0
13C δ (ppm)

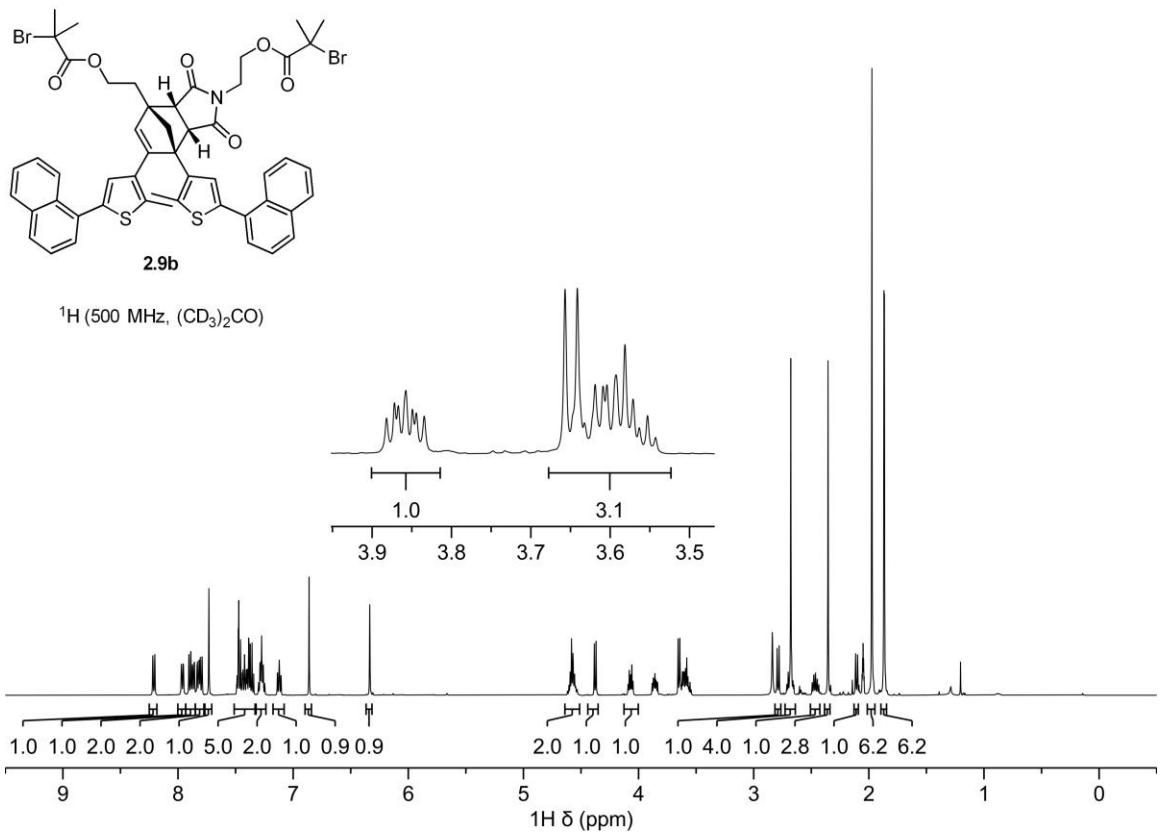
2.9b
^{1}H (500 MHz, $(CD_3)_2CO$)
1.0 3.1
3.9 3.8 3.7 3.6 3.5
1.0 1.0 2.0 2.0 1.0 5.0 2.0 1.0 0.9 0.9
2.0 1.0 1.0 1.0 4.0 1.0 2.8 1.0 6.2 6.2
9 8 7 6 5 4 3 2 1 0
1H δ (ppm)

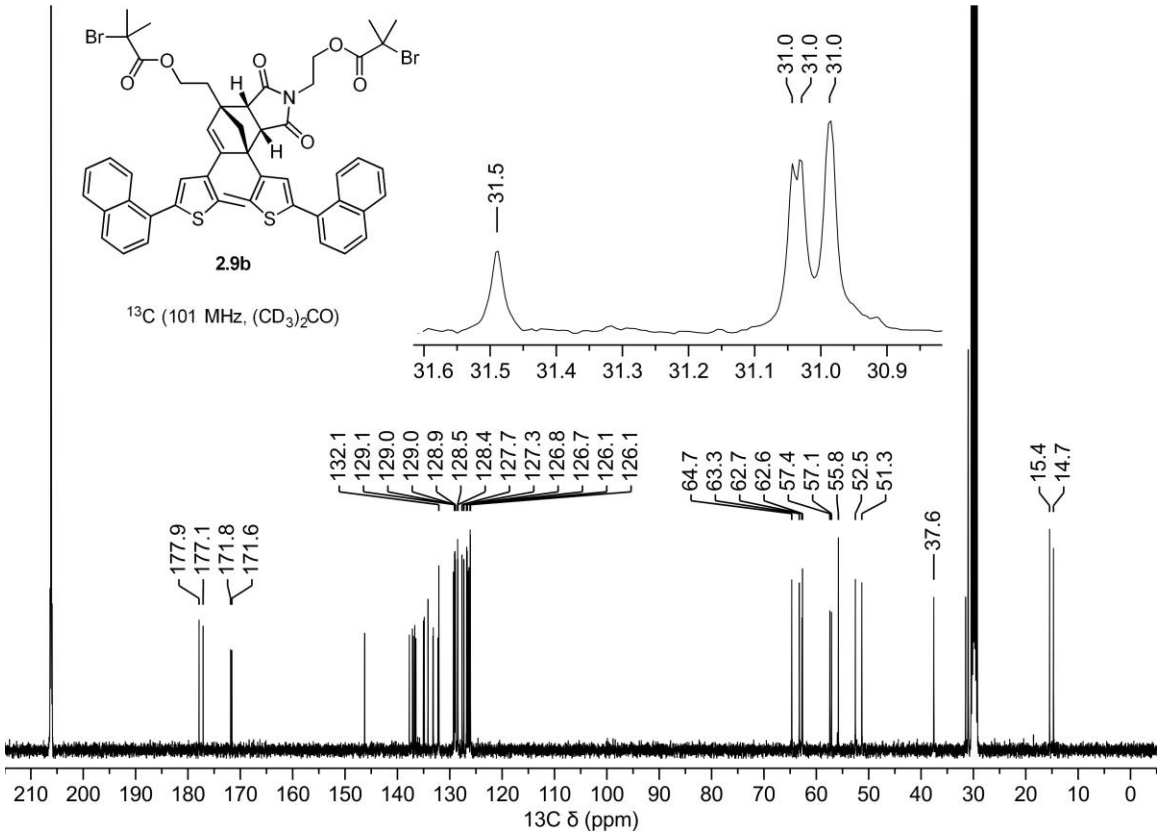
2.9b
^{13}C (101 MHz, $(CD_3)_2CO$)
31.0 31.0 31.0
31.5
31.6 31.5 31.4 31.3 31.2 31.1 31.0 30.9
132.1 129.1 129.0 129.0 128.9 128.5 128.4 127.7 127.3 126.8 126.7 126.1 126.1
64.7 63.3 62.7 62.6 57.4 57.1 55.8 52.5 51.3
37.6
15.4 14.7
177.9 177.1 171.8 171.6
210 200 190 180 170 160 150 140 130 120 110 100 90 80 70 60 50 40 30 20 10 0
13C δ (ppm)

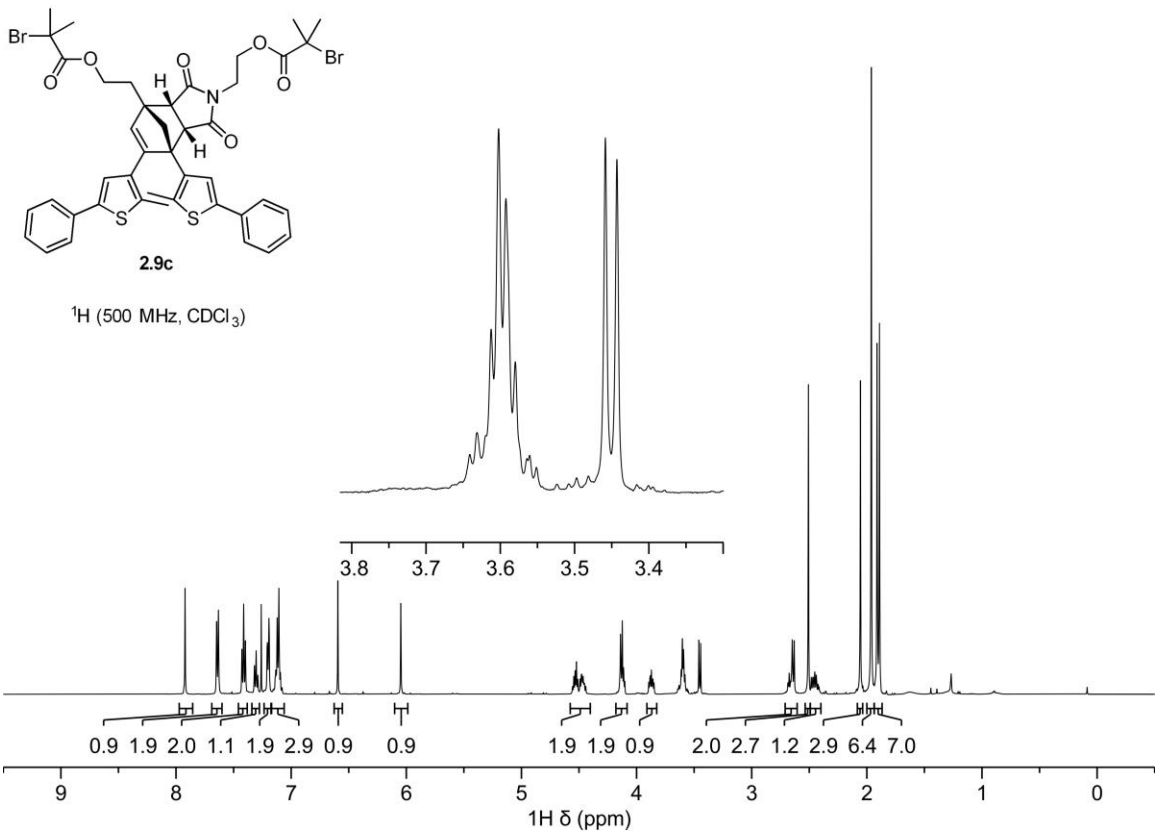
2.9c
^{1}H (500 MHz, CDCl$_3$)
3.8 3.7 3.6 3.5 3.4
0.9 1.9 2.0 1.1 1.9 2.9 0.9 0.9 1.9 1.9 0.9 2.0 2.7 1.2 2.9 6.4 7.0
9 8 7 6 5 4 3 2 1 0
1H δ (ppm)

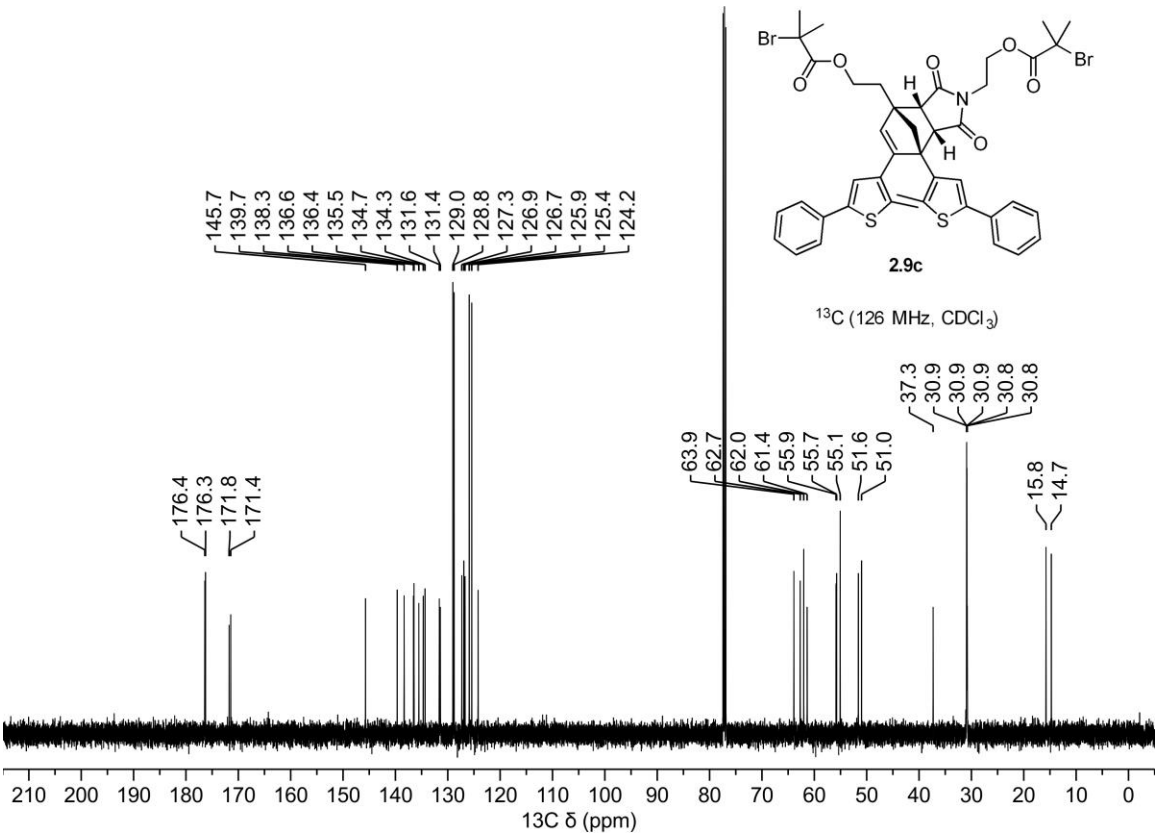
145.7 139.7 138.3 136.6 136.4 135.5 134.7 134.3 131.6 131.4 129.0 128.8 127.3 126.9 126.7 125.9 125.4 124.2
176.4 176.3 171.8 171.4
63.9 62.7 62.0 61.4 55.9 55.7 55.1 51.6 51.0
37.3 30.9 30.9 30.9 30.8 30.8
15.8 14.7
2.9c
^{13}C (126 MHz, CDCl$_3$)
210 200 190 180 170 160 150 140 130 120 110 100 90 80 70 60 50 40 30 20 10 0
13C δ (ppm)

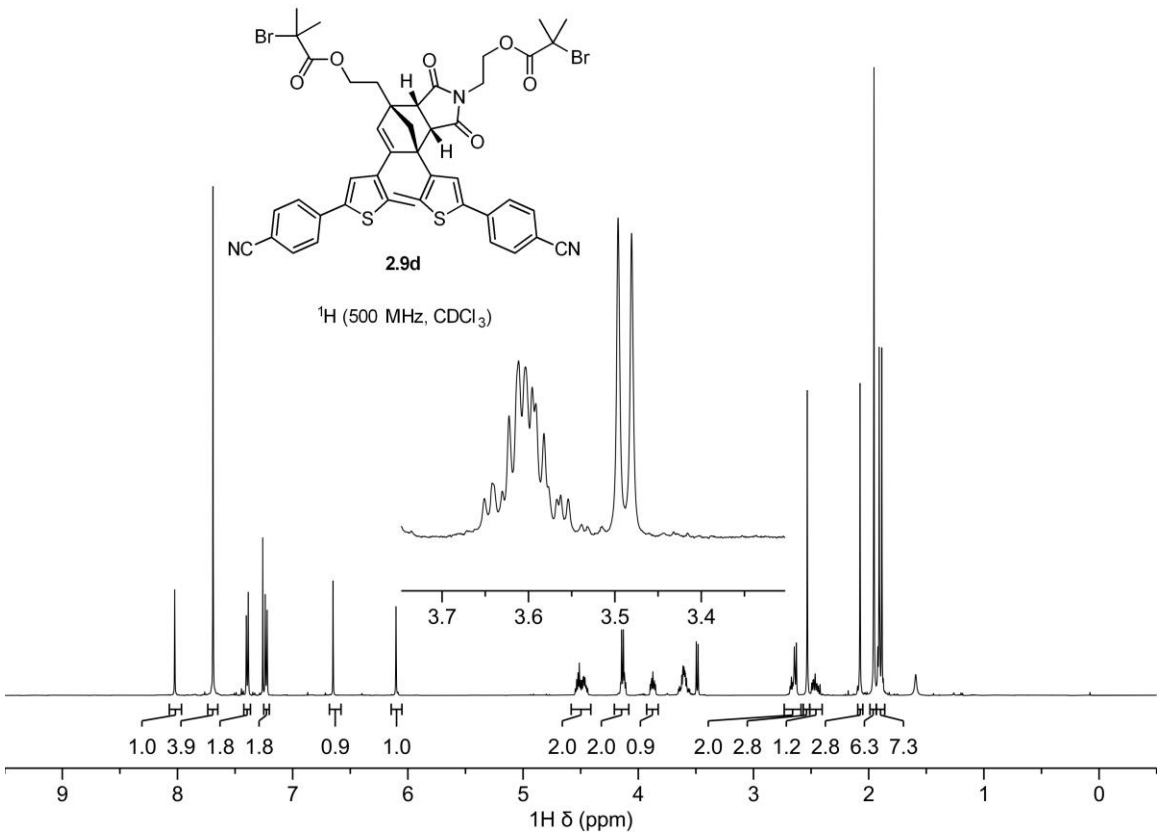
2.9d
1H (500 MHz, CDCl3)
1.0 3.9 1.8 1.8 0.9 1.0 2.0 2.0 0.9 2.0 2.8 1.2 2.8 6.3 7.3
1H δ (ppm)

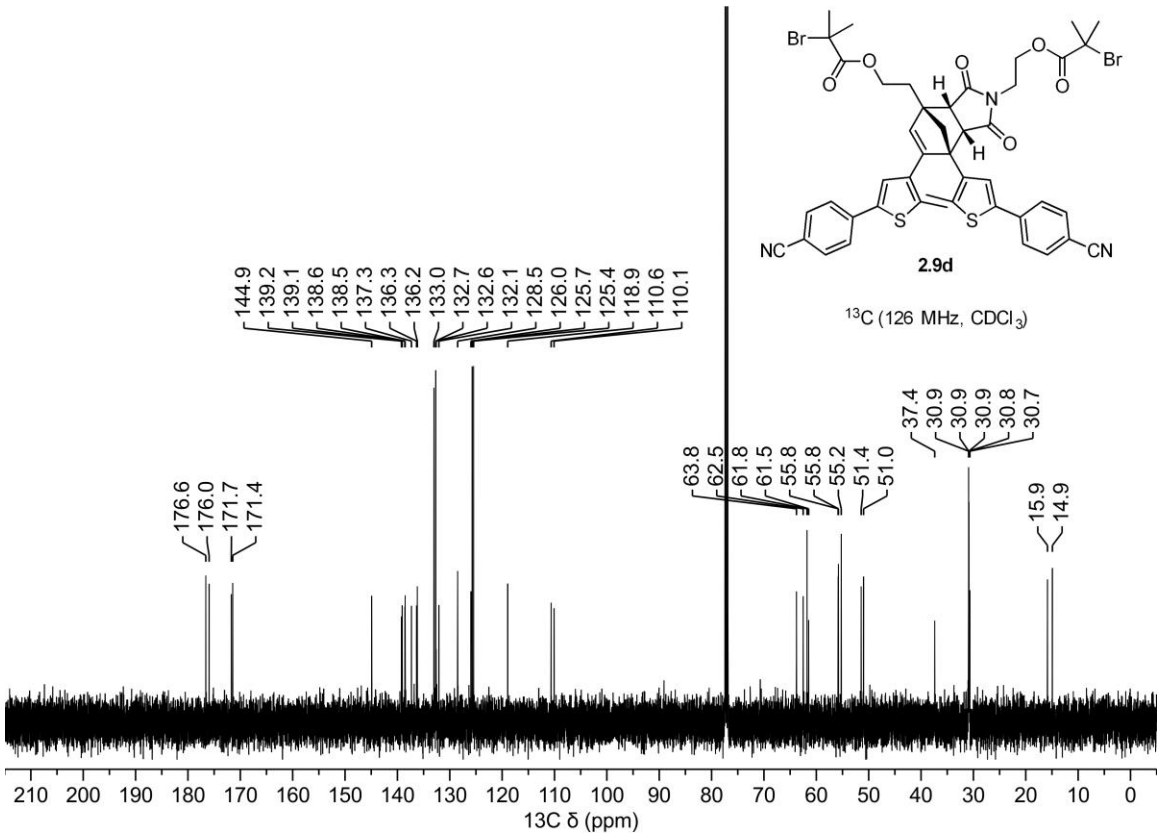
2.9d
13C (126 MHz, CDCl3)
144.9 139.2 139.1 138.6 138.5 137.3 136.3 136.2 133.0 132.7 132.6 132.1 128.5 126.0 125.7 125.4 118.9 110.6 110.1
176.6 176.0 171.7 171.4
63.8 62.5 61.8 61.5 55.8 55.8 55.2 51.4 51.0
37.4 30.9 30.9 30.9 30.8 30.7
15.9 14.9
13C δ (ppm)

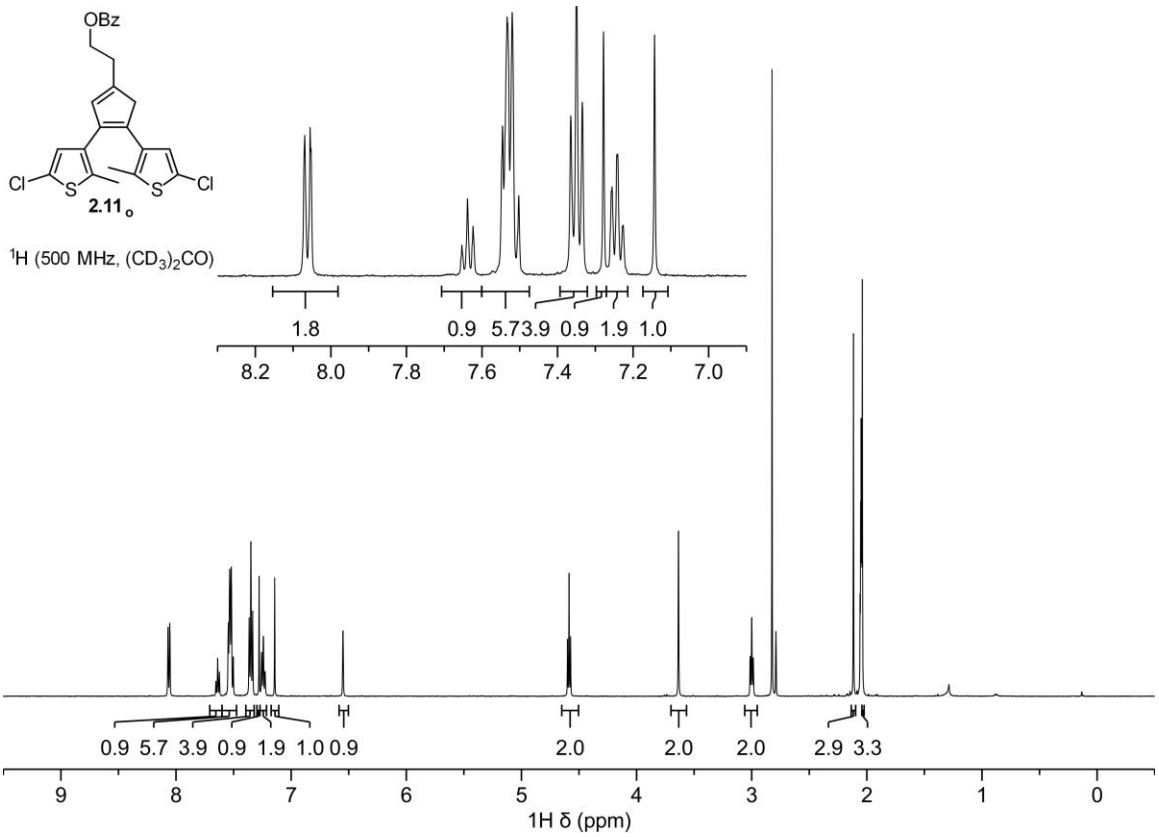
OBz
Cl
S
S
Cl
2.11o
1H (500 MHz, (CD3)2CO)
1.8
0.9 5.7 3.9 0.9 1.9 1.0
8.2 8.0 7.8 7.6 7.4 7.2 7.0
0.9 5.7 3.9 0.9 1.9 1.0 0.9
2.0
2.0
2.0
2.9 3.3
9 8 7 6 5 4 3 2 1 0
1H δ (ppm)

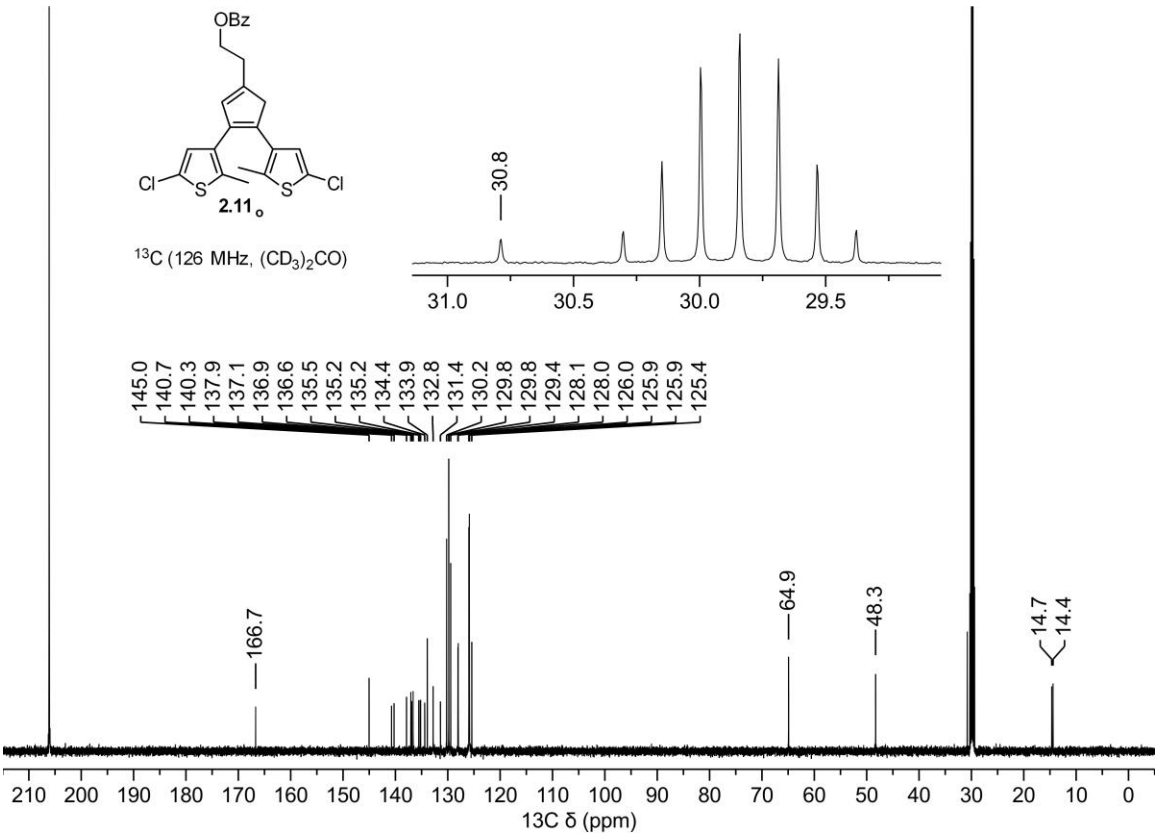
OBz
Cl
S
S
Cl
2.11o
13C (126 MHz, (CD3)2CO)
30.8
31.0 30.5 30.0 29.5
145.0
140.7
140.3
137.9
137.1
136.9
136.6
135.5
135.2
135.2
134.4
133.9
132.8
131.4
130.2
129.8
129.4
128.1
128.0
126.0
125.9
125.9
125.4
166.7
64.9
48.3
14.7
14.4
210 200 190 180 170 160 150 140 130 120 110 100 90 80 70 60 50 40 30 20 10 0
13C δ (ppm)

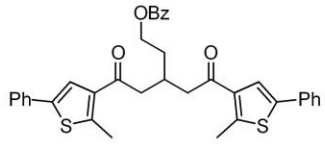

2.12

^{1}H (500 MHz, $CDCl_3$)

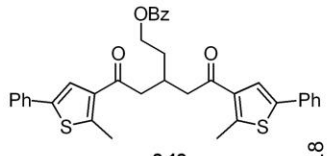

2.12

^{13}C (126 MHz, $CDCl_3$)

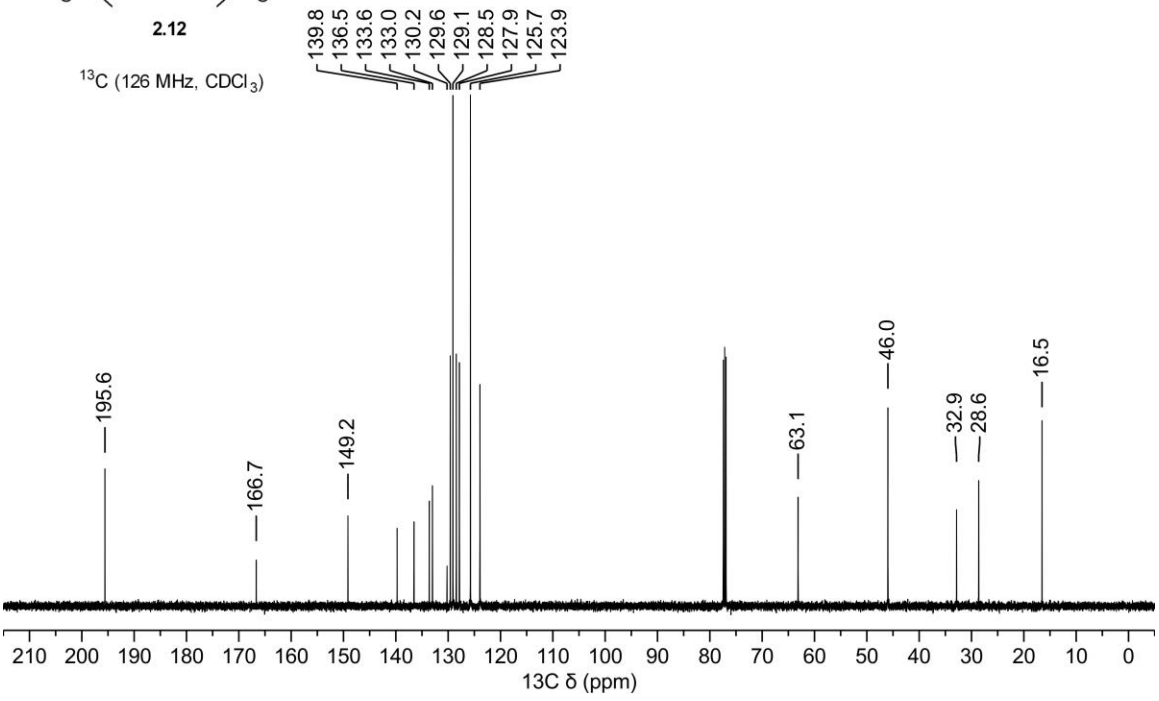

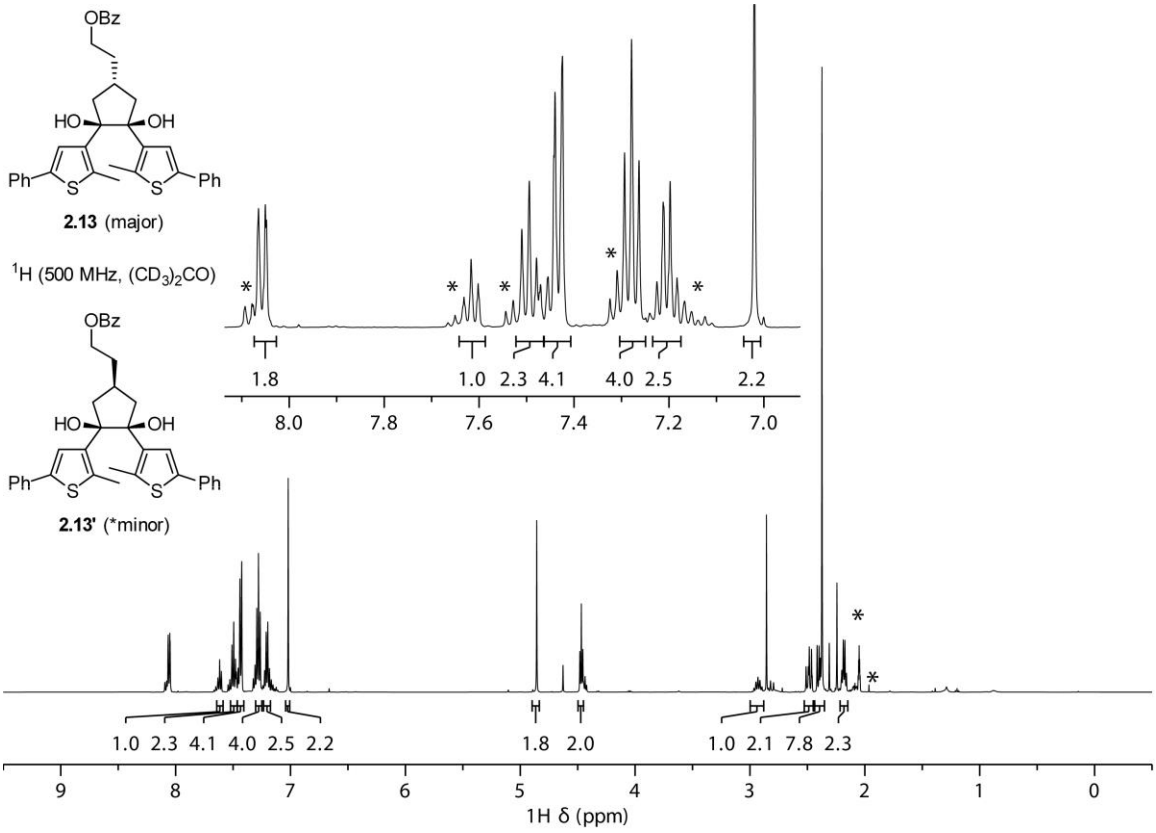
OBz
HO
OH
Ph
S
Ph
2.13 (major)
1H (500 MHz, (CD3)2CO)
2.13' (*minor)
1.8
1.0 2.3 4.1
4.0 2.5
2.2
1.0 2.3 4.1 4.0 2.5 2.2
1.8 2.0
1.0 2.1 7.8 2.3
1H δ (ppm)

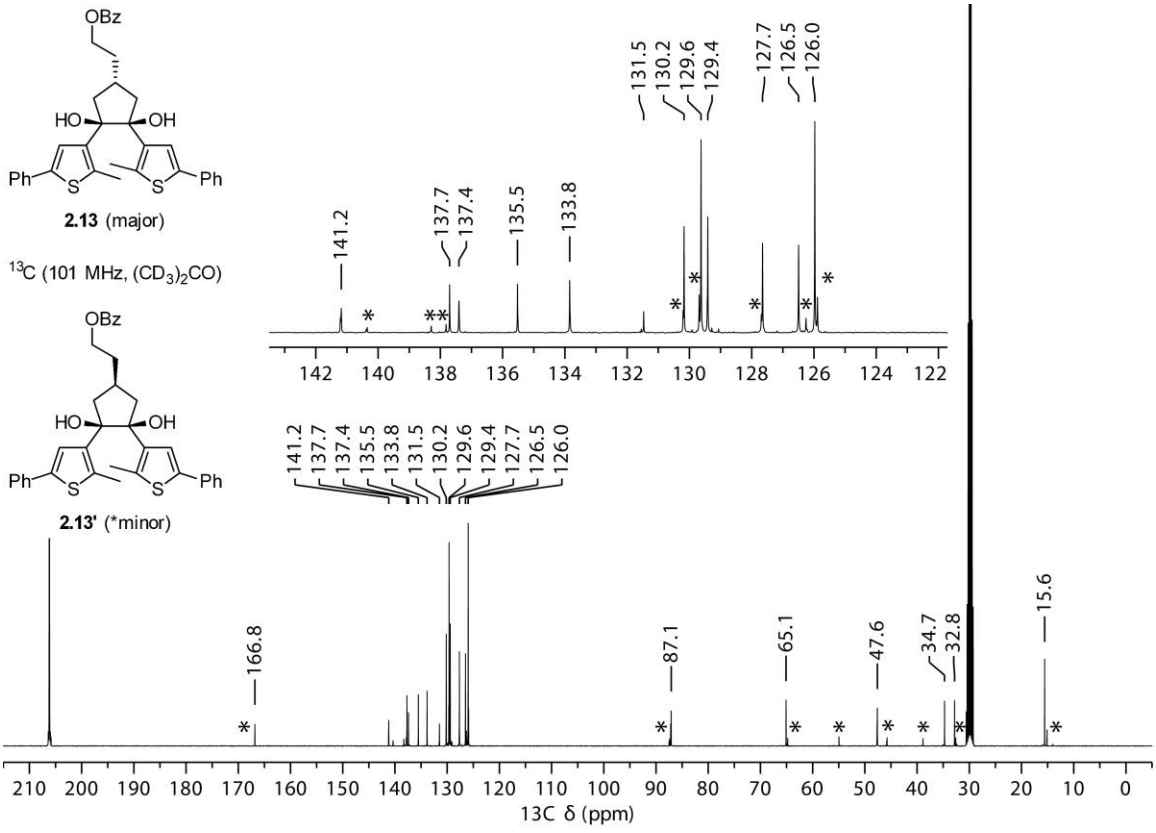
OBz
HO
OH
Ph
S
Ph
2.13 (major)
13C (101 MHz, (CD3)2CO)
2.13' (*minor)
141.2
137.7
137.4
135.5
133.8
131.5
130.2
129.6
129.4
127.7
126.5
126.0
166.8
87.1
65.1
47.6
34.7
32.8
15.6
13C δ (ppm)

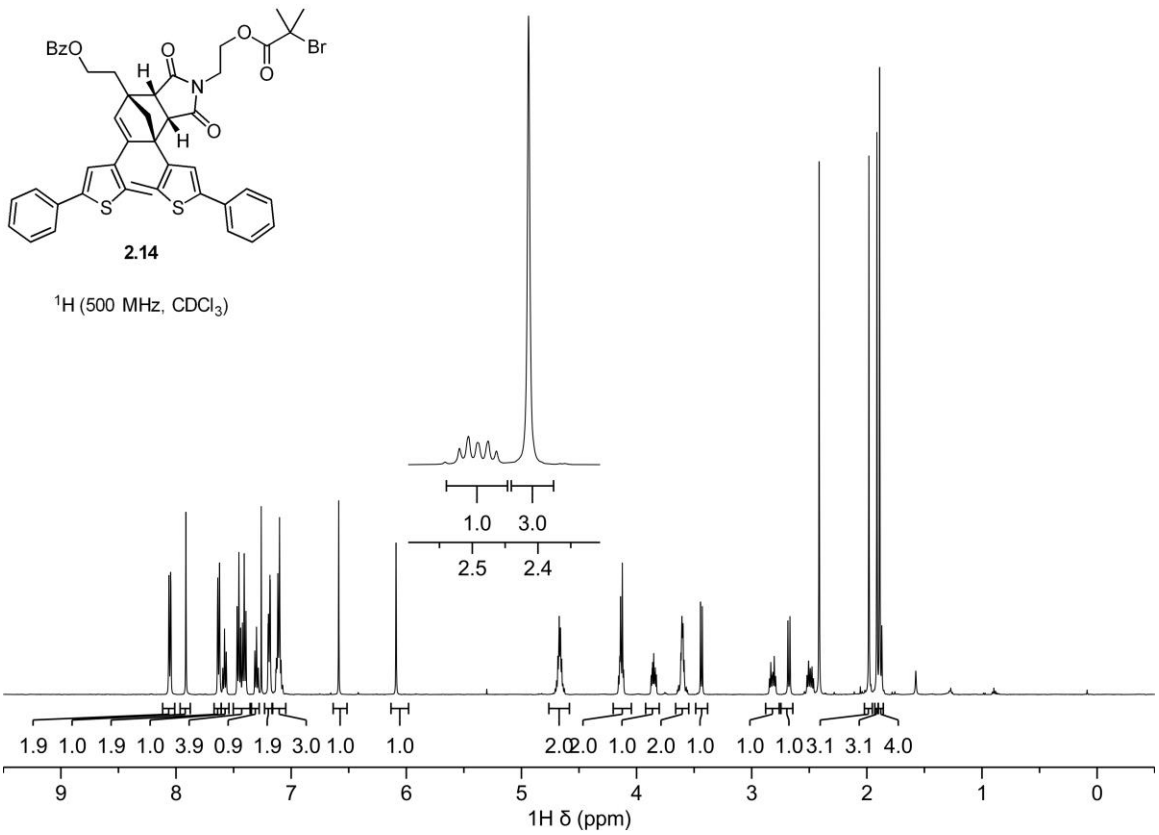
BzO
O
H
N
O
O
O
Br
H
S
S
2.14
^{1}H (500 MHz, $CDCl_3$)
1.0 3.0
2.5 2.4
1.9 1.0 1.9 1.0 3.9 0.9 1.9 3.0 1.0 1.0 2.0 2.0 1.0 2.0 1.0 1.0 1.0 3.1 3.1 4.0
9 8 7 6 5 4 3 2 1 0
1H δ (ppm)

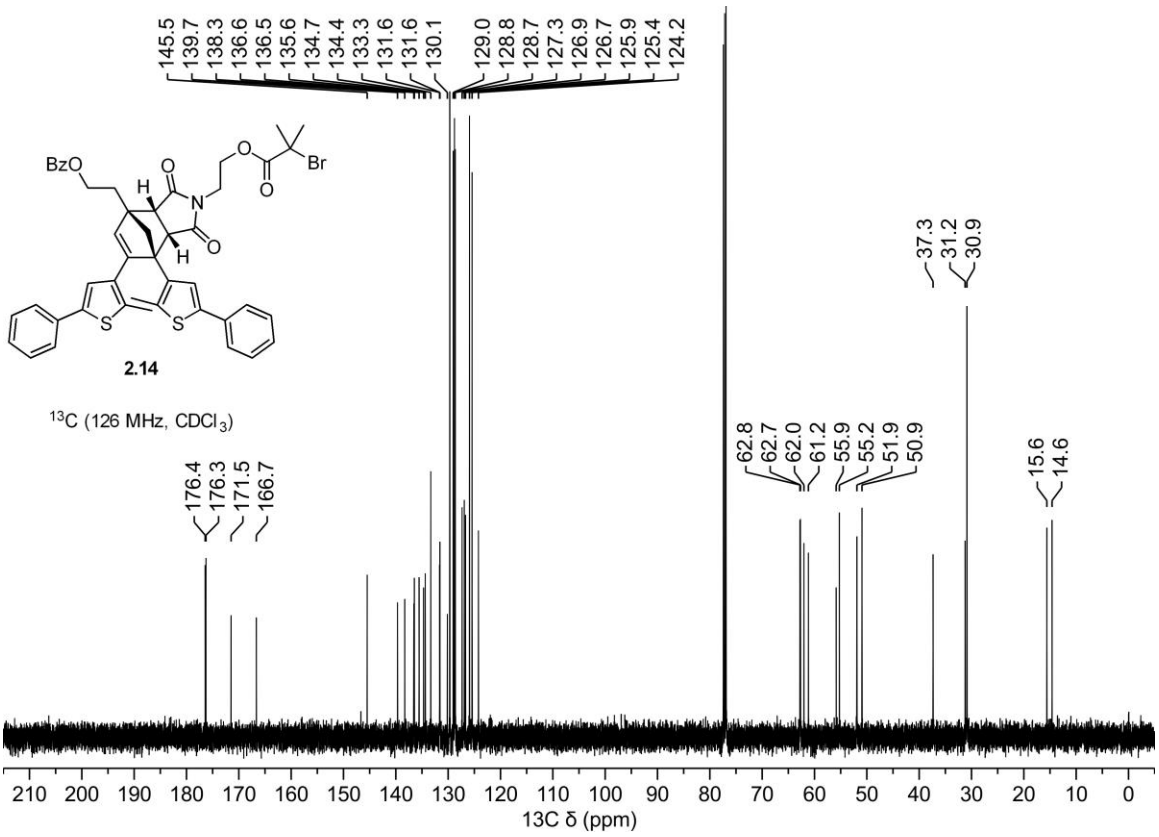
145.5
139.7
138.3
136.6
136.5
135.6
134.7
134.4
133.3
131.6
131.6
130.1
129.0
128.8
128.7
127.3
126.9
126.7
125.9
125.4
124.2
BzO
O
H
N
O
O
O
Br
H
S
S
2.14
^{13}C (126 MHz, $CDCl_3$)
176.4
176.3
171.5
166.7
62.8
62.7
62.0
61.2
55.9
55.2
51.9
50.9
37.3
31.2
30.9
15.6
14.6
210 200 190 180 170 160 150 140 130 120 110 100 90 80 70 60 50 40 30 20 10 0
13C δ (ppm)

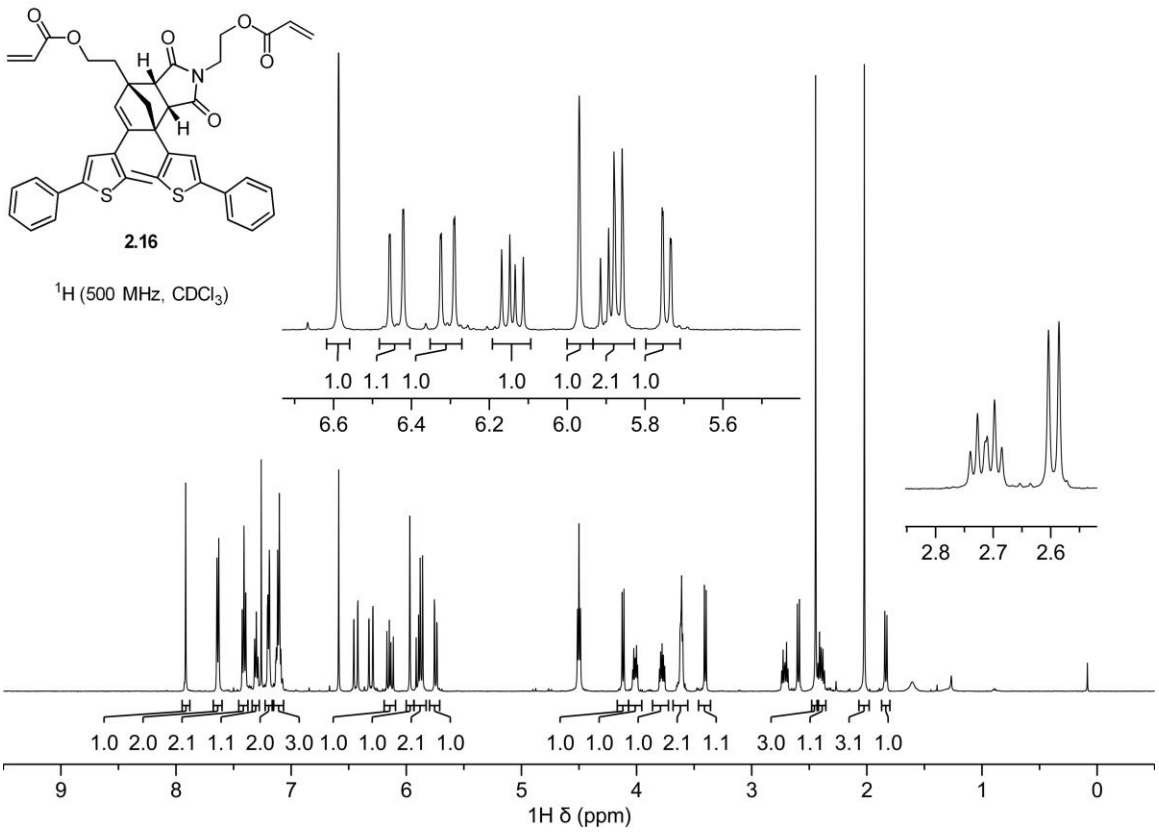
2.16
^{1}H (500 MHz, CDCl$_3$)
1.0 1.1 1.0 1.0 1.0 2.1 1.0
6.6 6.4 6.2 6.0 5.8 5.6
2.8 2.7 2.6
1.0 2.0 2.1 1.1 2.0 3.0 1.0 1.0 2.1 1.0 1.0 1.0 1.0 2.1 1.1 3.0 1.1 3.1 1.0
9 8 7 6 5 4 3 2 1 0
1H δ (ppm)

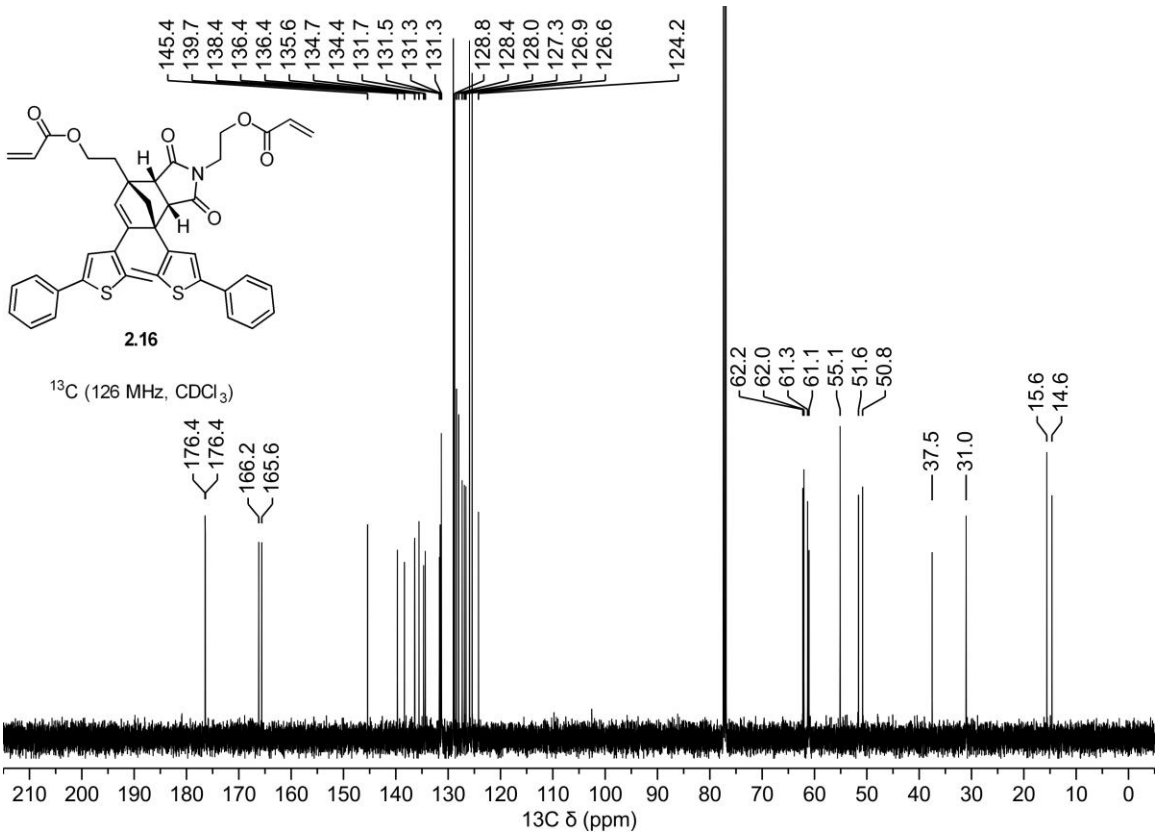
145.4 139.7 138.4 136.4 136.4 135.6 134.7 134.4 131.7 131.5 131.3 131.3 128.8 128.4 128.0 127.3 126.9 126.6 124.2
2.16
^{13}C (126 MHz, CDCl$_3$)
176.4 176.4 166.2 165.6
62.2 62.0 61.3 61.1 55.1 51.6 50.8 37.5 31.0 15.6 14.6
210 200 190 180 170 160 150 140 130 120 110 100 90 80 70 60 50 40 30 20 10 0
13C δ (ppm)

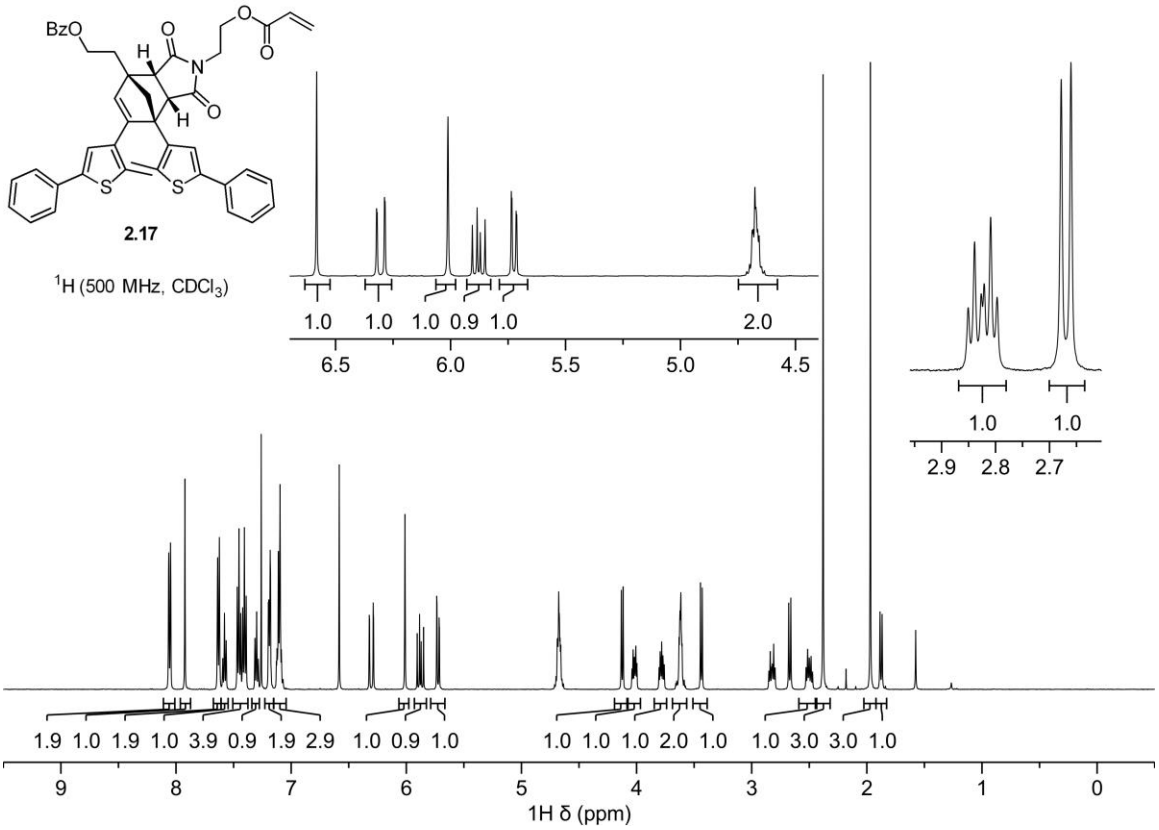
BzO
O
O
O
H
N
O
H
S
S
2.17
^{1}H (500 MHz, $CDCl_3$)
1.0 1.0 1.0 0.9 1.0 2.0
6.5 6.0 5.5 5.0 4.5
1.0 1.0
2.9 2.8 2.7
1.9 1.0 1.9 1.0 3.9 0.9 1.9 2.9 1.0 0.9 1.0 1.0 1.0 1.0 2.0 1.0 1.0 3.0 3.0 1.0
9 8 7 6 5 4 3 2 1 0
1H δ (ppm)

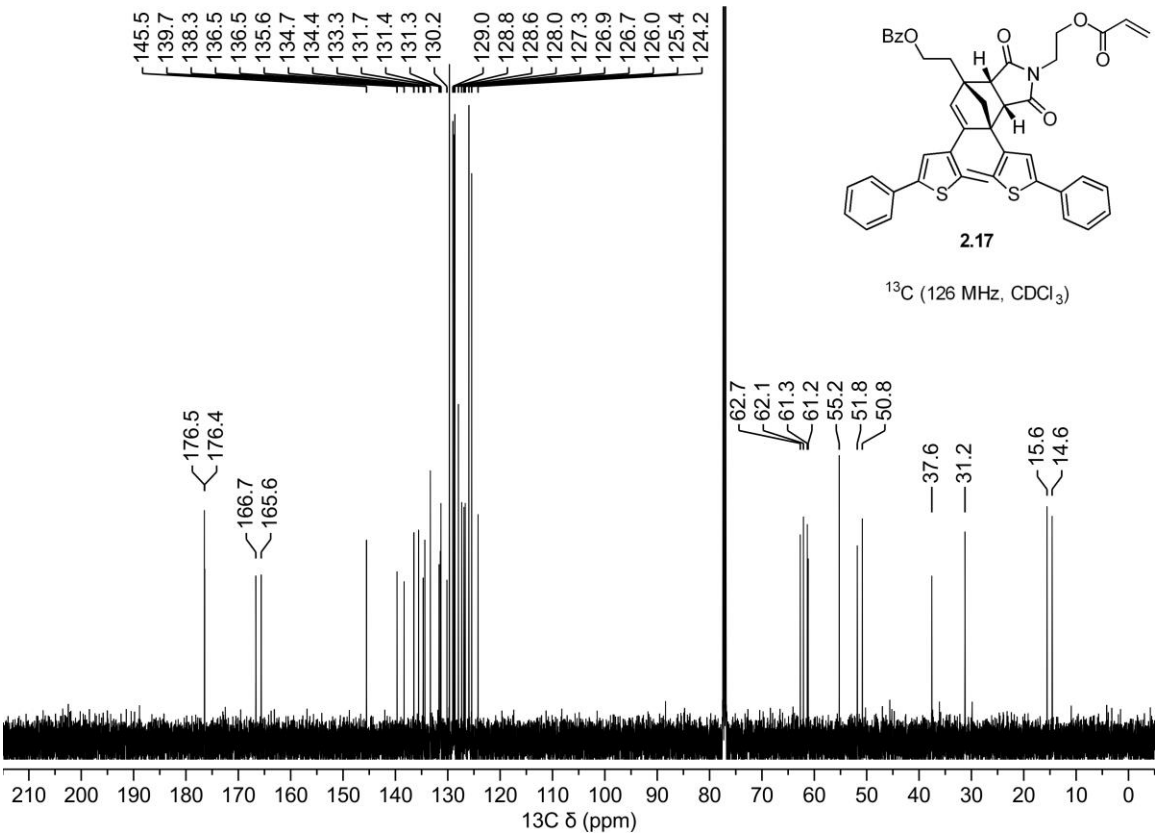
145.5
139.7
138.3
136.5
136.5
135.6
134.7
134.4
133.3
131.7
131.4
131.3
130.2
129.0
128.8
128.6
128.0
127.3
126.9
126.7
126.0
125.4
124.2
176.5
176.4
166.7
165.6
62.7
62.1
61.3
61.2
55.2
51.8
50.8
37.6
31.2
15.6
14.6
BzO
O
O
O
H
N
O
H
S
S
2.17
^{13}C (126 MHz, $CDCl_3$)
210 200 190 180 170 160 150 140 130 120 110 100 90 80 70 60 50 40 30 20 10 0
13C δ (ppm)

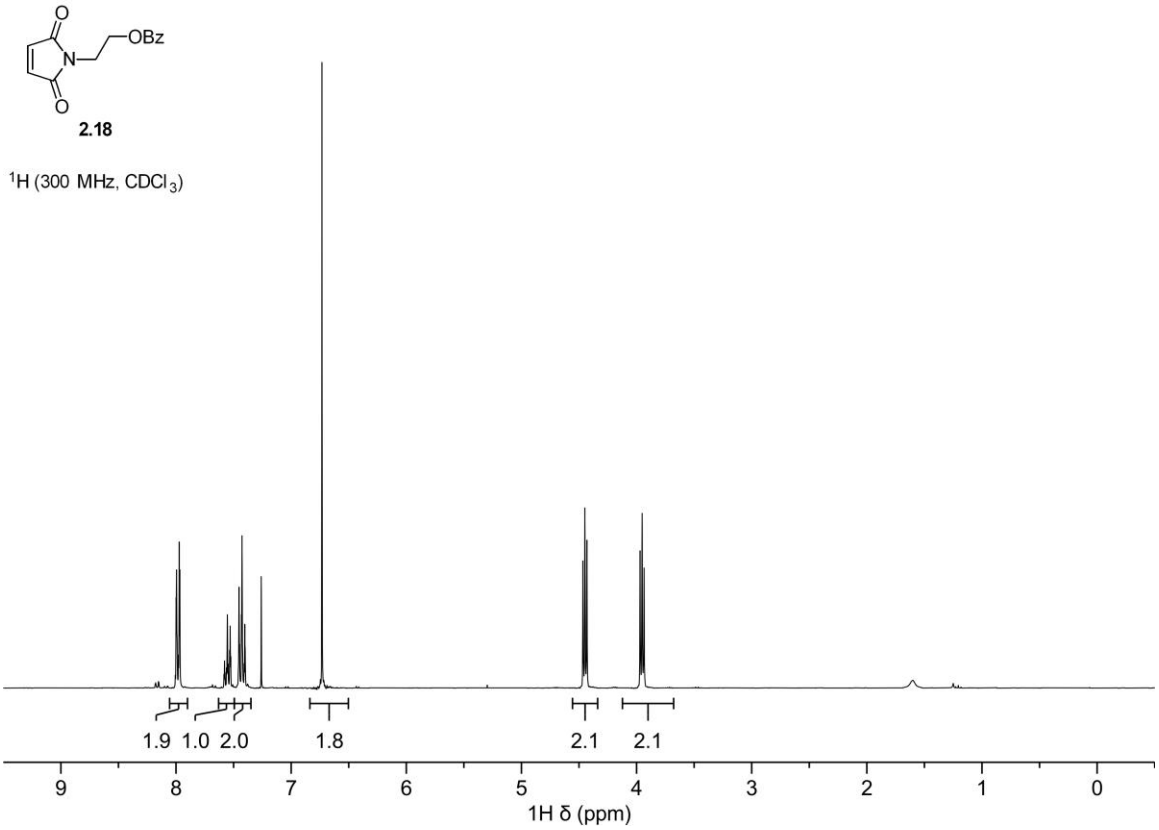
O
N
OBz
O
2.18
1H (300 MHz, CDCl3)
1.9 1.0 2.0 1.8 2.1 2.1
9 8 7 6 5 4 3 2 1 0
1H δ (ppm)

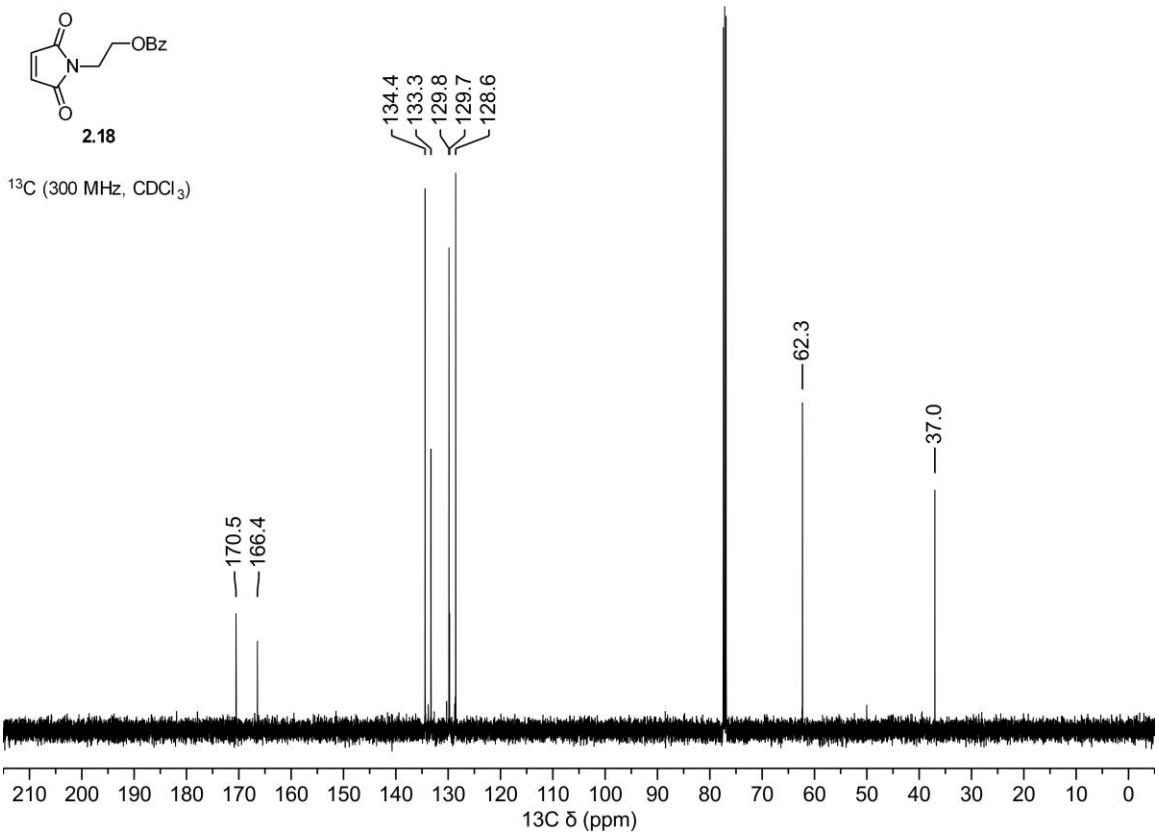
O
N
OBz
O
2.18
13C (300 MHz, CDCl3)
134.4
133.3
129.8
129.7
128.6
62.3
37.0
170.5
166.4
210 200 190 180 170 160 150 140 130 120 110 100 90 80 70 60 50 40 30 20 10 0
13C δ (ppm)

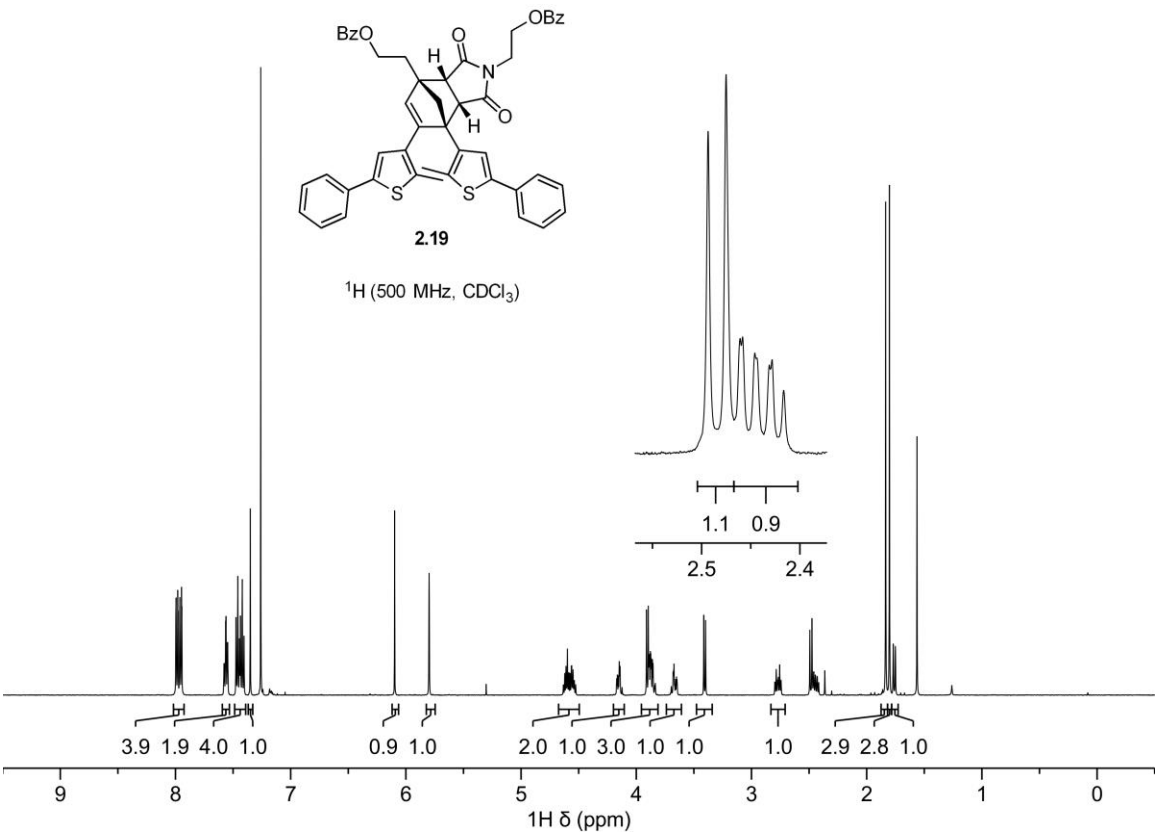
BzO
OBz
O
H
N
O
H
S
S
2.19
1H (500 MHz, CDCl3)
1.1 0.9
2.5 2.4
3.9 1.9 4.0 1.0
0.9 1.0
2.0 1.0 3.0 1.0 1.0
1.0
2.9 2.8 1.0
9 8 7 6 5 4 3 2 1 0
1H δ (ppm)

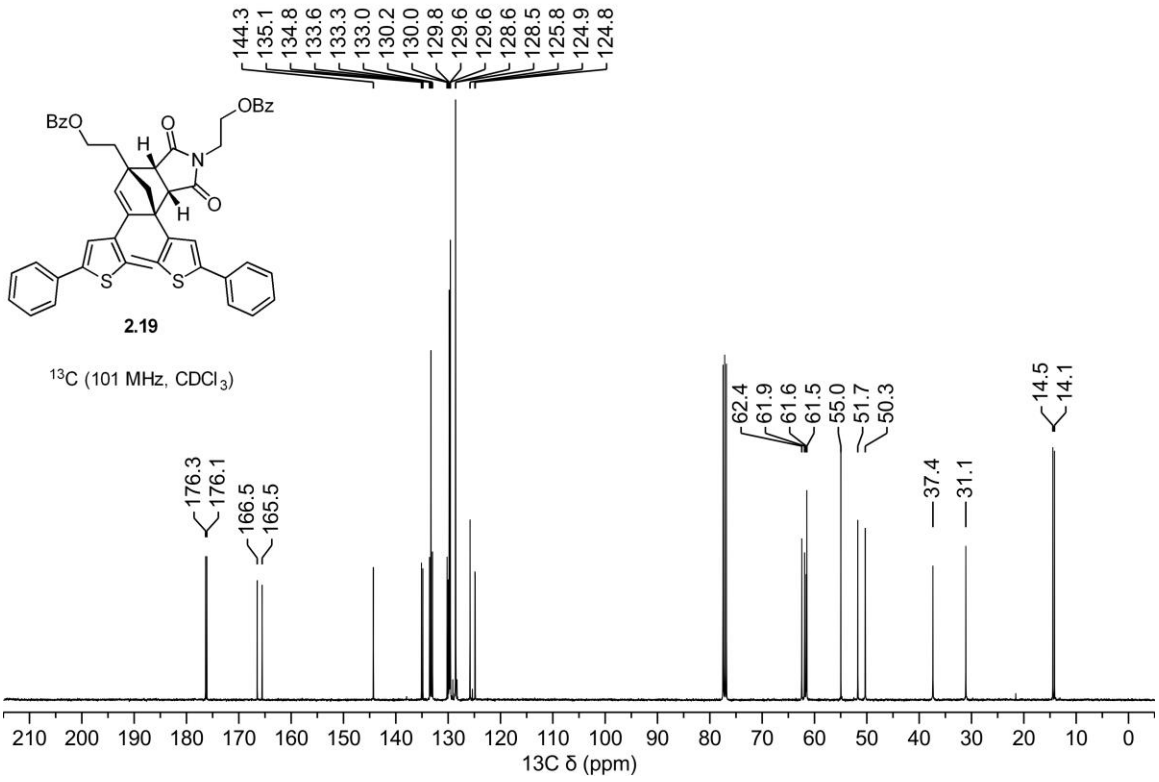
144.3
135.1
134.8
133.6
133.3
133.0
130.2
130.0
129.8
129.6
129.6
128.6
128.5
125.8
124.9
124.8
BzO
OBz
O
H
N
O
H
S
S
2.19
13C (101 MHz, CDCl3)
176.3
176.1
166.5
165.5
62.4
61.9
61.6
61.5
55.0
51.7
50.3
37.4
31.1
14.5
14.1
210 200 190 180 170 160 150 140 130 120 110 100 90 80 70 60 50 40 30 20 10 0
13C δ (ppm)

References

(1) Beyer, M. K.; Clausen-Schaumann, H. Mechanochemistry: The Mechanical Activation of Covalent Bonds. *Chem. Rev.* **2005**, *105*, 2921–2948.

(2) Caruso, M. M.; Davis, D. A.; Shen, Q.; Odom, S. A.; Sottos, N. R.; White, S. R.; Moore, J. S. Mechanically-Induced Chemical Changes in Polymeric Materials. *Chem. Rev.* **2009**, *109*, 5755–5798.

(3) Li, J.; Nagamani, C.; Moore, J. S. Polymer Mechanochemistry: From Destructive to Productive. *Acc. Chem. Res.* **2015**, *48*, 2181–2190.

(4) Paulusse, J. M. J.; Sijbesma, R. P. Ultrasound in polymer chemistry: Revival of an established technique. *J. Polym. Sci. Part Polym. Chem.* **2006**, *44*, 5445–5453.

(5) May, P. A.; Moore, J. S. Polymer mechanochemistry: techniques to generate molecular force via elongational flows. *Chem. Soc. Rev.* **2013**, *42*, 7497–7506.

(6) Davis, D. A.; Hamilton, A.; Yang, J.; Cremar, L. D.; Van Gough, D.; Potisek, S. L.; Ong, M. T.; Braun, P. V.; Martínez, T. J.; White, S. R.; Moore, J. S.; Sottos, N. R. Force-induced activation of covalent bonds in mechanoresponsive polymeric materials. *Nature* **2009**, *459*, 68–72.

(7) Sung, J.; Robb, M. J.; White, S. R.; Moore, J. S.; Sottos, N. R. Interfacial Mechanophore Activation Using Laser-Induced Stress Waves. *J. Am. Chem. Soc.* **2018**, *140*, 5000–5003.

(8) Sulkanen, A. R.; Sung, J.; Robb, M. J.; Moore, J. S.; Sottos, N. R.; Liu, G. Spatially Selective and Density-Controlled Activation of Interfacial Mechanophores. *J. Am. Chem. Soc.* **2019**, *141*, 4080–4085.

(9) Kim, G.; Lau, V. M.; Halmes, A. J.; Oelze, M. L.; Moore, J. S.; Li, K. C. High-intensity focused ultrasound-induced mechanochemical transduction in synthetic elastomers. *Proc. Natl. Acad. Sci.* **2019**, *116*, 10214–10222.

(10) Piermattei, A.; Karthikeyan, S.; Sijbesma, R. P. Activating catalysts with mechanical force. *Nat. Chem.* **2009**, *1*, 133–137.

(11) Michael, P.; Binder, W. H. A Mechanochemically Triggered "Click" Catalyst. *Angew. Chem. Int. Ed.* **2015**, *54*, 13918–13922.

(12) Chen, Z.; Mercer, J. A. M.; Zhu, X.; Romaniuk, J. A. H.; Pfattner, R.; Cegelski, L.; Martinez, T. J.; Burns, N. Z.; Xia, Y. Mechanochemical unzipping of insulating polyladderene to semiconducting polyacetylene. *Science* **2017**, *357*, 475–479.

(13) Yang, J.; Horst, M.; Romaniuk, J. A. H.; Jin, Z.; Cegelski, L.; Xia, Y. Benzoladderene Mechanophores: Synthesis, Polymerization, and Mechanochemical Transformation. *J. Am. Chem. Soc.* **2019**, *141*, 6479–6483.

(14) Boswell, B. R.; Mansson, C. M. F.; Cox, J. M.; Jin, Z.; Romaniuk, J. A. H.; Lindquist, K. P.; Cegelski, L.; Xia, Y.; Lopez, S. A.; Burns, N. Z. Mechanochemical synthesis of an elusive fluorinated polyacetylene. *Nat. Chem.* **2021**, *13*, 41–46.

(15) Larsen, M. B.; Boydston, A. J. "Flex-Activated" Mechanophores: Using Polymer Mechanochemistry To Direct Bond Bending Activation. *J. Am. Chem. Soc.* **2013**, *135*, 8189–8192.

(16) Hu, X.; Zeng, T.; Husic, C. C.; Robb, M. J. Mechanically Triggered Small Molecule Release from a Masked Furfuryl Carbonate. *J. Am. Chem. Soc.* **2019**, *141*, 15018–15023.

(17) Shi, Z.; Song, Q.; Göstl, R.; Herrmann, A. Mechanochemical activation of disulfide-based multifunctional polymers for theranostic drug release. *Chem. Sci.* **2021**, 10.1039.D0SC06054B.

(18) Göstl, R.; Sijbesma, R. P. π-extended anthracenes as sensitive probes for mechanical stress. *Chem. Sci.* **2016**, *7*, 370–375.

(19) Baumann, C.; Stratigaki, M.; Centeno, S. P.; Göstl, R. Multicolor Mechanofluorophores for the Quantitative Detection of Covalent Bond Scission in Polymers. *Angew. Chem. Int. Ed.* **2021**, *60*, 2–9.

(20) Karman, M.; Verde-Sesto, E.; Weder, C. Mechanochemical Activation of Polymer-Embedded Photoluminescent Benzoxazole Moieties. *ACS Macro Lett.* **2018**, *7*, 1028–1033.

(21) Kabb, C. P.; O'Bryan, C. S.; Morley, C. D.; Angelini, T. E.; Sumerlin, B. S. Anthracene-based mechanophores for compression-activated fluorescence in polymeric networks. *Chem. Sci.* **2019**, *10*, 7702–7708.

(22) Chen, Y.; Spiering, A. J. H.; Karthikeyan, S.; Peters, G. W. M.; Meijer, E. W.; Sijbesma, R. P. Mechanically induced chemiluminescence from polymers incorporating a 1,2-dioxetane unit in the main chain. *Nat. Chem.* **2012**, *4*, 559–562.

(23) Chen, Y.; Mellot, G.; Luijk, D. van; Creton, C.; Sijbesma, R. P. Mechanochemical tools for polymer materials. *Chem. Soc. Rev.* **2021**, *50*, 4100–4140.

(24) Robb, M. J.; Kim, T. A.; Halmes, A. J.; White, S. R.; Sottos, N. R.; Moore, J. S. Regioisomer-Specific Mechanochromism of Naphthopyran in Polymeric Materials. *J. Am. Chem. Soc.* **2016**, *138*, 12328–12331.

(25) Wang, Z.; Ma, Z.; Wang, Y.; Xu, Z.; Luo, Y.; Wei, Y.; Jia, X. A Novel Mechanochromic and Photochromic Polymer Film: When Rhodamine Joins Polyurethane. *Adv. Mater.* **2015**, *27*, 6469–6474.

(26) Imato, K.; Kanehara, T.; Ohishi, T.; Nishihara, M.; Yajima, H.; Ito, M.; Takahara, A.; Otsuka, H. Mechanochromic Dynamic Covalent Elastomers: Quantitative Stress Evaluation and Autonomous Recovery. *ACS Macro Lett.* **2015**, 1307–1311.

(27) Barber, R. W.; McFadden, M. E.; Hu, X.; Robb, M. J. Mechanochemically Gated Photoswitching: Expanding the Scope of Polymer Mechanochromism. *Synlett* **2019**, *30*, 1725–1732.

(28) Imato, K.; Nishihara, M.; Kanehara, T.; Amamoto, Y.; Takahara, A.; Otsuka, H. Self-Healing of Chemical Gels Cross-Linked by Diarylbibenzofuranone-Based Trigger-Free Dynamic Covalent Bonds at Room Temperature. *Angew. Chem. Int. Ed.* **2012**, *51*, 1138–1142.

(29) Wang, J.; Kouznetsova, T. B.; Boulatov, R.; Craig, S. L. Mechanical gating of a mechanochemical reaction cascade. *Nat. Commun.* **2016**, *7*, 13433.

(30) Hu, X.; McFadden, M. E.; Barber, R. W.; Robb, M. J. Mechanochemical Regulation of a Photochemical Reaction. *J. Am. Chem. Soc.* **2018**, *140*, 14073–14077.

(31) Irie, M.; Fukaminato, T.; Matsuda, K.; Kobatake, S. Photochromism of Diarylethene Molecules and Crystals: Memories, Switches, and Actuators. *Chem. Rev.* **2014**, *114*, 12174–12277.

(32) Stevenson, R.; De Bo, G. Controlling Reactivity by Geometry in Retro-Diels–Alder Reactions under Tension. *J. Am. Chem. Soc.* **2017**, *139*, 16768–16771.

(33) Alward, S. J.; Fallis, A. G. The synthesis of trisubstituted cyclopentadienes and their reactivity in the intramolecular Diels–Alder reaction. *Can. J. Chem.* **1984**, *62*, 121–127.

(34) Beyer, M. K. The mechanical strength of a covalent bond calculated by density functional theory. *J. Chem. Phys.* **2000**, *112*, 7307–7312.

(35) Klein, I. M.; Husic, C. C.; Kovács, D. P.; Choquette, N. J.; Robb, M. J. Validation of the CoGEF Method as a Predictive Tool for Polymer Mechanochemistry. *J. Am. Chem. Soc.* **2020**, *142*, 16364–16381.

(36) Lucas, L. N.; van Esch, J.; Kellogg, R. M.; Feringa, B. L. A new class of photochromic 1,2-diarylethenes; synthesis and switching properties of bis(3-thienyl)cyclopentenes. *Chem. Commun.* **1998**, No. 21, 2313–2314.

(37) Lemieux, V.; Gauthier, S.; Branda, N. R. Selective and Sequential Photorelease Using Molecular Switches. *Angew. Chem. Int. Ed.* **2006**, *45*, 6820–6824.

(38) Bruno, N. C.; Tudge, M. T.; Buchwald, S. L. Design and preparation of new palladium precatalysts for C–C and C–N cross-coupling reactions. *Chem. Sci.* **2013**, *4*, 916–920.

(39) Browne, W. R.; Jong, J. J. D. de; Kudernac, T.; Walko, M.; Lucas, L. N.; Uchida, K.; Esch, J. H. van; Feringa, B. L. Oxidative Electrochemical Switching in Dithienylcyclopentenes, Part 2: Effect of Substitution and Asymmetry on the Efficiency and Direction of Molecular Switching and Redox Stability. *Chem. – Eur. J.* **2005**, *11*, 6430–6441.

(40) Pu, S.; Yang, T.; Xu, J.; Shen, L.; Li, G.; Xiao, Q.; Chen, B. Synthesis and optoelectronic properties of four photochromic dithienylethenes. *Tetrahedron* **2005**, *61*, 6623–6629.

(41) Berkowski, K. L.; Potisek, S. L.; Hickenboth, C. R.; Moore, J. S. Ultrasound-Induced Site-Specific Cleavage of Azo-Functionalized Poly(ethylene glycol). *Macromolecules* **2005**, *38*, 8975–8978.

(42) Wilt, J. W.; Massie, S. N.; Dabek, R. B. Reaction of 2-(.DELTA.3-cyclopentenyl)ethyl bromide with tri-n-butyltin hydride. Cyclization to norbornane. *J. Org. Chem.* **1970**, *35*, 2803–2806.

(43) Lucas, L. N.; Jong, J. J. D. de; Esch, J. H. van; Kellogg, R. M.; Feringa, B. L. Syntheses of Dithienylcyclopentene Optical Molecular Switches. *Eur. J. Org. Chem.* **2003**, *2003*, 155–166.

(44) Heo, Y.; Sodano, H. A. Self-Healing Polyurethanes with Shape Recovery. *Adv. Funct. Mater.* **2014**, *24*, 5261–5268.

(45) Nguyen, N. H.; Rosen, B. M.; Lligadas, G.; Percec, V. Surface-Dependent Kinetics of Cu(0)-Wire-Catalyzed Single-Electron Transfer Living Radical Polymerization of Methyl Acrylate in DMSO at 25 °C. *Macromolecules* **2009**, *42*, 2379–2386.